JUSTUS-LIEBIG-UNIVERSITÄT GIESSEN

Justus-Liebig-Universität Gießen
Fachbereich 08: Biologie und Chemie
Institut für Anorganische und Analytische Chemie

Investigations on Enantioselective Copper Mediated Oxygenations using O_2 and H_2O_2 as Oxidants

Kumulativ-Dissertation zur Erlangung des Doktorgrades der Naturwissenschaften

−Dr. rer. nat.−

Vorgelegt von

Alexander Petrillo

aus Gießen

Oktober 2024

Selbstständigkeitserklärung

Ich erkläre: Ich habe die vorgelegte Dissertation selbstständig und ohne unerlaubte fremde Hilfe und nur mit den Hilfen angefertigt, die ich in der Dissertation angegeben habe. Alle Textstellen, die wörtlich oder sinngemäß aus veröffentlichten Schriften entnommen sind, und alle Angaben, die auf mündlichen Auskünften beruhen, sind als solche kenntlich gemacht. Ich stimme einer evtl. Überprüfung meiner Dissertation durch eine Antiplagiat-Software zu. Bei den von mir durchgeführten und in der Dissertation erwähnten Untersuchungen habe ich die Grundsätze guter wissenschaftlicher Praxis, wie sie in der „Satzung der Justus-Liebig-Universität Gießen zur Sicherung guter wissenschaftlicher Praxis“ niedergelegt sind, eingehalten.

Datum	Unterschrift

Erstgutachter: Prof. Dr. Siegfried Schindler

Zweitgutachter: Prof. Dr. Richard Göttlich

Danksagung

Zunächst möchte ich meinem Doktorvater Prof. Dr. Siegfried Schindler für die Aufnahme in seiner Arbeitsgruppe, die Unterstützung während der Promotion sowie weiterer Projekte, wie meine Auslandsaufenthalte in England und den USA, danken. Außerdem danke ich Prof. Dr. Richard Göttlich für das Zweitgutachten dieser Arbeit.

Weiterhin möchte ich der Arbeitsgruppe um Prof. Dr. Sonja Herres-Pawlis aus Aachen, der Arbeitsgruppe um Prof. Dr. Max Holthausen aus Frankfurt am Main und besonders Prof. Dr. Isaac Garcia-Bosch und seiner Gruppe aus Pittsburgh (Pennsylvania, USA), in der ich 4 Monate forschen durfte, für die Zusammenarbeit danken.

Auch möchte ich allen aktuellen und ehemaligen Mitgliedern unserer Arbeitsgruppe Dr. Pascal Specht, Alexander Granichny, Dr. Thomas Rotärmel, Lars Schneider, Chiara Campi, Christian Noß, Dr. Fabian Stöhr, Dr. Tim Brückmann, Dr. Markus Lerch, Dr. Christopher Gawlig, Stefan Schaub, Azar Rezaei, Dr. Miriam Wern und Dr. Florian Ritz für das freundschaftliche Arbeitsklima und die zahlreichen wissenschaftlichen Diskussionen danken.

Außerdem danke ich allen Studierenden Helene Walter, Giacomo Rubin, Kevin Keller und Remy Goldberg, die an meinen Forschungsprojekten mitgearbeitet haben.

Des Weiteren danke ich meinen ehemaligen Kommilitonen, insbesondere Steffen Schröder, auf dessen freundschaftliche Unterstützung ich stets zählen konnte. Allen Mitgliedern des JCF Gießen danke ich für die zahlreichen spannenden und spaßigen Projekte, allen voran die Organisation der Frühjahressymposiums 2023 in Gießen.

Ich danke außerdem der Studienstiftung des Deutschen Volkes für die finanzielle Unterstützung, insbesondere Dr. Peter Antes und Prof. Dr. Claudia Hattendorff für die Hilfsbereitschaft und Vernetzung unserer Regionalgruppe.

Weiter danke ich Dr. Jonathan Becker und Dr. Christian Würtele für die Einführung in die Kristallographie und Lisa Wagner für das Messen meiner Einkristalle. Außerdem danke ich allen Mitarbeitenden der OC-Analytik, der Glasbläserei, der Chemikalienausgabe und der Materialausgabe für die nette Zusammenarbeit.

Vor allem aber möchte ich Emily Lea Pfeiff, meiner Familie und meinen Freunden für die Unterstützung während meines gesamten Studiums und der Promotion danken.

“Die Wissenschaft fängt eigentlich erst da an, interessant zu werden, wo sie aufhört.”

Justus von Liebig

List of Abbreviations

AO	Amine oxidase
CDA	Copper dioxygen adduct
CT	Charge transfer
DG	Directing group
DβM	Dopamine β-monooxygenase
DFT	Density functional theory
EDG	Electron donating group
EPR	Electron paramagnetic resonance
er	Enantiomeric ratio
EWG	Electron withdrawing group
EXAFS	Extended X-ray absorption fine structure
FG	Functional group
HAA	Hydrogen atom abstraction
HAT	Hydrogen atom transfer
IR	Infrared
LMCT	Ligand to metal charge transfer
LPMO	Lytic polysaccharide monooxygenase
PHM	Peptidylglycine α-hydroxylating monooxygenase
PPO	Polyphenol oxidase
rds	Rate determining step
rR	Resonance Raman
SC-XRD	Single crystal X-ray diffraction
SET	Single electron transfer
SOD	Superoxide dismutase
XAS	X-ray absorption spectroscopy

Abstract

Stereoselective oxygenations play a crucial role in the chemical and pharmaceutical industry since the biological activity of a compound can be dictated by a single stereogenic center. Performing such oxygenations with O_2 or H_2O_2 as oxidants would be desirable from an ecological perspective because they possess the highest O atom economy and form H_2O or H_2O_2 as only by-products. However, appropriate catalysts are required to direct the selectivity of oxygenation reactions. For the development of such catalysts, a biomimetic approach based on Cu-enzymes is promising, since they carry out catalytic and stereoselective oxygenations under ambient conditions, using O_2 or H_2O_2 as oxidants. This research is focused on the development of Cu-mediated enantioselective oxygenations using O_2 and H_2O_2 as oxidants, based on the knowledge gained from enzymatic models.

The first approach to reaching enantioselective Cu-mediated oxygenations is described in **Chapter 3.1**. A chiral ligand in combination with Cu^I and O_2 was used for the formation of a chiral Cu-O_2 intermediate, which was proposed to oxygenate an external substrate enantioselectively. The stoichiometric oxygenation of thioanisole was observed. However, enantiomeric ratios (er´s) of only 52:48 were reached. Studying the intermediates involved in this reaction helped understand how ligand design, i.e. chelate ring size, dictates if an intramolecular or intermolecular oxygenation occurs. This knowledge can be applied in the design of novel ligands for Cu complexes in the future.

In **Chapter 3.2** the second approach, enantioselective intramolecular oxygenations with chiral directing groups, is described. Using Cu^I in combination with O_2 resulted in the isolation of (*R*)-1-acetyladamant-2-ol with er´s up to >99:1 and yields up to 37%. The product represents a rare example of enantiopure 1,2-difunctionalized adamantanes which have potential pharmaceutical applications. Low-temperature stopped-flow UV-vis studies revealed that the reaction proceeds via a Cu^{III} bis(μ-oxido) intermediate. In contrast, using Cu^{II} in combination with H_2O_2 resulted in lower er´s of 72:28, but higher yields of up to 63%. This study demonstrates that Cu-mediated oxygenations with the green oxidants O_2 and H_2O_2 can be carried out enantioselectively. The knowledge gained on the important parameters that influence the yield and er in such reactions, e.g. choice of directing group and oxidative conditions, can be used in the future for the development of a catalytic variant of the reaction.

Zusammenfassung

Stereoselektive Oxygenierungen spielen in der chemischen und pharmazeutischen Industrie eine entscheidende Rolle, da die biologische Aktivität einer Verbindung durch ein einzelnes stereogenes Zentrum bestimmt werden kann. Solche Oxygenierungen mit O_2 oder H_2O_2 als Oxidationsmittel wären aus ökologischer Perspektive wünschenswert, da diese die höchste O-Atomökonomie aufweisen und H_2O bzw. H_2O_2 als einzige Nebenprodukte bilden. Um die Selektivität von Oxygenierungen zu steuern, sind jedoch geeignete Katalysatoren erforderlich. Für die Entwicklung solcher Katalysatoren ist ein biomimetischer Ansatz auf Basis von Cu-Enzymen vielversprechend, da diese unter milden Bedingungen katalytische und stereoselektive Oxygenierungen durchführen und O_2 bzw. H_2O_2 als Oxidationsmittel nutzen. Diese Forschung konzentriert sich daher auf die Entwicklung Cu-mediierter enantioselektiver Oxygenierungen, unter Verwendung von O_2 und H_2O_2 als Oxidationsmittel, basierend auf den Erkenntnissen aus enzymatischen Modellen.

Der erste Ansatz zur Erreichung enantioselektiver Cu-mediierter Oxygenierungen wird in **Kapitel 3.1** beschrieben. Ein chiraler Ligand in Kombination mit Cu^I und O_2 wurde zur Bildung eines chiralen Cu-O_2-Intermediats verwendet, von dem angenommen wurde, dass es ein externes Substrat enantioselektiv oxygenieren kann. Die stöchiometrische Oxygenierung von Thioanisol wurde beobachtet. Allerdings wurden Enantiomerenverhältnisse von lediglich 52:48 erreicht. Die Untersuchung der zugrunde liegenden Intermediate half zu verstehen, wie das Liganden-Design, in diesem Fall die Chelat-Ringgröße, bestimmt, ob eine intramolekulare oder intermolekulare Oxygenierung auftritt. Dieses Wissen kann in der Zukunft beim Design neuartiger Liganden für Cu-Komplexe angewendet werden.

In **Kapitel 3.2** wird der zweite Ansatz, die enantioselektiven intramolekularen Oxygenierungen mit chiralen dirigierenden Gruppen, beschrieben. Die Verwendung von Cu^I in Kombination mit O_2 führte zur Isolierung von (*R*)-1-Acetyladamant-2-ol mit einem Enantiomerenverhältnis von bis zu >99:1 und einer Ausbeute von bis zu 37%. Das Produkt stellt ein seltenes Beispiel enantiomerenreiner 1,2-difunktionalisierter Adamantane dar, welche potenziell pharmazeutische Anwendungen haben. Mittels Tief-Temperatur Stopped-Flow UV-vis Spektroskopie konnte gezeigt werden, dass die Reaktion über ein Cu^{III} bis(μ-oxido) Intermediat verläuft. Im Gegensatz dazu führte die Verwendung von Cu^{II} in Kombination mit H_2O_2 zu einem niedrigeren Enantiomerenverhältnis von 72:28, aber

höheren Ausbeuten von bis zu 63%. Diese Arbeit zeigt, dass Cu-mediierte Oxygenierungen mit den grünen Oxidationsmitteln O_2 und H_2O_2 enantioselektiv durchführbar sind. Die gewonnenen Erkenntnisse über die wichtigen Parameter, welche die Ausbeuten und Enantiomerenverhältnisse beeinflussen, z.B. die Wahl der dirigierenden Gruppe bzw. der oxidativen Bedingungen, können künftig für die Entwicklung einer katalytischen Variante der Reaktion genutzt werden.

Table of Contents

List of Abbreviations I

Abstract II

Zusammenfassung III

1 Introduction 1

1.1 Enantioselective Oxygenations as Key Technology 1

1.2 Copper Enzymes 3

1.2.1 Type I Copper Enzymes 4

1.2.2 Type II Copper Enzymes 5

1.2.3 Type III Copper Enzymes 7

1.2.4 Lytic Polysaccharide Monooxygenases 8

1.3 Copper Dioxygen Adducts 9

1.4 (Per-)Oxygenases as Biomimetic Models 15

2 Research Goals 21

2.1 Intermolecular Oxygenations 21

2.2 Intramolecular Oxygenations 22

3 Publications 24

3.1 Copper Mediated Intramolecular vs. Intermolecular Oxygenations: The Spacer makes the Difference! 24

3.2 Expanding the Clip-and-Cleave Concept: Approaching Enantioselective C−H Hydroxylations by Copper Imine Complexes Using O_2 and H_2O_2 as Oxidants 32

4 References 45

1 Introduction

1.1 Enantioselective Oxygenations as Key Technology

Oxidations and oxygenations are among the most industrially relevant reaction types and make up 20% of all processes in the chemical industry value chain, which equals approximately 600 million tonnes of chemicals produced via oxidation and oxygenation reactions annually.[1] These reactions are mainly used for the functionalization of hydrocarbons to form more useful synthetic building blocks or functional materials.[1] Thus far oxidations and oxygenations are often carried out using oxidants such as HNO_3, H_2SO_4, Cl_2, CrO_3, and H_2O_2, of which the first four produce toxic waste.[2] It would be much more desirable to use O_2 gas as the greenest and cheapest available oxidant[2] or H_2O_2, which produces only water as a by-product. Furthermore, H_2O_2 has better handling properties for industrial applications as an aqueous solution, compared to O_2.[3] Using O_2 as an oxidant can also be economically viable in large-scale productions when an annual production of 10^4-10^5 tonnes is surpassed, depending on the product.[2] An example of such a historically relevant industrial oxidation using O_2 as an oxidant is the Wacker-Hoechst process for the production of acetaldehyde from ethylene (**Scheme 1**).

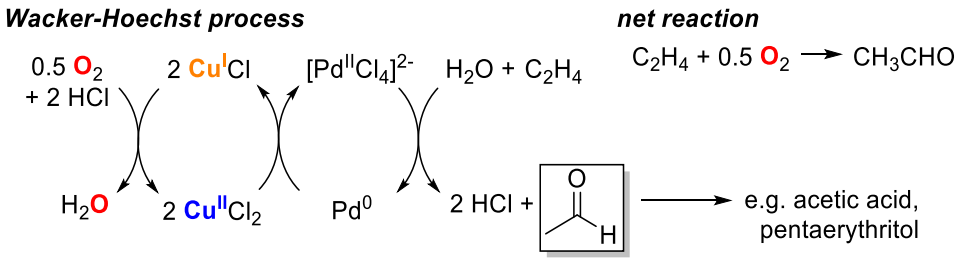

Scheme 1. Wacker-Hoechst process as an example of a historically relevant industrial oxygenation using O_2 as an oxidant.[4]

One class of such oxidation/oxygenation reactions is the direct functionalization of un-activated C–H bonds (C–H activation),[1] which are often relatively inert due to their high bond dissociation energy, e.g. 105.0 kcal/mol for methane.[5] However, such direct C–H activations carry a high economic and ecological potential in the large-scale production of more complex organic molecules, such as pharmaceuticals, food chemicals, and agricultural chemicals, since they can substitute traditional expensive multistep functionalizations that produce waste in each step.[1,6,7] A concise example is the production of pharmaceuticals in which up to 100 times more waste is generated than the target compound.[8]

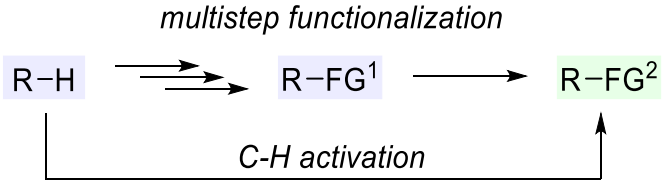

Scheme 2. Substitution of traditional multistep functionalizations (top) by C–H activation.[6] FG = functional group

Moreover, the modification of a single specific position of a molecule is often crucial for its biological activity.[9] Therefore, pharmaceutical research can utilize C–H activation for late-stage diversification of lead compounds.[9,10] This enables rapid screening of analogues, related to the lead compound, regarding their pharmacological activity.[9,10] Such a rapid diversification would give faster access to viable drug candidates and accelerate the upstream drug development process. Even though the toolbox of efficient C–H activation reactions is growing, they are often met with issues such as scalability, harsh conditions, or narrow substrate scopes, making it clear that further development is required.[9] Additionally, pharmaceutical production is highly reliant on enantiomerically pure compounds. Enantiomers are molecules that are not superimposable with their mirror image and biological activity can solely rely on a single stereogenic center. This is demonstrated by the thalidomide tragedy in the late 1950s and early 1960s.[11] Thalidomide was prescribed as a racemic mixture to pregnant women as a sedative. It was soon recognized that babies delivered by women who were given thalidomide during early pregnancy show a significant increase in congenital abnormalities[11] and later discovered that only (*R*)-thalidomide has sedative effects and that (*S*)-thalidomide acts teratogenic.[12,13]

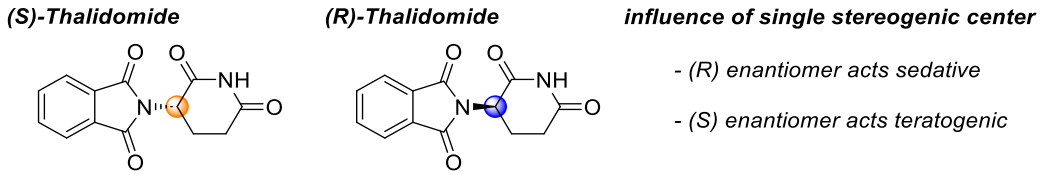

Scheme 3. (*S*)- and (*R*)-thalidomide and their effects.[12,13]

This event drove the development of enantiomerically pure pharmaceuticals, which is reflected in the fact that chiral drug approval increased from 58% to 75% between 1992 and 2006, and enantiopure compounds reached a global trade volume of 123 billion USD in 2000.[14] Furthermore, 6 out of the 15 worldwide most sold pharmaceuticals in 2017, i.e. $5-10 billion annual net sales each, are based on chiral synthetic compounds. [15] This underlines

the growing significance of enantioselective functionalizations for pharmaceutical production.[15]

In addition to the previously described problems, C–H activation reactions often use toxic and expensive precious metals, e.g. Pd, Ir, Rh, and Ru.[6,16] These could be substituted by Cu, which is not only able to activate O_2 and H_2O_2, but is also much cheaper and has a higher tolerable concentration in pharmaceuticals.[6] Ultimately, the development of Cu-mediated enantioselective oxygenations using O_2 or H_2O_2 as green oxidants would bring significant ecological and economic advantages to the chemical- and pharmaceutical industry. The best-performing O_2 activating catalysts known today are Fe- and Cu-containing enzymes, of which the latter will be discussed in the following chapter.

1.2 Copper Enzymes

Dioxygen usually does not react under ambient conditions with organic compounds, due to its triplet ground state, which makes the reaction with singlet ground state organic compounds spin-forbidden.[17] However, biological systems readily utilize O_2 as an oxidant for organic transformations by activation at metal centers, e.g. Fe and Cu-centers.[17] Enzymes with Cu in their active site serve multiple roles in biological systems such as binding, activation, reduction, and transport of O_2 and ultimately oxidation or oxygenation of bioactive compounds (oxidases and oxygenases).[18] These biological processes are mediated by the Cu^{II}/Cu^{I} redox pair.[19] The inner sphere activation of O_2 in biological systems is accomplished by the formation of so-called "*copper dioxygen adducts*" (CDAs) in the active sites.[20,21]

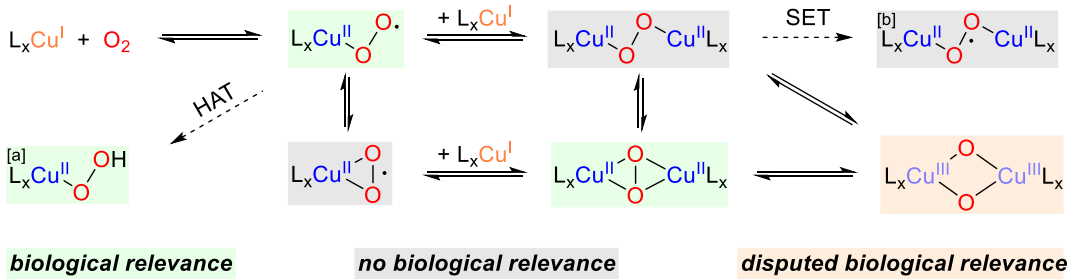

Scheme 4. Examples of mono- and dinuclear copper dioxygen adducts and potential equilibria.[22] [a]forms from a copper dioxygen intermediate by hydrogen atom transfer (HAT); [b]forms from a copper dioxygen adduct by single electron transfer (SET).[23]

Numerous such intermediates are known today, but only a few have been found in biological systems (**Scheme 4**).[20,21] The properties and reactivity of the intermediates will be discussed

in more detail in **Chapter 1.3**. Historically, Cu-containing enzymes were classified into three types based on the coordination sphere around the Cu-center and their UV-vis and electron paramagnetic resonance (EPR) features.[18]

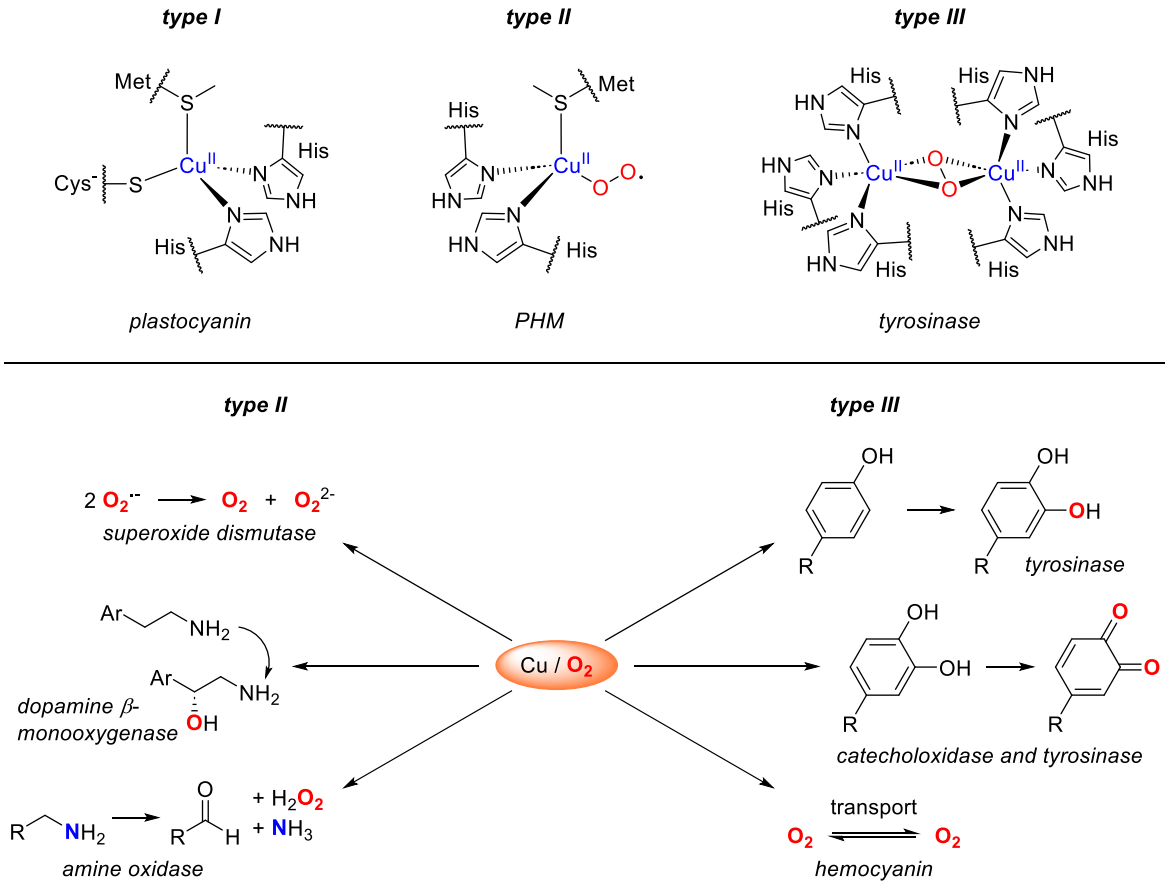

Scheme 5. Examples of coordination spheres of type I (plastocyanin)[24], type II (peptidylglycin α-hydroxylating monooxygenase, PHM)[25], and type III (tyrosinase)[26] copper enzymes and typical transformations catalyzed by type II and type III copper enzymes.[18] Active centers are shown in oxidized form.

Crystallographic and spectroscopic advances allowed the classification of new types of Cu enzymes i.e., seven in total today, but only the traditional three types[18] and a recently discovered class of Cu enzymes, the lytic polysaccharide monooxygenases (LPMOs),[27] will be briefly outlined in the following.

1.2.1 Type I Copper Enzymes

Type I Cu enzymes possess a characteristic cysteine thiolate coordination to the Cu-center that causes an intense ligand to metal charge transfer (LMCT) in the oxidized state and a deep blue colour of the enzyme,[28] which is why this type of enzyme is often referred to as

"*blue copper proteins*".[18] Furthermore, the Cu-center is coordinated by two histidine and one methionine ligand, usually in a tetrahedral coordination sphere.[18] In some cases, e.g. in azurin, an additional weakly coordinated peptide carbonyl from the enzyme backbone is present, forming a trigonal bipyramidal coordination sphere.[29] Typical representatives of this type are plastocyanin (**Scheme 5**), azurin, and amicyanin.[18,24,29] Most type I Cu enzymes are oxidases responsible for outer sphere electron transfers between other enzymes.[19]

1.2.2 Type II Copper Enzymes

Type II Cu enzymes in their oxidized state have similar EPR features as regular Cu^{II} complexes, hence they are sometimes referred to as "*normal copper proteins*".[18] They possess a light blue colour in their oxidized form, which is caused by symmetry-forbidden d-d transitions and not by an LMCT as in type I Cu enzymes.[18] On the one hand, type II Cu enzymes demonstrate oxidase activity, e.g. superoxide dismutase (SOD),[30] which catalyzes the disproportionation of superoxides to dioxygen and peroxides or amine oxidase (AO), where O_2 is reduced to H_2O_2 and an amine is oxidized to an aldehyde (**Scheme 5**).[20,21] However, in the case of AO the carbonyl oxygen in the product aldehyde is not transferred from O_2, but from a cofactor in the enzyme, which is regenerated by transferring its electrons in the O_2 reduction process, hence oxidase and not oxygenase activity.[20,21] On the other hand, type II Cu enzymes are also known to show oxygenase activity (**Scheme 5**), such as stereoselective hydroxylations by peptidylglycin α-hydroxylating monooxygenase (PHM) or dopamine β-monooxygenase (DβM).[25,31] The stereoselective benzylic hydroxylation of dopamine to noradrenaline by DβM plays an important role in the physiological regulation of neurotransmitters.[20] Both PHM and DβM possess two Cu-centers, one coordinated by three histidine residues (Cu_H site) and one by two histidine and one methionine residue (Cu_M site), with a distance of 11 Å between them.[25] It is generally accepted that the initial step of the reaction is the formation of a Cu^{II} end-on superoxido complex (**^{E}S**) at the Cu_M site and the subsequent formation of a hydroperoxido (**Hp**) intermediate.[20,21] In contrast, the Cu_H site is believed to be responsible for electron tunneling to the Cu_M site to close the catalytic cycle.[32] While early kinetic isotope effect studies suggest that **Hp** formation occurs via hydrogen atom transfer (HAT) by the superoxide intermediate (**Scheme 6**),[33] computational studies indicate that different pathways are possible.[34] The subsequent steps leading to hydroxylation allow various radical recombination scenarios involving for example Cu oxyl

(**Cp**) species, leading to five mechanistic scenarios that are currently debated.[20] However, it was recently demonstrated that DβM has a dimeric active site in an open form (Cu_H–Cu_M = 14 Å) and a closed form (Cu_H–Cu_M = 4-5 Å), which opened the debate around the involvement of dinuclear intermediates in the catalytic cycle of PHM and DβM.[31]

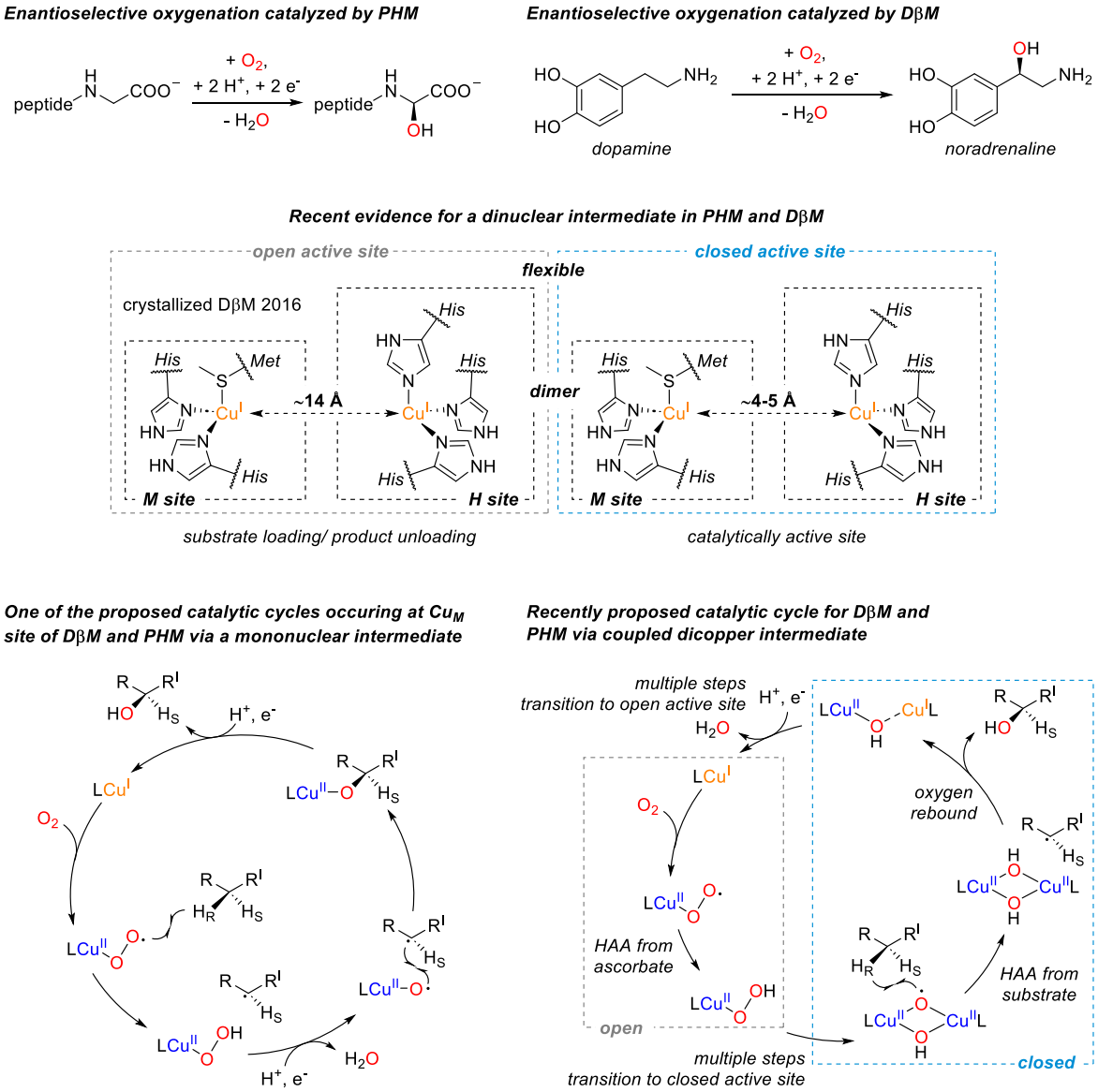

Scheme 6. General reaction scheme for the enantioselective oxygenations by PHM and DβM (top)[20]. Open and closed active sites of the DβM dimer based on the crystal structure reported by Vendelboe *et al.* in 2016 (middle).[31] Prosed reaction path of PHM and DβM via a mononuclear intermediate (bottom left) [25,35]. Proposed reaction path by Wu *et al.* involving a coupled dicopper intermediate (bottom right).[36]

Recent computational studies indicate that the open active site allows the entry of the co-substrate ascorbate, which is involved in hydrogen atom abstraction (HAA) by the ^{E}**S** intermediate to ultimately form the **Hp** intermediate.[31,36] Facile transition into the closed active site is then proposed to allow the formation of the dinuclear reactive species (μ-O•)(μ-OH)$Cu^{II}Cu^{II}$ that ultimately performs the hydroxylation (**Scheme 6**).[36] The exact reaction mechanisms of PHM and DβM are still disputed and subject to current research.

1.2.3 Type III Copper Enzymes

Type III Cu enzymes have two Cu-centers in their active site which are coordinated by three histidine residues each.[26,37,38] The enzyme is EPR silent in its oxidized form, due to the antiferromagnetic coupling caused by the O_2 bridge between the Cu-centers (**Scheme 5**).[18] A prominent example of type III Cu enzymes is the O_2-transport protein hemocyanin, which substitutes the Fe-containing hemoglobin in the breathing mechanism of molluscs and arthropods.[37,39] However, besides O_2-transport type III Cu enzymes are also known to perform oxygenase and oxidase reactions.[39] Tyrosinase catalyzes the aerobic *ortho*-hydroxylation of tyrosine to the catechol L-DOPA and the subsequent aerobic oxidation to L-dopaquinone (**Scheme 5**).[39] The latter step is also catalyzed by the enzyme catechol oxidase and both enzymes are classified as polyphenol oxidases (PPOs).[39] In contrast to catechol oxidase, tyrosinase shows both oxygenase and oxidase activity. The described reactions are the initial steps of melanogenesis and are followed by the non-enzymatic polymerization of L-dopaquinone to melanin.[40] Melanins are pigments responsible for the brown colouration of eyes, skin, and hair, the browning of fruits and play a role in UV light protection of the skin and wound healing.[41,42] Various intermediates of the tyrosinase catalytic cycle have been crystallized and it starts at the reduced form of the enzyme by activation of dioxygen in the form of a side-on peroxido (^{S}**P**) complex (**Scheme 7**).[26] There is a consensus that the phenol hydroxylation proceeds by electrophilic aromatic substitution.[43] However, it is debated if the ^{S}**P** intermediate is performing the reactions, or if the ^{S}**P** is in equilibrium with a Cu^{III} bis(μ-oxido) (**O**) species, which ultimately accomplishes the hydroxylation.[21]

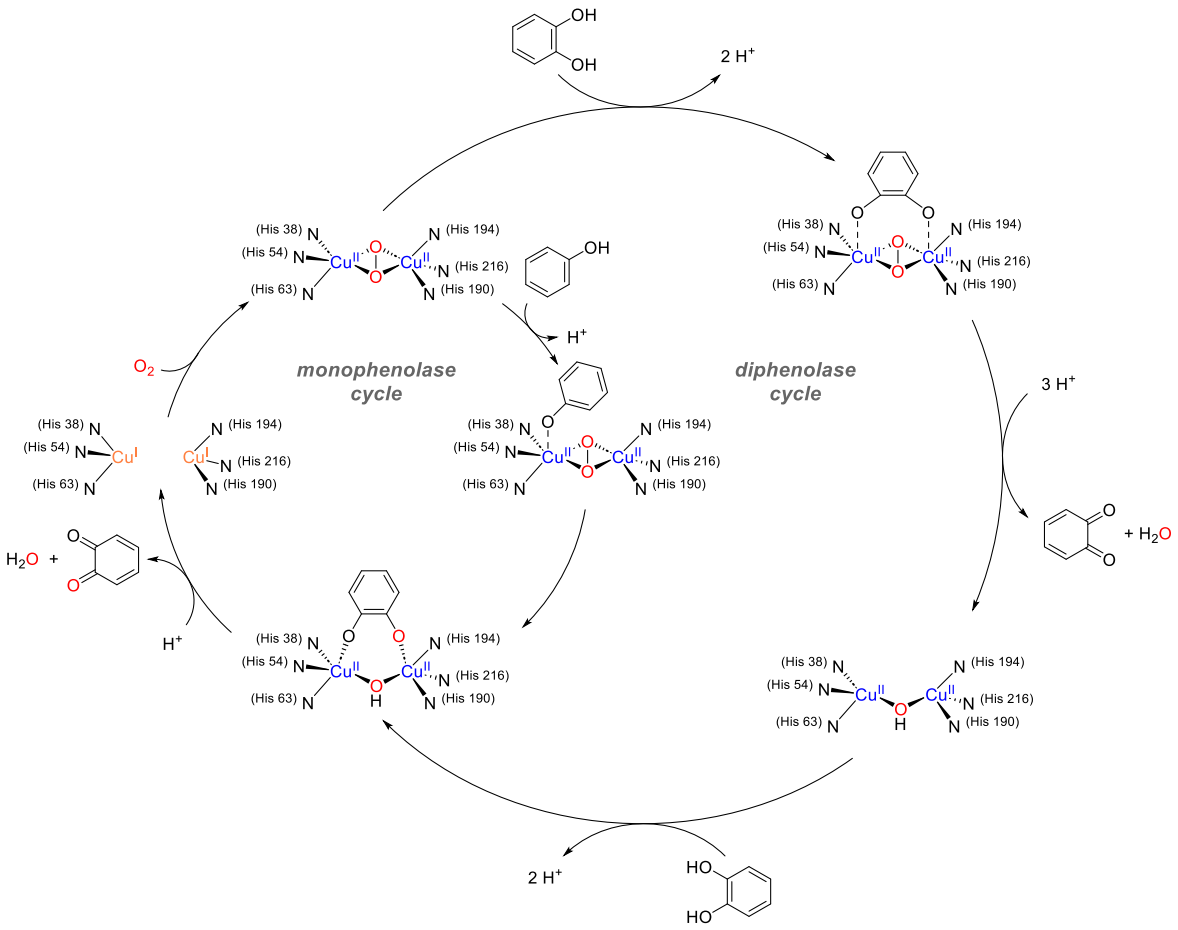

Scheme 7. Proposed mono- and diphenolase cycle of tyrosinase.[44] Nitrogen atoms belong to histidine residues and the numbers indicate the position of the residue in the enzyme starting from the N-terminus.

1.2.4 Lytic Polysaccharide Monooxygenases

The most recently discovered class of Cu-enzymes are the LPMOs, which are responsible for the oxidative cleavage of the glycosidic bonds in polysaccharides (**Scheme 8**).[45] LPMOs are distinct from the classic types of Cu-enzymes, because of a characteristic bis-chelating N-terminal histidine in the active site, referred to as the "*histidine brace*". The histidine brace possesses an N-methylated imidazole in some fungal LPMOs.[46] Together with a second coordinating histidine, a T-shaped coordination sphere is present in this enzyme class in its reduced form.[46] The exact mechanism is still debated and the presence of multiple subclasses of LPMOs could even result in varying mechanisms.[46] Originally, analogous pathways as proposed for PHM (**Scheme 6**) were suspected for LPMOs.[20,21] However, it was demonstrated that LPMOs can run their catalytic cycle under anaerobic conditions using H_2O_2 as an oxidant and that LPMOs are able to generate H_2O_2 in the absence of a

substrate.[47–50] Therefore, the most recent studies indicate that LPMOs generate H_2O_2 from O_2 in a cofactor-assisted process first and then activate H_2O_2 for the oxygenation of the C1 or C4 position of a polysaccharide unit.[50] Hence, its reactivity can be described as peroxygenase reactivity.[48,51] The cofactor is suspected to be ascorbate which reduces the resting state to start the catalytic cycle and assists the process by making HATs in various steps possible.[50]

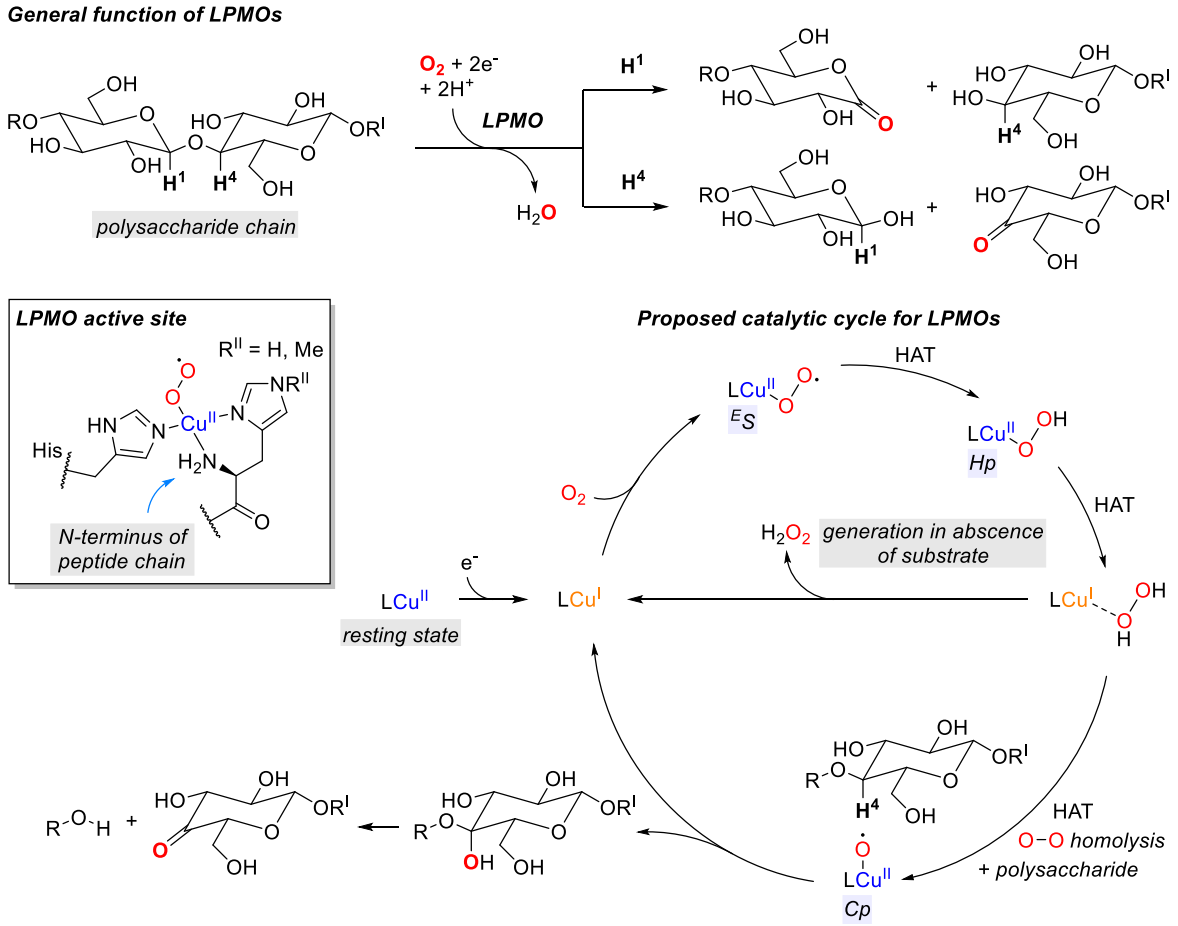

Scheme 8. General scheme of the glycosidic bond cleavage by LPMOs (top).[20] LPMO active site in its superoxide form (left).[52] Proposed catalytic cycle of LPMOs (right).[47,48,50]

1.3 Copper Dioxygen Adducts

As briefly indicated in the previous chapter, Cu activates O_2 and H_2O_2 by forming intermediates referred to as "*copper dioxygen adducts*" (CDAs). A plethora of model complexes have been studied to understand the mechanisms of dioxygen activation by Cu and ultimately the mechanisms behind enzymatic oxidations and oxygenations.[20–22,53,54] Nowadays, more CDAs are known than indicated in **Scheme 4** and **Table 1**,[55] but this chapter focuses only on the displayed examples.

Table 1. Examples of characteristic spectroscopic data of CDAs. The spectroscopic data listed was collected using the ligands below. All intermediates shown were confirmed by single crystal X-ray diffraction (SC-XRD).[23,56,57–59]

intermediate	name (abbreviation)	UV-vis λ / nm	Raman $\tilde{\upsilon}$ / cm^{-1} (Δ[$^{18}O_2$])	IR $\tilde{\upsilon}$ / cm^{-1}
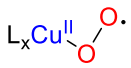	η^1-superoxido (***E*S**)	442, 690	1117 (58)	1122
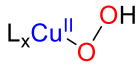	η^1-hydroperoxido (***Hp***)	375, 628, 819	861 (47)	/
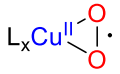	η^2-superoxido (***S*S**)	352	1111 (49)	1112
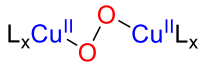	trans-μ-1,2-peroxido (***T*P**)	525, 615	832 (44)	/
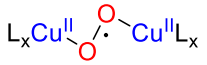	trans-μ-1,2-superoxido (***T*S**)	444	1073 (60)	/
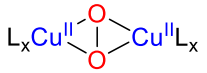	μ-η^2:η^2-peroxido (***S*P**)	338, 530	725 (39)	/
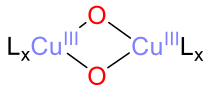	bis(μ-oxido) (***O***)	324, 448	600 (20)	/

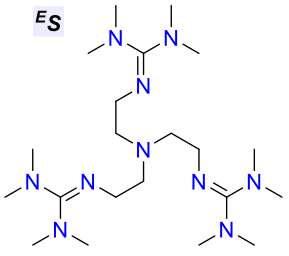

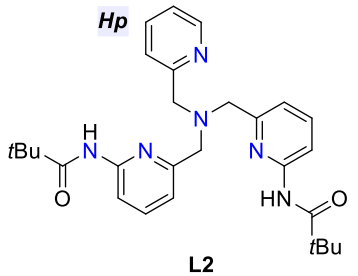

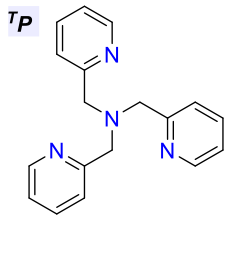

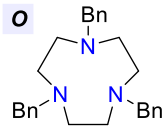

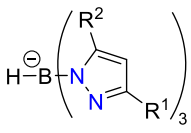

L5 $R^1 = R^2 =$ Me ***S*S**

L6 $R^1 = t$Bu; $R^2 =$ Me ***S*P**

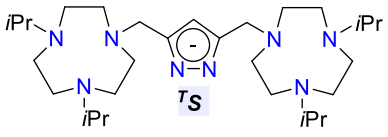

CDAs are often short-lived intermediates, but their lifetime can be increased at low temperatures (−80 °C to −135 °C) to make them spectroscopically detectable.[53,60,61] Low temperatures support the reaction by lowering the entropic cost of formation of a CDA from O_2 gas and attenuating the subsequent decomposition.[22] Although single crystal X-ray diffraction (SC-XRD) is the most precise method for the characterization of CDAs, multiple

diagnostic spectroscopic features have been found (**Table 1**), i.e. UV-vis, resonance Raman (rR), infrared (IR), X-ray absorption spectroscopy (XAS) and extended X-ray absorption fine structure (EXAFS) spectroscopy features.[22,53,54,60] These allow easier characterization without necessarily relying on the crystallization of such compounds. CDAs possess highly covalent Cu-O_2 bonds, resulting in a charge transfer (CT) that is diagnostic for most intermediates. Therefore, it is possible to differentiate between ^{T}**P**, ^{S}**P,** and **O** by UV-vis spectroscopy, despite them being isoelectronic.[22] In addition to UV-vis spectroscopy, rR spectroscopy can be used to confirm the intermediate, since the O-O vibration is indicative of the oxidation state of O_2.[22,54] Furthermore the Cu_2O_2 core vibration, Cu-O, and O-O vibration can be probed by using $^{18}O_2$ and measuring the shift of the Raman signal to lower wavenumbers in comparison to the signals resulting from $^{16}O_2$.[22,54] Mononuclear superoxido complexes can also be confirmed using IR spectroscopy.[57,59] XAS is used to probe the oxidation state of Cu, which has characteristic 1s→3d transitions for Cu^{I}, $Cu^{II,}$ and Cu^{III}.[22,54,62] For structural confirmation EXAFS can be used, by measuring the Cu···Cu and Cu-N/O interatomic distances, which are also diagnostic for the intermediates, e.g. the average Cu···Cu distance in the **O** core of 2.80 Å vs. the ^{S}**P** core of 3.51 Å.[22,54]

The first CDA to be characterized by SC-XRD was a ^{T}**P** complex by Karlin and co-workers in 1988.[63] They were using the ligand tris(2-pyridylmethyl)amine (tmpa, **L3**) and oxygenated its Cu^{I} complex at −85 °C.[63] Brief heating of the ^{T}**P** complex under vacuum results in O_2 de-coordination, which can be reversed by rechilling the solution followed by the introduction of O_2 gas (**Scheme 9**).[63] Later the **L3**-based ^{T}**P** complex was used for aerobic toluene oxygenations and was assigned a rather nucleophilic character.[64,65] Furthermore, the effect of the chelate ring size on CDA formation was studied by subsequently elongating the spacers between the N and pyridine in **L3** by one CH_2 group to afford ligands **L8** – **L10** (**Scheme 9**) and it was demonstrated that the chelate ring size alters the reaction significantly, e.g. the destabilization of the ^{E}**S** intermediate when **L8** was used or total diminishment of reactivity towards O_2 when **L10** was used.[66] In the decades after the discovery of the ^{T}**P** complex with **L3,** the improvement of low-temperature techniques for sample handling and spectroscopy led to the discovery and SC-XRD characterization of multiple CDAs using **L1** – **L7** (**Table 1**).[53,60] The mechanisms of formation and subsequent reaction of CDAs are determined by kinetic analyses often employing low-temperature stopped-flow techniques, which allow the rapid detection of short-lived intermediates and monitoring the temporal evolution of their UV-vis signals.[53,60,67]

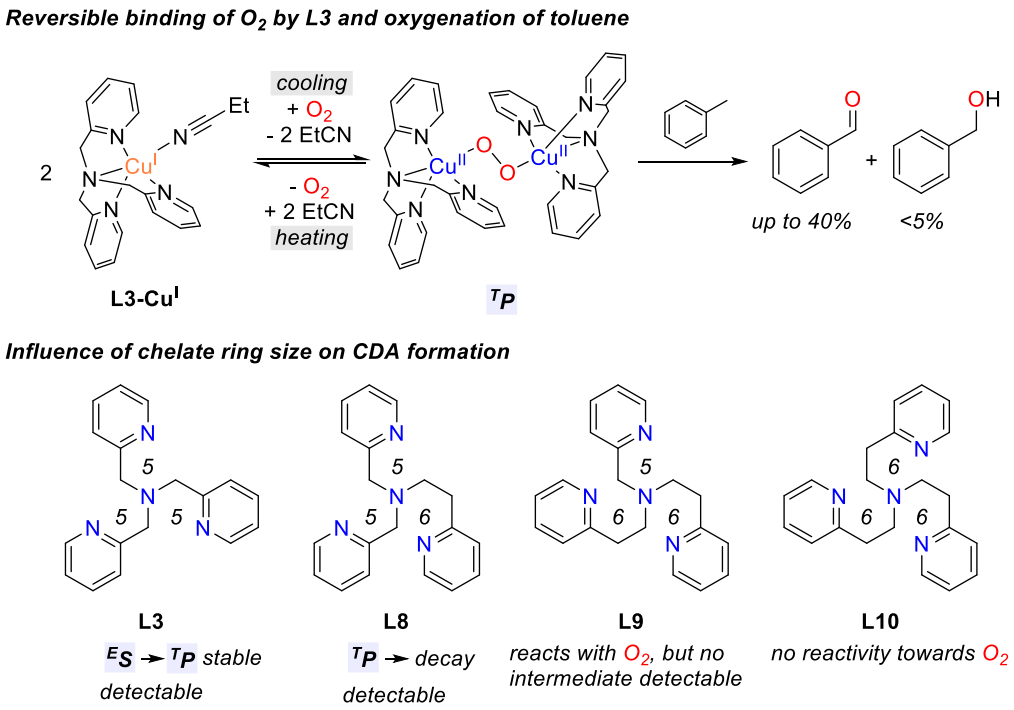

Scheme 9. Reversible dioxygen binding of the **L3**-Cu^{I} complex and oxygenation capability of the resulting ^{T}**P** complex (top).[63,64] Ligands that were used to study the effect of the chelate ring size on CDA formation (bottom).[66] Chelate ring sizes are indicated by the numbers in the ligands.

Typically, the formation of an ^{E}**S** intermediate is the rate-determining step (rds) followed by rapid dimerization to a dinuclear CDA, which often does not allow accumulation and spectroscopic detection of a mononuclear superoxido intermediate (**Scheme 10**).[53,60]

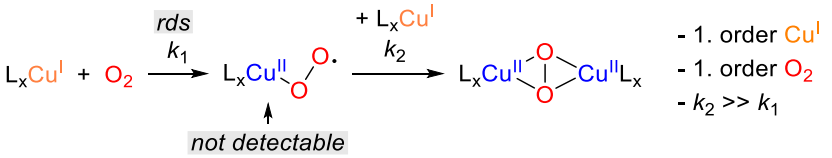

Scheme 10. Example of a kinetic scenario observed for the reaction of Cu^{I} with O_2.[53,60]

However, kinetic parameters, i.e. the reaction order of one with respect to Cu^{I} and O_2, are indicative of the initial formation of a mononuclear superoxido complex prior to dimerization.[53,60] Anyhow, other kinetic scenarios, in which superoxido intermediates are detectable or in which subsequent dimerization is rate determining, are possible, but will not be discussed in detail in this work.[68–70] Which CDA is formed predominantly depends on various ligand parameters, such as denticity, chelate ring size, charge, and steric effects, but also on parameters such as temperature and solvent choice.[22]

The Cu^{I} precursor complexes have a $3d^{10}$ electronic configuration and their complex geometry is determined by steric factors of the ligand.[22] The most common coordination geometries for such precursor complexes are trigonal monopyramidal, square planar, T- and Y-shaped, or in some cases linear.[22] Tetrahedral Cu^{I} complexes are also common but often lack inner sphere oxygen activation capabilities, due to the required geometrical reorganization of the coordination sphere to open a vacancy for O_2 association.[22,29] However, tetrahedral complexes with labile ligands, e.g. MeCN or THF, are usually exceptions to this rule.[71] The CDAs resulting from O_2 activation are usually present as square pyramidal (^{S}**P** and **O** with tridentate ligands), square planar (**O** with bidentate ligands), or trigonal bypyramidal (^{E}**S** and ^{T}**P** with tetradentate ligands) complexes.[22] The denticity has a significant influence on which CDA is forming, e.g. tetradentate ligands almost exclusively form end-on species such as ^{T}**P** and ^{E}**S** complexes, due to the tendency of Cu^{II} to be five coordinated. In contrast, bidentate ligands almost only form **O** complexes, due to the inclination of Cu^{III} to be square planar.[22] Anyhow, there are exceptions such as Me_2tmpa, which is a tetradentate ligand and readily forms an **O** complex.[72]

Tolman and co-workers demonstrated in 1996 that ^{S}**P** complexes can be in equilibrium with **O** complexes using 1,4,7-triisopropyl-1,4,7-triazacyclononane (**L11**) and that the equilibrium is highly dependent on the solvent.[58] They observed that the **O** complex forms in THF and the ^{S}**P** complex in DCM (**Scheme 11**) and that the addition of the respective other solvent caused a shift in the equilibrium.[58] Furthermore, later studies found that the equilibrium is altered by ligand parameters, e.g. electron-rich ligands tend to stabilize the Cu^{III}-center and prefer the formation of **O** complexes and sterically bulky ligands rather form ^{S}**P** complexes, due to the greater Cu···Cu distance of ^{S}**P** complexes in comparison to **O** complexes.[22,54,73–75] Computational studies indicate that the ^{S}**P**/**O** equilibrium can be the rds followed by rapid oxygenation of a substrate by the resulting **O** complex in C–H activation reactions.[76] In such a scenario the ^{S}**P** complex would be spectroscopically observable, but the **O** complex would be the actual oxidizing species and not be spectroscopically observable due to rapid consumption in the C–H activation step.[76] This finding indicates that many oxygenations that were assigned to ^{S}**P** intermediates could in reality be performed by **O** intermediates instead, which brought up in the discussion of the potential role of **O** intermediates in nature.[21]

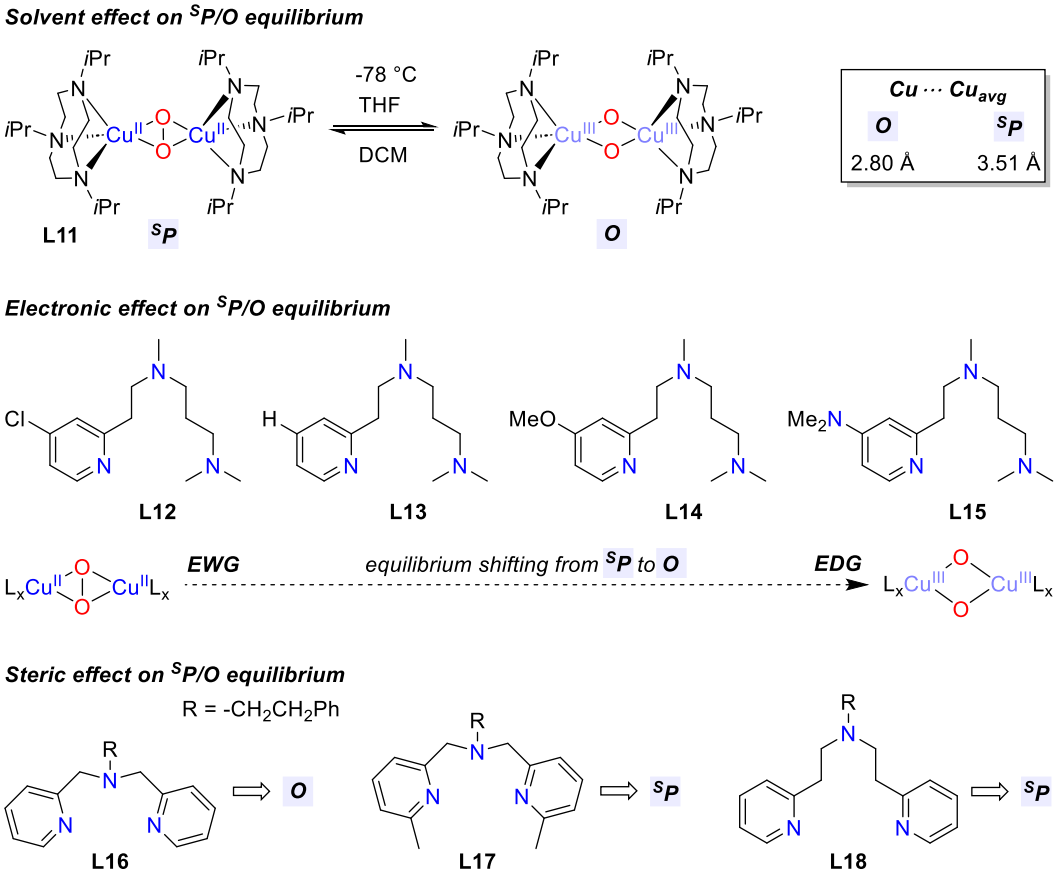

Scheme 11. Examples of parameters that are influencing the **^{S}P/O** equilibrium.[58,73–75]

Despite the problem of rapid dimerization of **^{E}S** intermediates, the crystallization and characterization of such a complex was achieved in 2006 by using the sterically bulky and superbasic ligand tris(tetramethylguanidino)tren (TMG$_3$tren, **L1**).[59] The resulting **^{E}S** complex showed reversible dioxygen binding as previously observed for the **^{T}P** complex with **L3**.[59,63] Furthermore, it was observed that the addition of an H atom source, e.g. 1-hydroxy-2,2,6,6-tetramethylpyperidine (TEMPO-H), causes the formation of a **Hp** intermediate that undergoes intramolecular ligand hydroxylation (**Scheme 12**).[77] This was also observed when the Cu^{II} complex with **L1** was used and H_2O_2 was added together with NEt_3.[77] It is thought to be reminiscent of a monooxygenase-like reaction, with reaction steps analogous to PHM.[77] The superoxide without an H atom source did not show such reactivity.[77] A recent study investigated the reaction of [Cu^{I}(**L1**)]$^{+}$ with anhydrous H_2O_2 ((*o*-Tol$_3$P=O · H_2O_2)$_2$) and found a different reaction path that leads to the same intramolecular ligand hydroxylation product (**Scheme 12**).[78] In contrast to the previous study, a peroxygenase-like reaction is proposed that follows a mechanism reminiscent of LPMOs.[78]

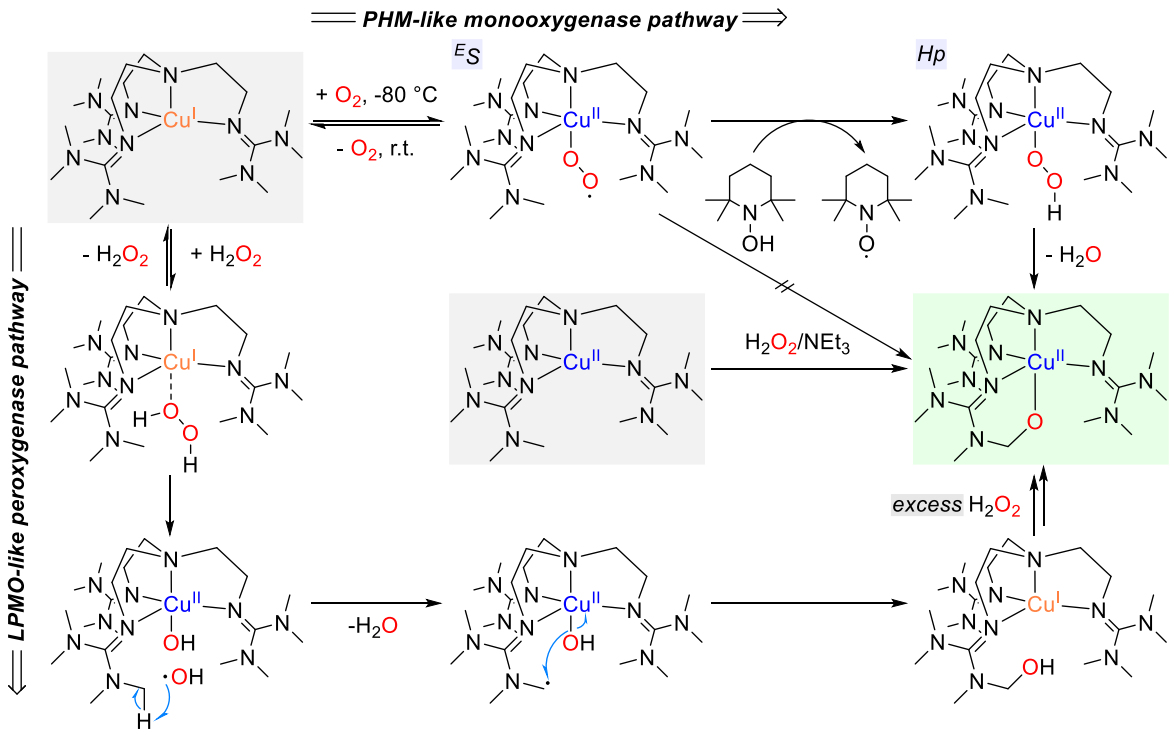

Scheme 12. Monooxygenase- and peroxygenase-like reaction pathways of **L1**-Cu complexes leading to intramolecular ligand hydroxylation ((*o*-Tol$_3$P=O · H$_2$O$_2$)$_2$ was used as anhydrous H$_2$O$_2$ source in the peroxygenase pathway).[59,77,78]

Using an excess of Cu^{I} complex resulted in the formation of hydroxylated ligand coordinated to Cu^{I} in an equivalent amount to the applied H$_2$O$_2$, demonstrating that Cu^{I} is regenerated during the hydroxylation.[78] The Cu^{II} complex of the hydroxylated ligand only formed when an excess of H$_2$O$_2$ was applied.[78]

1.4 (Per-)Oxygenases as Biomimetic Models

Originally, model complexes and CDAs were primarily studied to extrapolate the mechanistic insights onto enzymatic systems and gain indirect information on Cu-enzyme mechanisms. Nowadays, the knowledge gained about Cu-enzyme active sites is rather used as a model for the design of novel catalysts or oxygen mediators. The first example of a tyrosinase model system was reported by Karlin and co-workers in 1981.[79] They used *N*,*N*,*N*′,*N*′-tetrakis[2-(2-pyridyl)ethyl]-α,α′-diamino-*m*-xylene (*m*-xyl(py), **L19**), which possesses two tridentate ligand units bridged by a *m*-xylene group.[79,80] This ligand forms a dinuclear Cu^{I} complex that activates dioxygen via a ^{S}**P** intermediate and selectively hydroxylates the arene bridge,[81] which is why it is considered a tyrosinase model system. The scaffold has later been modified to a Schiff base ligand with two bidentate units bridged by an *m*-xylene group (**L20**), which also performs arene hydroxylation.[82] Kinetic studies

support a hydroxylation via a ^{S}**P** intermediate, but no such intermediate was spectroscopically detected for **L20**.[82] In 1999 Tolman and co-workers reported the selective hydroxylation of 2-(diethylaminoethyl)-6-phenylpyridine (PPN, **L21**), which is a ligand that kept the bidentate character as in **L20**, but substituted the *m*-xylene bridge by a pendant phenyl group.[83]

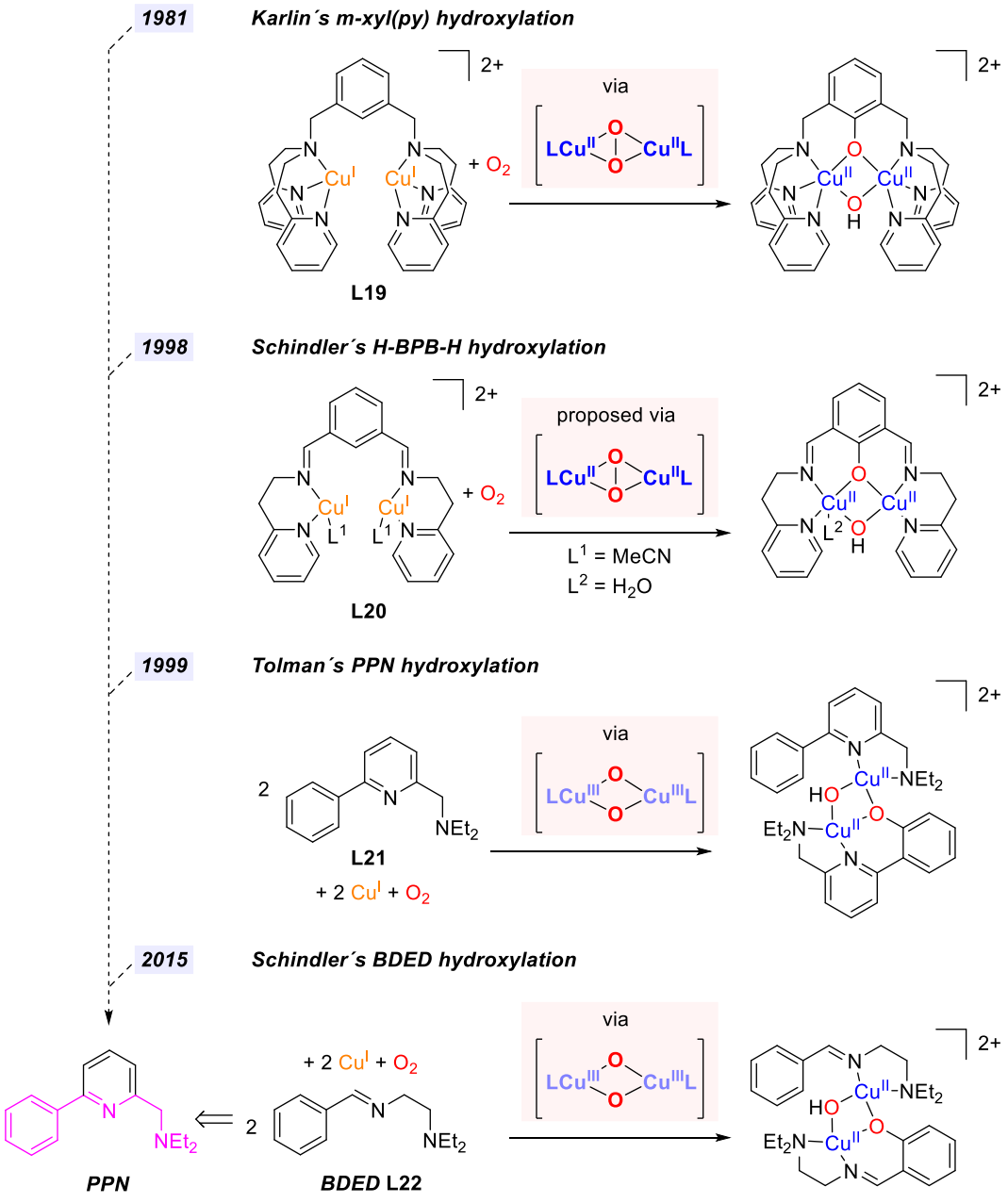

Scheme 13. Evolution of selected tyrosinase model systems.[79,82–84]

Therefore, **L21** does not pre-organize the Cu^{I} complex to form a dinuclear CDA, in contrast to **L19** and **L20**.[83] However, the key observation using **L21** was that the hydroxylation proceeds via an **O** intermediate.[83] These findings in combination with the previously

reported and in **Chapter 1.3** discussed low barrier ^{S}**P**/**O** equilibrium raised the question if the **O** intermediate is the active oxygenating species in tyrosinase instead of a ^{S}**P** intermediate.[83] This question is still debated in current research.[21] A detailed reinvestigation of the mechanism behind the hydroxylation of **L21** was published by Schindler and co-workers in 2015.[84] In this study, *N*`-benzylidene-*N*,*N*-diethylethylenediamine (BDED, **L22**) was reported, which possesses a scaffold that evolved from **L21** but is more easily accessible by a single-step imine condensation.[84] The hydroxylation of **L22** follows a similar mechanism as the hydroxylation of **L21**, also proceeding via an **O** intermediate.[84] The first example of a synthetic application of aerobic copper-mediated oxygenations using diamines as directing groups (DGs) on ketone substrates was published by Schönecker *et al.* in 2003.[85,86] They used 17-ketosteroids with 2-picolylamine to form bidentate Schiff base ligands, comparable to **L22**, that coordinate to $Cu^{I/II}$ and could be readily hydroxylated to diastereoselectively form 12β-hydroxy-17-ketosteroids. Yields up to 50% were reached, using dioxygen as an oxidant in the case of Cu^{I} and dioxygen and a reducing agent in the case of Cu^{II} (**Scheme 14**).[85,86] The reaction was significantly improved by Baran and co-workers in 2015 by the application of Na ascorbate as a reducing agent, ultimately reducing the reaction time to 1-6 h and increasing the yield to up to 94%.[87] The mechanism of the reaction was proposed to work via a dinuclear CDA,[86,87] a hypothesis supported by computational studies.[88] However, a detailed mechanistic study by Garcia-Bosch, Baran, and co-workers revealed that the formation of a **Hp** intermediate, which forms from H_2O_2 that is generated from O_2 by the Cu^{I} complex in a multistep process, is also possible.[89] Furthermore, they rationalized their findings by comparing their mechanism to key steps in the catalytic cycle of LPMOs, which could be similar due to the similar coordination sphere around the Cu-center (histidine brace in LPMOs vs. their bidentate ligands).[90] The reaction conditions were adjusted based on the mechanistic proposal, thus Cu^{II} and H_2O_2 could be used directly, making initial anaerobic preparations with anhydrous degassed solvent redundant and thereby increasing the practicability of the reaction.[89] It was recognized that the accessibility of substrate ligands by simple imine condensation allows potential synthetic application of aerobic hydroxylations on various aldehyde and ketone substrates.[91–93] This idea was pursued by the Schindler group and Garcia-Bosch group and the resulting concept was termed the clip-and-cleave concept (**Scheme 15**).[84,89,91–93]

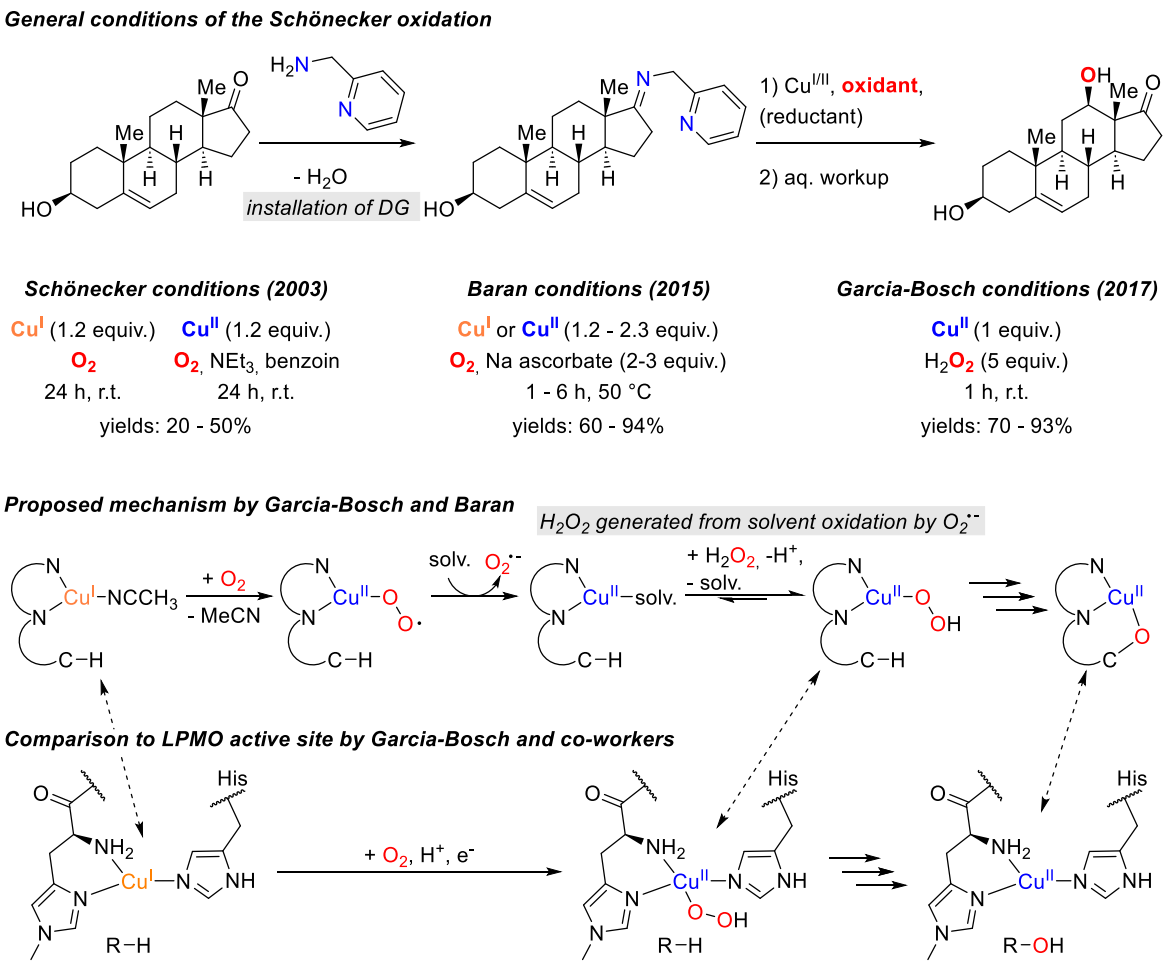

Scheme 14. General conditions of the Schönecker oxidation with dehydro-epi-androsterone as exemplary substrate and conditions applied by Schönecker, Baran, and Garcia-Bosch (yields vary between substrates).[85–87,89] Proposed mechanism for the Schönecker oxidation[89] and comparison of the mechanism to intermediates in LPMOs.[90]

Garcia-Bosch and co-workers additionally established the use of Cu^{I} and H_2O_2 in benzophenone hydroxylation as a third oxidative condition, besides the original Cu^{I}/O_2 and Cu^{II}/H_2O_2 conditions.[92] These conditions were previously not considered for regioselective hydroxylations, since Cu^{I} in combination with H_2O_2 potentially generates unselective hydroxyl radicals.[94]

General scheme of the clip-and-cleave concept

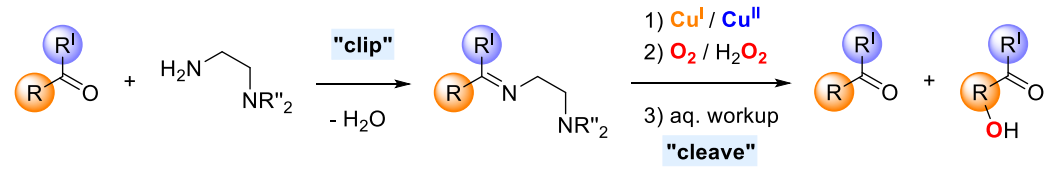

Products from sp^2 and sp^3 hydroxylations by clip-and-cleave reactions

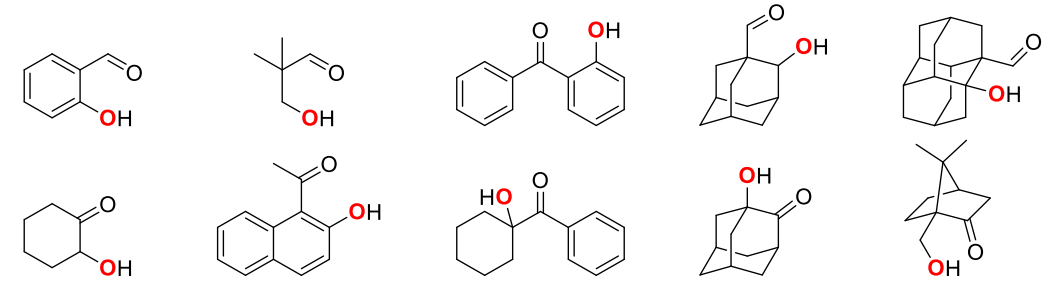

Scheme 15. General scheme of the clip-and-cleave concept (top). Exemplary hydroxylation products generated by clip-and-cleave reactions.[84,89,91–93]

Furthermore, Specht *et al.* found a third path for copper-mediated intramolecular ligand hydroxylations, besides hydroxylation via dinuclear or mononuclear CDAs, using Cu^{II}/O_2.[93] This path follows a dioxygen-mediated series of electron transfers between the ligand and copper ultimately opening the ligand for nucleophilic attack by water to yield the hydroxylation product (**Scheme 16**).[93] This mechanism has previously been reported by Schindler and co-workers.[95] However, this path has not been studied in detail yet and has no practical use in clip-and-cleave chemistry so far.

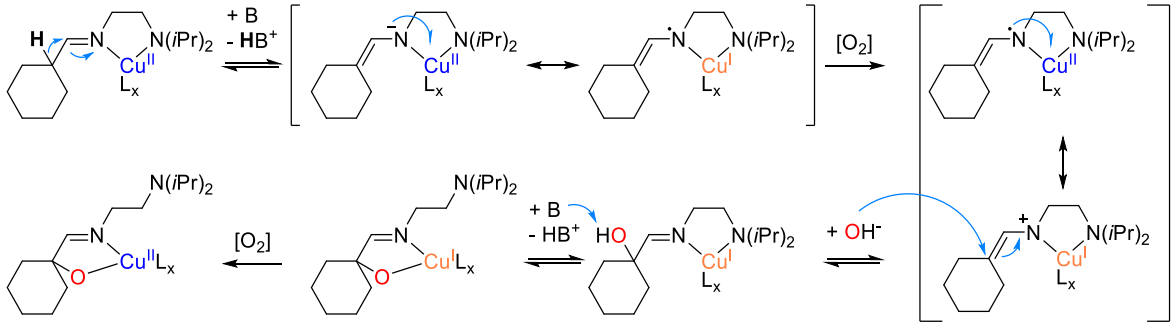

Scheme 16. Proposed mechanism for the hydroxylation of cyclohexanecarboxaldehyde using Cu^{II}/O_2.[93]

Various aliphatic and aromatic substrates were regioselectively hydroxylated, but reliable structure reactivity relationships, which determine the intermediate responsible for the hydroxylation and allow the rational choice of optimal oxidative conditions, are still elusive.[84,89–93] As a concise example, benzaldehyde is hydroxylated via an **O** complex, but the structurally related benzophenone is hydroxylated via a **Hp** intermediate.[84,92] As a key

problem in Cu^{I}-based hydroxylations, the formation of homoleptic 2:1 [L:Cu] complexes, which are either unreactive towards O_2 or only perform outer sphere oxidation of the Cu ion, was determined.[93] To overcome this problem two concepts have been attempted (**Scheme 17**).

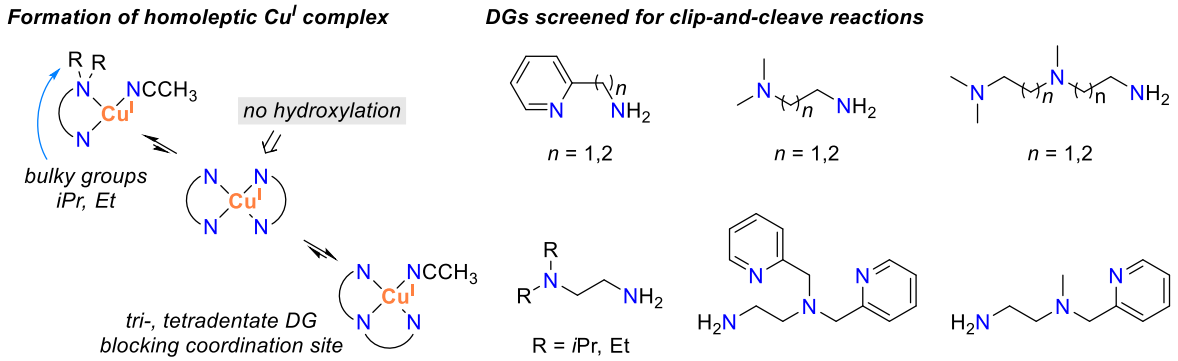

Scheme 17. Formation of the unproductive 2:1 [L:Cu] complex (left). DGs that have been screened for clip-and-cleave reactions.[90,93]

On the one hand, DGs with bulky *N*-substituents, i.e. iPr or Et, were used to sterically hinder the formation of the 2:1 [L:Cu] complex.[93] This concept was demonstrated to be successful in benzaldehyde and cyclohexanone hydroxylations.[93] On the other hand, the use of tri- and tetradentate DGs was attempted to block the coordination sphere of the Cu ion and only allow the coordination of small monodentate ligands, e.g. O_2 or H_2O_2.[90,93] This concept was counterproductive and in the best case, only low yields were obtained.[90,93] Furthermore, the screening revealed that ligands that form six-membered chelate rings often give lower yields in intramolecular ligand hydroxylations.[90,93]

All in all, it has been demonstrated that the clip-and-cleave concept is applicable to complex synthetic problems and useful organic transformations, e.g. steroid or adamantane hydroxylations, using the green oxidants O_2 and H_2O_2.[87,91,92] However, the herein presented key publications demonstrate that the outcome of clip-and-cleave reactions cannot be rationalized by a single factor. It is determined by a combination of multiple factors, mainly substrate choice, DG choice, and oxidative conditions, i.e. Cu^{I}/O_2, Cu^{I}/H_2O_2, or Cu^{II}/H_2O_2. Additionally, a key problem remains the use of stoichiometric amounts of DG and Cu to perform the hydroxylations in high yields, which need to be reduced to catalytic amounts to make the clip-and-cleave concept truly sustainable. Therefore, more research in this field is required to make clip-and-cleave a viable class of predictable lab scale or even industrial oxygenations with green oxidants, i.e. O_2 and H_2O_2, in the future.

2 Research Goals

The significant role of oxidation and oxygenation reactions in the chemical and pharmaceutical industry, e.g. for chemical feedstock production and late-stage diversification of bioactive compounds, was outlined in **Chapter 1.1**. The greenest oxidants with the highest O atom economy are O_2 and H_2O_2. Therefore, substituting common oxidants, such as HNO_3, H_2SO_4, CrO_3, or Cl_2, in industrial oxygenations by O_2 and H_2O_2 would be desirable to reduce waste in large-scale productions. Furthermore, the importance of chirality in bioactive compounds was briefly discussed. For the development of enantioselective oxygenations using O_2 and H_2O_2 as oxidants, a biomimetic approach based on Cu-enzymes is very promising. Biological Cu-enzyme-based aerobic oxidations and oxygenations are chemo-, regio- and stereoselective, catalytic, work under ambient conditions, and only produce H_2O or H_2O_2 as by-products. In addition, Cu has a comparatively high tolerable concentration in pharmaceuticals.

The Schönecker oxidation and the clip-and-cleave concept are concise examples that Cu-mediated oxygenations with O_2 and H_2O_2 as oxidants have the potential to perform challenging organic transformations and yield valuable products, e.g. diastereomerically pure 12β-hydroxy-17-ketosteroids or 1,2-disubstituted adamantanes. However, the stereoselectivity of the Schönecker oxidation is determined by the chiral steroid substrate. An enantioselective variant of the clip-and-cleave concept to hydroxylate achiral substrates is still elusive. Therefore, the goal of this work is the development of enantioselective Cu-mediated oxygenations with O_2 and H_2O_2 as oxidants. Two approaches were considered (intermolecular vs. intramolecular oxygenations).

2.1 Intermolecular Oxygenations

The first approach was the design of a chiral CDA that oxygenates an external substrate. An initial investigation of **L24** showed that it does not undergo intramolecular ligand hydroxylation, in contrast to the related ligand **L23** (**Scheme 18**). Therefore, the goal was a detailed investigation of the reaction of **L24** with $Cu^{I/II}$ and O_2 or H_2O_2, to see if it is a potential candidate for enantioselective intermolecular substrate oxygenations. The Cu^{I} complex of **L24** could stoichiometrically oxygenate thioanisole with O_2. A rather low enantiomeric ratio of 52:48 was obtained.

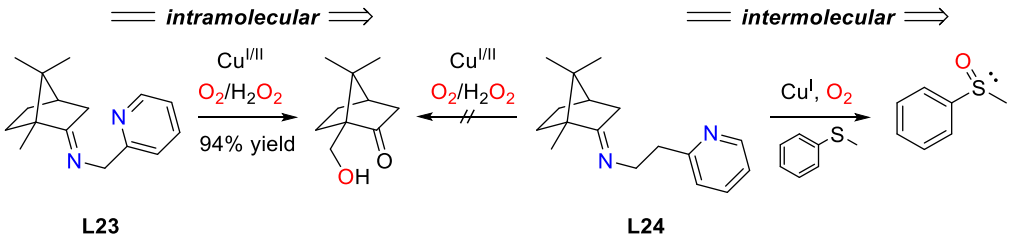

Scheme 18. Intramolecular oxygenation of **L23** vs. intermolecular oxygenation of thioanisole by **L24**.

However, the intermediates could be investigated in detail by low-temperature stopped-flow UV-vis spectroscopy, SC-XRD, $^{18}O_2$ labelling, and ESI-MS and were additionally supported by DFT computations. The findings help understanding how the ligand design influences whether Cu mediates an intermolecular or an intramolecular oxygenation. Details of this study are described in **Chapter 3.1** and have been published in *European Journal of Inorganic Chemistry*.

2.2 Intramolecular Oxygenations

The second approach was the development of an enantioselective variant of the clip-and-cleave concept. Chiral directing groups have been chosen by comparing the structural features of directing groups that were previously successfully applied in clip-and-cleave reactions (**Scheme 19**).

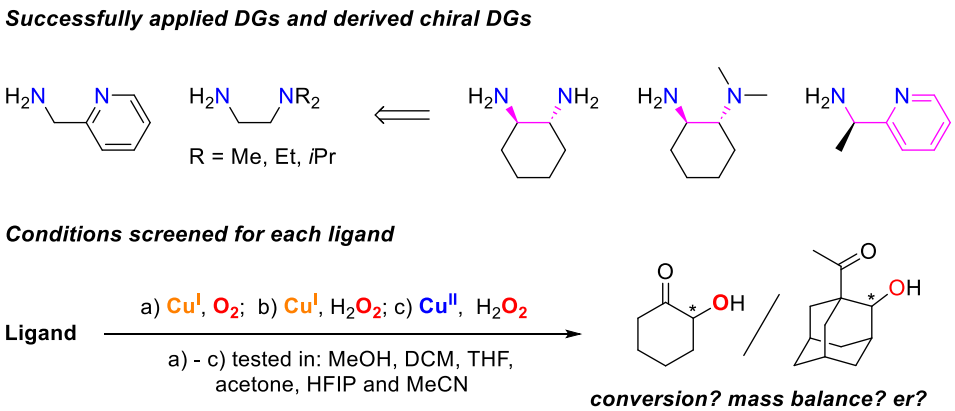

Scheme 19. DGs that were previously successfully applied and derived chiral DGs (top). Conditions screened for each ligand and hydroxylation products obtained (bottom).

Cyclohexanone was chosen as a test substrate for *proof of principle* since it was previously hydroxylated by application of the clip-and-cleave concept. To highlight the synthetic potential, 1-acetyladamantane was chosen as the second substrate. Enantioselective 1,2-

functionalizations of adamantanes are rare, but the products have potential pharmaceutical applications. Six different ligands were screened under various conditions (six solvents, Cu^{I}/O_2, Cu^{I}/H_2O_2, Cu^{II}/H_2O_2) and conversions and enantiomeric ratios were determined. It has been successfully demonstrated that the clip-and-cleave concept can be expanded to enantioselective reactions. The highlight of this study was the isolation of (*R*)-1-acetyl-2-adamantol with a yield of 37% and an enantiomeric ratio of >99:1. The mechanism behind the key reaction was studied in detail using low-temperature stopped-flow UV-vis spectroscopy and was further supported by DFT computations. Details of this study are described in **Chapter 3.2** and have been published in the *Journal of the American Chemical Society*.

3 Publications

3.1 Copper Mediated Intramolecular vs. Intermolecular Oxygenations: The Spacer makes the Difference!

This article has been published in

European Journal of Inorganic Chemistry

Alexander Petrillo, Alexander Hoffmann, Jonathan Becker, Sonja Herres-Pawlis and Siegfried Schindler

Eur. J. Inorg. Chem. **2022**, e202100970

https://doi.org/10.1002/ejic.202100970

EurJIC
European Journal of Inorganic Chemistry

Research Article
doi.org/10.1002/ejic.202100970

Chemistry Europe
European Chemical Societies Publishing

www.eurjic.org

Copper Mediated Intramolecular vs. Intermolecular Oxygenations: The Spacer makes the Difference!

Alexander Petrillo,[a] Alexander Hoffmann,[b] Jonathan Becker,[a] Sonja Herres-Pawlis,[b] and Siegfried Schindler*[a]

Copper complexes in combination with dioxygen are important as potential catalytic systems for regio- and stereoselective aerobic oxygenations of aromatic and aliphatic C–H bonds at ambient temperatures. In that context we herein describe a copper(I) complex with an imine ligand derived from (+)-camphor and 2-(2-aminoethyl)pyridine that forms a bis(μ-hydroxido) dicopper complex upon reaction with dioxygen at room temperature. It is detectable by UV-vis for several hours up to a few days, depending on the solvent and could be structurally characterized. In contrast to previous observations this complex rather oxygenates acetone or thioanisole as external substrates instead of undergoing an intramolecular ligand hydroxylation.

Introduction

Copper enzymes such as tyrosinase or dopamine-β-monoxygenase catalyze[1] reactions that are potentially highly desirable for chemical industry.[2,3] The active species responsible for these oxygenations often are investigated by applying model complexes which are usually short lived and often only accessible at low temperatures (around −80 °C).[4] So far only a few examples of copper "dioxygen adduct" species are known, which are persistent at room temperature for an extended time range.[5,6] Especially copper complexes with tetradentate and tridentate ligands have been investigated in that regard. They demonstrated a large influence of chelate ring size as well as substituents on nitrogen donor atoms on the reactivity of the complexes towards dioxygen.[7,8] Less reports have been published on complexes with bidentate ligands that tend to form either side-on peroxido or bis(μ-oxido) dicopper copper complexes. Groups by Itoh, Karlin, Tolman and Stack, as well as us, demonstrated the large influence of the ligand system with regard to the outcome of the reaction.[9,10]

Previously, Baran, Garcia-Bosch and co-workers successfully hydroxylated an aminomethylpyridine based imine ligand **1** in high yields (up to 94 %) according to Scheme 1.[11,12]

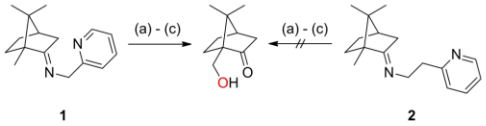

Scheme 1. (a) 1) 2.3 eq. $[Cu(MeCN)_4]PF_6$, 3 eq. Na ascorbate, acetone, 2) O_2, 50 °C, 6 h, 3) Na_4EDTA workup; (b) 1) 1.1 eq. $Cu(NO_3)_2 \cdot 3\,H_2O$, THF, 2) 15 eq. H_2O_2, 50 °C, 4.5 h, 3) Na_4EDTA workup; (c) 1) 1 eq. $[Cu(MeCN)_4]PF_6$, acetone, 2) 15 eq. H_2O_2, r.t., 4.5 h, 3) Na_4EDTA workup.

To compare reactivities we investigated the closely related copper system with literature known ligand **2** (Scheme 1)[13,14] at room temperature, which only differs by applying 2-(2-aminoethyl)pyridine instead of aminomethylpyridine. However, despite the minor difference in the ligand system, no intramolecular ligand γ-hydroxylation was observed with **2** (Figure S22–Figure S24).

Hydroxylation reactions of this type, a so called "clip and cleave" concept,[10,15,16] in general proceed either via copper hydroperoxido complexes or 2:1 copper dioxygen species (e.g. bis(μ-oxido) or μ-η^2:η^2-peroxido dicopper complexes) as key intermediates (Scheme 2), or via a dioxygen mediated series of electron transfers between the ligand and copper ultimately opening the ligand for nucleophilic attack by water to yield the hydroxylation product.[10,12,15,17] If such a reaction takes place and which path it takes is determined by very subtle structural and electronic changes in the ligand structure.[10,18]

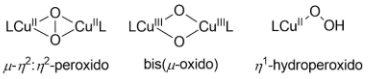

Scheme 2. Common intermediates in copper mediated ligand hydroxylations.

[a] *A. Petrillo, Dr. J. Becker, Prof. Dr. S. Schindler*
Institute of Inorganic and Analytical Chemistry
Justus-Liebig-University Giessen
Heinrich-Buff-Ring 17, 35392 Giessen, Germany
E-mail: siegfried.schindler@anorg.chemie.uni-giessen.de
https://www.uni-giessen.de/fbz/fb08/Inst/iaac/schindler
[b] *Dr. A. Hoffmann, Prof. Dr. S. Herres-Pawlis*
Institute of Inorganic Chemistry
RWTH Aachen University
Landoltweg 1a, 52074 Aachen, Germany
https://www.bioac.ac.rwth-aachen.de/go/id/ictk/

Supporting information for this article is available on the WWW under https://doi.org/10.1002/ejic.202100970

EurJIC
European Journal of Inorganic Chemistry

Research Article
doi.org/10.1002/ejic.202100970

Chemistry Europe
European Chemical Societies Publishing

Results and Discussion

To gain better insight into these reactions in general, we investigated the reaction of the copper complex with ligand **2** in more detail. Intriguingly, in contrast to most imines, ligand **2** resists hydrolysis during aqueous workup and could be crystallized in its protonated form under air (molecular structure and crystallographic data are reported in SI 3.5.6).

The 1:1 copper(I) complex of **2** crystallized as a dimer with two linear coordinated copper centers bridging two ligands (Figure 1). Similar molecular structures were reported e.g. by Specht *et al.* for a related ligand, where (+)-camphor is substituted by cyclohexanone, and by Ray and co-workers.[10,19] In contrast to our complexes, the copper(I) complexes of the methylene bridged ligand **1** and complexes of the related ligands by Specht *et al.* were crystallized as trigonal planar mono copper complexes with one acetonitrile ligand or as 2:1 ligand:copper ratio coordinated complexes.[12] Both species were detectable for copper complexes with ligand **2** as well by ESI-MS, indicating equilibria between the three copper(I) species (Figure S32). The $[Cu(\mathbf{2})_2]^+$ species is unreactive towards dioxygen (Figure S8), we therefore propose that this species plays no significant role during dioxygen activation. Despite several attempts to crystallize this copper(I) species, only the copper(II) analogue could be structurally characterized (SI 3.5.2). However, even though the dimer was the most prominent species in the ESI-MS spectrum, thorough NMR analysis confirmed that the mono acetonitrile coordinated species $[Cu(\mathbf{2})(MeCN)]PF_6$ is the preferred species in solution (Figure S14–Figure S21).

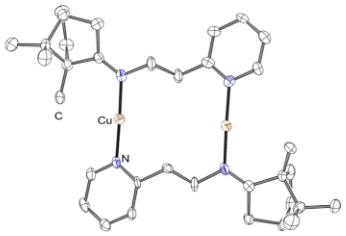

Figure 1. ORTEP Plot of the molecular structure of $[Cu_2(\mathbf{2})_2](PF_6)_2$. Anions and hydrogen atoms are omitted for clarity. Ellipsoids are drawn at 50% probability.

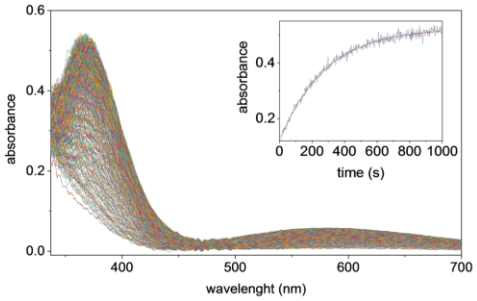

Figure 2. Time-resolved UV-vis spectra of the reaction of $[Cu(\mathbf{2})(MeCN)]PF_6$ ($4.7 \cdot 10^{-4}$ mol · L^{-1}) with dioxygen ($5.7 \cdot 10^{-3}$ mol · L^{-1})[3] in acetone at −7 °C over a period of 1000 s. The inset displays the time dependent change in absorbance at 365 nm (blue: experimental, red: exponential fit, first-order rate constant $k_{obs} = 3.6 \cdot 10^{-3}\,s^{-1}$).

Stopped-flow measurements in acetone (Figure 2) were carried out to investigate the reaction of $[Cu(\mathbf{2})(MeCN)]PF_6$ with dioxygen to detect the formation of reactive intermediates. No reactions were observed at low temperatures (−93 °C). Furthermore, oxygenation in acetonitrile afforded only a very slow color change to purple (within days) and no observable LMCT bands within hours. Stopped-flow measurements in acetone: MeCN (2.5% V/V MeCN) revealed a strong inhibition of the reaction by the presence of small amounts of MeCN. The significance of de-coordination of additional ligands (such as MeCN) during or prior to dioxygen activation has been thoroughly studied in the past.[20]

Time resolved UV-vis spectra were collected in acetone between −10 °C and +10 °C. Absorbance maxima were observed at 365 nm and at 570 nm, which would be the typical region for μ-η^2:η^2-peroxido dicopper complexes.[21] Furthermore, similar spectra were assigned to bis(μ-oxido) dicopper complexes in the past.[6,22] However, the product complex formed was stable enough to be crystallized and turned out to be the bis(μ-hydroxido) dicopper complex $[Cu_2(\mathbf{2})_2(\mu\text{-}OH)_2](PF_6)_2$ (Figure 3). We were able to confirm that the UV-vis spectrum can be assigned to the bis(μ-hydroxido) by isolation of the complex and the measurement of a UV-vis spectrum at room temperature. Additionally, DFT calculations (see below and SI 1.5) supported this assignment.

The crystallization of two conformers of the bis(μ-hydroxido) dicopper complex was achieved (Figure 3). The presence of such bis(μ-hydroxido) conformers in solution was supported by Ray and co-workers using helium tagging infrared photodissociation spectroscopy.[19] It is a common decomposition product of μ-η^2:η^2-peroxido and bis(μ-oxido) complexes and was also clearly detectable by ESI-MS (SI 3.4).[15,19,23]

Ray and co-workers recently reported the formation of a bis(μ-oxido) complex that subsequently reacts to a reactive bis(μ-hydroxido) with similar UV-vis features that we

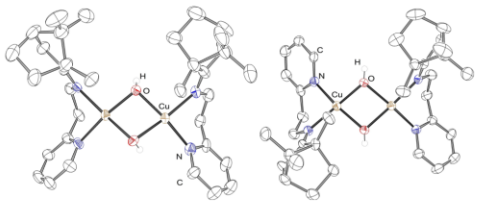

Figure 3. ORTEP Plots of the molecular structures of the C_1 and C_2 form of $[Cu_2(\mathbf{2})_2(\mu\text{-}OH)_2](PF_6)_2$. Anions and carbon bound hydrogen atoms are omitted for clarity. Ellipsoids are drawn at 50% probability.

EurJIC
European Journal of Inorganic Chemistry

Research Article
doi.org/10.1002/ejic.202100970

Chemistry Europe
European Chemical Societies Publishing

observed.[19] However, they could not crystallize their complex. In contrast we did not observe the formation of the presumed bis(μ-oxido) complex, but obtained instead a stable bis(μ-hydroxido) complex. The temperature range and the time of full formation of the band at 365 nm of approximately 1000 s (Figure 2) is quite exceptional for copper dioxygen species and demonstrates the high stability of the copper(I) complexes of **2**. It is known that copper(I) complexes can be stabilized by six membered chelate rings.[8,10] Furthermore, it was observed in the past that the bite angle of a ligand can determine which type of adduct forms.[24]

The observed adduct does not decompose significantly at room temperature (Figure 4a–d). It is even detectable by UV-vis in DCM for at least 5 d (Figure 4b). Considering that the copper(I) complexes of **1** undergo intramolecular hydroxylation via a copper hydroperoxido complex within hours, makes [Cu(**2**)(MeCN)]PF_6 an outstanding example for the influence of chelate ring size and bite angle on the reactivity of copper(I) complexes towards dioxygen.

Bis(μ-oxido) dicopper complexes are common intermediates for intramolecular ligand hydroxylations, which makes it particularly interesting how our "substrate" ligand forms copper dioxygen species without subsequent oxygenation.[10,15,16,25] Anyhow, the molecular structure of the bis(μ-hydroxido) complex reveals a γ-H···O distance of 2.34–2.50 Å, which could potentially be too far for an insertion of O into the C–H bond or even radical H abstraction, under the assumption that similar distances are present in the actual dioxygen adduct.

The temporal evolution of the absorbance at 365 nm (inset Figure 2) can be fitted by a single exponential function, indicating pseudo first order kinetics. Furthermore, kinetic measurements in dependency O_2 concentration confirmed the first order kinetics with respect to $c(O_2)$ leading to the overall rate law:

$$\frac{dc([Cu_2(\mathbf{2})_2(\mu{-}OH)_2](PF_6)_2)}{dt} = k \cdot c([Cu(\mathbf{2})(MeCN)]^+) \cdot c(O_2)$$

Thus, the initial formation of a 1:1 Cu:O_2 superoxido species should be representing the rate determining step followed by fast consecutive steps to the final product. Despite the small temperature range we calculated the activation parameters $\Delta H^{\neq} = +21.9 \pm 0.7\ kJ\,mol^{-1}$ and $\Delta S^{\neq} = -166 \pm 2\ J\,K^{-1}\,mol^{-1}$ from an Eyring plot (Figure S4; Table S2). The quite negative activation entropy is in line with an associative mechanism (substitution of MeCN) that also explains the suppression of the reaction if the concentration of MeCN is raised.

Density functional theory (DFT) calculations were performed to investigate the nature of the Cu_2O_2 species that forms prior to the bis(μ-hydroxido) complex and confirmed the overall reaction mechanism. The calculations reveal the bis(μ-oxido) species as favored by app. 9 kcal mol^{-1} over the peroxido species (Figure S10; Table S5). As the UV-vis spectrum together with the observation of no characteristic Cu_2O_2 modes in the Raman spectrum of this species indicates the formation of the

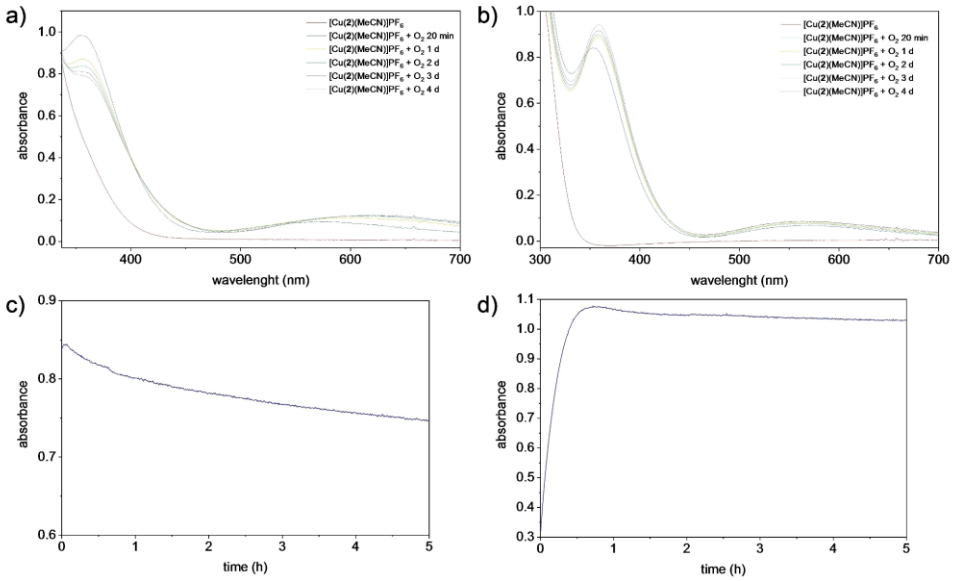

Figure 4. UV-vis spectra of the reaction of [Cu(**2**)(MeCN)]PF_6 with O_2 a) in acetone over 4 d and b) in DCM over 4 d; c) Time trace of the absorption at 365 nm in acetone; d) Time trace the absorption at 365 nm of the reaction in DCM.

EurJIC
European Journal of Inorganic Chemistry

Research Article
doi.org/10.1002/ejic.202100970

Chemistry Europe
European Chemical Societies Publishing

hydroxido species, it was also investigated via DFT calculations. The key parameters of the triplet hydroxido species (favored by 14.1 kcal/mol compared to the singlet hydroxido species; Table S6) agree very well with the bond length and angles determined by single crystal X-ray crystallography (Table S8). Furthermore, the time-dependent (TD) DFT UV-vis spectrum of the triplet hydroxido species corresponds to the experimental spectrum (Figure S13). Therefore, the bis(μ-hydroxido) most likely forms from a bis(μ-oxido) core by hydrogen atom abstraction from the acetone, as observed by Ray and co-workers.[19]

This was further confirmed by the formation of a dinuclear copper complex with an acetate and hydroxide bridge (Figure 5), upon oxygenation of [Cu(**2**)(MeCN)]PF_6 in acetone after a few days at room temperature (A species which was not observable by ESI-MS measurements). Furthermore, the bis(μ-hydroxido) must play a role in oxygen mediation during acetone oxidation, since it slowly decomposes in acetone, but not in DCM (Figure 4c, Figure 4d).

The molecular structure demonstrates that the dioxygen adduct is able to oxidize substrates after all. Acetic acid is a typical product from oxygenation of acetone to methyl glyoxal and subsequent oxidative decomposition.[26] Anyhow, this process seems to be very slow, which is why the acetate bridged complex was not observable by ESI-MS. The stability of the complex in DCM thus can be easily explained by the lack of the observed acetone oxidation.

Stereoselective oxygenations of prochiral substrates with dioxygen as oxidant are mostly carried out utilizing enzyme catalysis, which have the drawback of high substrate specificity and therefore relatively narrow substrate scope.[27] However, some non-enzymatic examples are known, but to the best of our knowledge no prochiral substrates were enantioselectively oxygenated applying copper dioxygen chemistry.[28] Thioanisole was chosen as a target substrate to test potential stereoselective oxygenations by $[Cu_2(\mathbf{2})_2(OH)_2]^{2+}$, since aryl sulfides are enantioselectively oxidizeable to their corresponding sulfoxides (Scheme 3).[29,30] Chiral sulfoxides are particularly interesting due to their biological activity, but this reaction is rather a proof of concept to demonstrate that copper "dioxygen adduct" complexes can be designed to be stereoselective oxygen mediators.[29,31]

Conversions up to 97% were achieved using one equivalent of the copper(I) complex, yielding almost exclusively the sulfoxide and ee's up to 4%. Furthermore, $^{18}O_2$ experiments revealed that dioxygen is the sole oxygen source for the oxygenation. Since the thioanisole oxidation is a 2 e^- process a conversion up to 50% (with respect to copper(I)) was expected. The higher conversion could indicate a catalytic reaction with two turnovers. However, attempts to run the reaction with catalytic amounts (5% and 10%) of copper(I) failed. Furthermore, considering the fact that the reactions have the best outcome in acetone and that the dioxygen complex clearly reacts with acetone (Figure 5), the direct oxygenation of thioanisole by the bis(μ-hydroxido) species, as observed by Ray and co-workers, seems likely. However, the *in situ* formation of H_2O_2 and formation of a copper hydroperoxido species as active oxidizing species, as observed by the Baran and Garcia-Bosch groups, cannot be completely excluded.[12,19] The presence of the bis(μ-hydroxido) complex in the C_2 and C_1 symmetric form (crystallographic characterization) in solution causes many possible transition states during oxygenation that most likely do not yield the same enantiomer, which could be a reason for the lack of enantioselectivity. Furthermore, the (+)-camphor moieties might not be sufficiently bulky to induce higher ee's for this type of reaction. Despite the low ee's this reaction proofs that with further optimization and according ligand design enantioselective oxygenations utilizing chiral copper dioxygen adducts as oxygen mediators could potentially be developed.

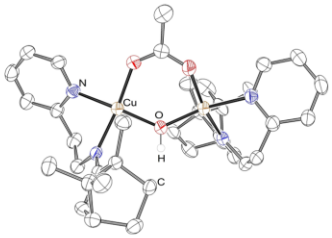

Figure 5. ORTEP Plot of the molecular structure of $[Cu_2(\mathbf{2})_2(\mu\text{-OAc})(\mu\text{-OH})](PF_6)_2$. Anions and carbon bound hydrogen atoms are omitted for clarity. Ellipsoids are drawn at 50% probability.

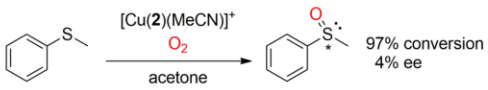

Scheme 3. Oxygenation of thioanisole to the chiral methyl phenyl sulfoxide.

Conclusion

Our observations are a concise example for the often observed stabilization of copper(I) complexes by six membered chelate rings, an effect that was previously elucidated.[8,10] However, such a dramatic effect of the chelate ring size on the ultimate reactivity of copper(I) towards dioxygen (hydroperoxido vs. bis(μ-oxido) and bis(μ-hydroxido)) was not expected here. The methyl bridged ligand readily undergoes intramolecular ligand hydroxylation in high yields (up to 94%) when reacted with copper(I) and O_2 or H_2O_2. Complexes of the ethyl bridged ligand on the other hand oxygenates the solvent rather than the γ-C–H bond and is able to selectively oxygenate thioanisole to its according sulfoxide.

Chiral copper dioxygen adducts are rare (only one has been crystallized so far).[32] Further investigations on simple chiral ligands are required for the development of useful enantioselective non-enzymatic oxygenations using dioxygen as oxidant and chiral copper(I) complexes as catalysts.

EurJIC
European Journal of Inorganic Chemistry

Research Article
doi.org/10.1002/ejic.202100970

Chemistry Europe
European Chemical Societies Publishing

Experimental Section

Materials and Methods: Solvents and reagents were purchased from common suppliers. $[Cu(MeCN)_4]PF_6$ and $[Cu(MeCN)_4]OTf$ were prepared according to literature procedures and stored in an argon filled glove box.[33] The used solvents were purchased as anhydrous solvents under nitrogen atmosphere and were distilled under argon prior to transferring them into an argon filled glove box. ^1H and ^{13}C NMR spectra were measured on a Bruker Avance II 400 MHz or Bruker Avance III 400 MHz HD. The NMR analysis of the copper(I) complex was carried out on a Bruker Avance III 600 MHz HD NMR-spectrometer. Elemental analysis was carried out on a Thermo FlashEA–1112 Series CHN-analysator. Reactions under inert conditions were carried out in an argon 5.0 filled glove box (MBraun, Garching, Germany). UV-vis measurements were carried out using an Agilent 8453 spectrometer at 20 °C. GC-MS measurements were carried out using an Agilent Technologies 5977B mass detector with a 7820 A GC system. Chiral HPLC was carried out using a CHIRALPAK IC column and a Dionex UVD 170 U detector (eluent mixture: 70% n-hexane, 30% IPA). ESI-MS was measured using a Bruker Daltonics micrOTOF. SC-XRD analysis was carried out on a Bruker D8 Venture system, which was equipped with an IμS microfocus Mo-K_α and Cu-K_α X-ray source. Moreover, the system was equipped with an OXFORD CRYOSYSTEMS 700 low temperature system and a PHOTON100 CMOS-detector. The molecular structures were solved and refined using SHELXT2014/5[34] and SHELXL2018/3[35], respectively.

Preparation of Ligand 2: A modified version of a literature known synthesis was used to obtain **2**.[13] (+)-Camphor (2.119 g, 13.92 mmol) was added to a round bottom flask and dissolved in anhydrous toluene (50 mL). Afterwards 2-(2-pyridyl)-ethylamine (1.711 g, 14.01 mmol) and $BF_3 \cdot Et_2O$ (0.1 mL, 0.8 mmol) were added to the solution and the flask was attached to a Dean-Stark apparatus equipped with a reflux condenser and a drying tube filled with $CaCl_2$. The mixture was refluxed overnight. After cooling to room temperature the solvent was removed *in vacuo* and the crude product was purified by Kugelrohr distillation. The pure product was obtained as a colorless oil (2.022 g, 7.886 mmol; 57%). ^1H NMR(400 MHz, $CDCl_3$): δ (ppm) = 8.48 (d, *J* = 4.5 Hz, 1H), 7.51 (tt, *J* = 7.7, 1.7 Hz, 1H), 7.13 (d, *J* = 7.7 Hz, 1H), 7.05 (t, *J* = 7.6 Hz, 1H), 3.71–3.51 (m, 2H), 3.15–3.00 (m, 2H), 2.18 (dt, *J* = 17.0, 3.9 Hz, 1H), 1.79 (t, *J* = 4.6 Hz, 1H), 1.77–1.66 (m, 1H), 1.6 (d, *J* = 16.9 Hz, 1H), 1.53 (td, *J* = 12.0, 4.2 Hz, 1H), 1.21–1.10 (m, 1H), 1.01–0.91 (m, 1H), 0.90 (s, 3H), 0.83 (s, 3H), 0.53 (s, 3H); ^{13}C NMR (101 MHz, $CDCl_3$) δ (ppm) = 182.6, 160.6, 149.2, 136.0, 124.0, 121.1, 53.5, 52.3, 46.7, 43.7, 38.4, 35.5, 32.2, 27.3, 19.3, 18.9, 11.5; HRMS (ESI): *m/z* calcd for $C_{17}H_{24}N_2 + H^+$: 257.2013 $[M+H]^+$, found: 257.2014.

Preparation of [Cu(2)(MeCN)]PF_6: In an argon filled glovebox $[Cu(MeCN)_4]PF_6$ (1.480 mg, 3.971 mmol) was dissolved in anhydrous acetone (20 mL). Ligand **2** (1.016 mg, 3.963 mmol) was also dissolved in anhydrous acetone (15 mL) and added dropwise while stirring the copper(I) solution. The pale yellow solution was stirred at room temperature for 2 h. Subsequently anhydrous diethyl ether (250 mL) was added to precipitate the colorless copper complex. The suspension was stirred overnight. The colorless solid was filtered off and washed with anhydrous diethyl ether (3 · 10 mL). The product was dried *in vacuo*. A colorless solid was obtained as final product (1.705 mg, 3.370 mmol, 85%). ^1H NMR(600 MHz, acetone-*d6*): δ (ppm) = 8.70 (d, *J* = 5.4 Hz, 1H), 8.10 (t, *J* = 7.5 Hz, 1H), 7.78 (d, *J* = 7.5 Hz, 1H), 7.58 (t, *J* = 5.8 Hz, 1H), 4.18-4.04 (m, 1H), 4.04-3.93 (m, 1H), 3.63 (s, 2H), 2.69 (dt, *J* = 18.4, 3.8 Hz, 1H), 2.30 (s, 3H), 2.09 (d, *J* = 18.4 Hz, 1H), 2.02 (t, *J* = 4.5 Hz, 1H), 1.90-1.82 (m, 1H), 1.79 (td, *J* = 12.2, 3.7 Hz, 1H), 1.50 (s, 3H), 1.32-1.23 (m, 1H), 1.17–1.08 (m, 1H), 0.95 (s, 3H), 0.66 (s, 3H); ^{13}C NMR (151 MHz, acetone-*d6*) δ (ppm) = 195.9 (q, broad), 161.0 (q), 150.6 (CH), 140.9 (CH), 126.5 (CH), 124.7 (CH), 118.7 (q, MeCN), 56.2 (q), 54.0 (CH_2), 49.3 (q), 44.3 (CH), 40.8 (CH_2, broad), 39.1 (CH_2), 32.6 (CH_2), 27.3 (CH_2), 19.7 (CH_3), 19.1 (CH_3), 13.0 (CH_3), 1.8 (CH_3); elemental analysis calcd (%) for $C_{19}H_{27}CuF_6N_3P$: C 45.10, H 5.38, N 8.31; found: C 45.02, H 5.55, N 8.16.

Crystallization of [Cu(**2**)(MeCN)]PF_6 was attempted in MeCN, acetone and DCM. However, the copper(I) complex always crystallized as the $[Cu_2(\mathbf{2})_2](PF_6)_2$ dimer complex (SI 3.5.1), whether the isolated complex [Cu(**2**)(MeCN)]PF_6 was used or the complex was generated *in situ* by careful addition of **2** to $[Cu(MeCN)_4]PF_6$.

Stopped-Flow UV-vis Spectroscopy: Stopped-Flow measurements were carried out on a commercial HI-TECH SF-61SX2 stopped-flow unit (TgK Scientific, Bratford-on-Avon, UK). The collected data was processed using Kinetic Studio version 5.02 Beta. The procedure for kinetic measurements was described in detail in previous work.[36]

UV-vis Experiments: A $8.1 \cdot 10^{-4}$ mol · L^{-1} solution of $[Cu(\mathbf{2})(MeCN)]^+$ was prepared by mixing equimolar amounts of $[Cu(MeCN)_4]PF_6$ and **2** in anhydrous degassed acetone or DCM in an argon filled glovebox. A UV-vis spectrum of the copper(I) complex was recorded at 20 °C. Afterwards dioxygen was led through the solution for about 4 min. Spectra were recorded after further 16 min, 1 d, 2d, 3 d and 4 d. The experiment was repeated in both solvents and the intensity at 365 nm was traced over 5 h at 20 °C.

Oxygenation Reactions: The oxygenation of thioanisole by the bis(*μ*-hydroxido) complex was investigated, to test if the complex is suitable for enantioselective oxygenations. In an argon filled glovebox [Cu(**2**)(MeCN)]PF_6 (216.7 mg; 0.4283 mmol) was dissolved in anhydrous acetone (20 mL). Subsequently, thioanisole (50 μL; 0.43 mmol) was added to the solution under stirring. Pure dioxygen was lead through the solution for 5 min at r.t. causing the solution to turn to a deep purple color. The solution was stirred at r.t. for 4 h and quenched by the addition of 1 mol · L^{-1} NH_3 solution (30 mL). The acetone was removed *in vacuo* and the aqueous layer was washed with DCM (4 · 15 mL). The combined organic layers were dried over Na_2SO_4. After removal of the drying agent, the solvent was removed *in vacuo* and the product mixture was analysed by GC-MS and chiral HPLC. The procedure was repeated in DCM and THF (DCM: green solution after oxygenation; THF: purple suspension that turned into a blue solution after oxygenation).

Crystallizations

$[Cu_2(\mathbf{2})_2](PF_6)_2$: One equivalent of $[Cu(MeCN)_4]PF_6$ and one equivalent of **2** were dissolved in small amounts of anhydrous degassed acetone in separate vials. The ligand solution was carefully added to the copper salt solution resulting in a highly concentrated pale yellow complex solution. Colorless crystals were obtained by slow ether diffusion over a few days at room temperature.

$[Cu(\mathbf{2})_2](BF_4)_2 \cdot 2\ C_3H_6O$: One equivalent of $[Cu(MeCN)_4]BF_4$ and one equivalent of **2** were dissolved in small amounts of anhydrous degassed DCM in separate vials. The ligand solution was carefully added to the copper salt solution resulting in a highly concentrated pale yellow complex solution. Approximately 10 equivalents of S_8 were added in an attempt to crystallize potential sulfido complexes. The solution was stirred overnight and filtered using a syringe filter resulting in a purple solution. Red crystals were obtained by slow pentane diffusion over three months at −30 °C. The sulfur most likely oxidized the Cu(I) complex to the observed $[Cu(\mathbf{2})_2](BF_4)_2$. However the crystallization of sulfido complexes remained unsuccessful.

$[Cu_2(\mathbf{2})_2(\mu\text{-}OH)_2](PF_6)_2 \cdot 2$ THF (C_2): One equivalent of $[Cu(MeCN)_4]PF_6$ and one equivalent of **2** were dissolved in small amounts of anhydrous degassed THF in separate vials. The ligand solution was

EurJIC
European Journal of Inorganic Chemistry

Research Article
doi.org/10.1002/ejic.202100970

Chemistry Europe
European Chemical Societies Publishing

carefully added to the copper salt solution resulting in a highly concentrated pale yellow complex solution. Dioxygen gas was passed through the solution at room temperature for 2 min resulting in a deep purple colored solution. Blue crystals were obtained by slow pentane diffusion over 10 d at −30 °C.

$[Cu_2(2)_2(\mu\text{-}OH)_2](PF_6)_2 \cdot 2\ C_3H_6O$ (C_1): One equivalent of $[Cu(MeCN)_4]PF_6$ and one equivalent of **2** were dissolved in small amounts of anhydrous degassed acetone in separate vials. The ligand solution was carefully added to the copper salt solution resulting in a highly concentrated pale yellow complex solution. One equivalent of NaBArF was added in an attempt to exchange the anion. Dioxygen gas was passed through the solution at room temperature for 2 min resulting in a deep purple colored solution. Blue crystals were obtained by slow ether diffusion over a week at room temperature.

$[Cu_2(2)_2(\mu\text{-}OAc)(\mu\text{-}OH)](PF_6)_2$: One equivalent of $[Cu(MeCN)_4]PF_6$ and one equivalent of **2** were dissolved in small amounts of anhydrous degassed acetone in separate vials. The ligand solution was carefully added to the copper salt solution resulting in a highly concentrated pale yellow complex solution. Dioxygen gas was passed through the solution at room temperature for 2 min resulting in a deep purple colored solution. Blue crystals were obtained by slow ether diffusion over a week at room temperature.

$2\text{-}H_2(OTf)_2 \cdot H_2O$: One equivalent of $Cu(OTf)_2$ and one equivalent of **2** were dissolved in small amounts of DCM in separate vials. The ligand solution was carefully added to the copper salt solution resulting in a highly concentrated green complex solution. The solvent was removed and the complex was re-dissolved in acetone. Colorless crystals were obtained by slow ether diffusion over a few days at room temperature.

Computational Details: Density functional theory (DFT) calculations were performed with Gaussian 16, Revision B01[37]. The geometry optimizations were optimized by using the TPSSh functional[38] and with the Ahlrichs type basis set def2-TZVP[39] basis set as implemented in Gaussian 16, Revision B01.[37] As solvent model, we used the Polarizable Continuum Model (PCM) as implemented in Gaussian 16. As empirical dispersion correction, we used the D3 dispersion with Becke–Johnson damping as implemented in Gaussian16, Revision B.01.[40]

Deposition Numbers 2118500 (for $[Cu_2(\mathbf{2})_2(\mu\text{-OAc})(\mu\text{-OH})](PF_6)_2$), 2118501 (for $\mathbf{2}\text{-}H_2(OTf)_2 \cdot H_2O$), 2118502 (for $[Cu_2(\mathbf{2})_2(\mu\text{-OH})_2](PF_6)_2 \cdot C_3H_6O$), 2118503 (for $[Cu_2(\mathbf{2})_2](PF_6)_2$), 2118504 (for $[Cu_2(\mathbf{2})_2(\mu\text{-OH})_2](PF_6)_2 \cdot 2$ THF), 2118505 (for $[Cu(\mathbf{2})_2](BF_4)_2 \cdot 2\ C_3H_6O$) contain the supplementary crystallographic data for this paper. These data are provided free of charge by the joint Cambridge Crystallographic Data Centre and Fachinformationszentrum Karlsruhe Access Structures service at www.ccdc.cam.ac.uk/structures.

Acknowledgements

We thank the Regional Computing Center of the University of Cologne (RRZK) for providing computing time on the DFG-funded High Performance Computing (HPC) system CHEOPS as well as support. Furthermore, Alexander Petrillo thanks the German Academic Scholarship Foundation (Studienstiftung des deutschen Volkes) for financial support. We thank Prof. Dr. Michael A. Rübhausen and Dr. Benjamin Grimm-Lebsanft for performing Raman measurements. Open Access funding enabled and organized by Projekt DEAL.

Conflict of Interest

The authors declare no conflict of interest.

Data Availability Statement

The data that support the findings of this study are available from the corresponding author upon reasonable request.

Keywords: Chiral · Copper · DFT · Dioxygen · Oxygenations

[1] a) E. I. Solomon, D. E. Heppner, E. M. Johnston, J. W. Ginsbach, J. Cirera, M. Qayyum, M. T. Kieber-Emmons, C. H. Kjaergaard, R. G. Hadt, L. Tian, *Chem. Rev.* **2014**, *114*, 3659; b) D. A. Quist, D. E. Diaz, J. J. Liu, K. D. Karlin, *J. Biol. Inorg. Chem.* **2017**, *22*, 253.
[2] S. E. Allen, R. R. Walvoord, R. Padilla-Salinas, M. C. Kozlowski, *Chem. Rev.* **2013**, *113*, 6234.
[3] H. Sterckx, B. Morel, B. U. W. Maes, *Angew. Chem. Int. Ed.* **2019**, *58*, 7946.
[4] C. E. Elwell, N. L. Gagnon, B. D. Neisen, D. Dhar, A. D. Spaeth, G. M. Yee, W. B. Tolman, *Chem. Rev.* **2017**, *117*, 2059.
[5] G. J. Karahalis, A. Thangavel, B. Chica, J. Bacsa, R. B. Dyer, C. C. Scarborough, *Inorg. Chem.* **2016**, *55*, 1102.
[6] M. Paul, A. Hoffmann, S. Herres-Pawlis, *J. Biol. Inorg. Chem.* **2021**.
[7] a) S. Itoh, H. Fujii in *Comprehensive Coordination Chemistry III*, Vol. 3 (Eds.: E. C. Constable, G. Parkin, L. Q. Que Jr), Elsevier, **2021**, pp. 200–237; b) S. Itoh, T. Abe, Y. Morimoto, H. Sugimoto, *Inorg. Chim. Acta* **2018**, *481*, 38; c) L. Q. Hatcher, K. D. Karlin, *J. Biol. Inorg. Chem.* **2004**, *9*, 669.
[8] M. Schatz, M. Becker, F. Thaler, F. Hampel, S. Schindler, R. R. Jacobson, Z. Tyeklár, N. N. Murthy, P. Ghosh, Q. Chen, J. Zubieta, K. D. Karlin, *Inorg. Chem.* **2001**, *40*, 2312.
[9] a) T. Brückmann, J. Becker, C. Würtele, M. Seuffert, D. Heuler, K. Müller-Buschbaum, M. Weiß, S. Schindler, *J. Inorg. Biochem.* **2021**, 111544; b) A. P. Cole, V. Mahadevan, L. M. Mirica, X. Ottenwaelder, T. D. P. Stack, *Inorg. Chem.* **2005**, *44*, 7345; c) T. Osako, K. Ohkubo, M. Taki, Y. Tachi, S. Fukuzumi, S. Itoh, *J. Am. Chem. Soc.* **2003**, *125*, 11027; d) T. Osako, S. Nagatomo, Y. Tachi, T. Kitagawa, S. Itoh, *Angew. Chem. Int. Ed.* **2002**, *114*, 4501; e) S. Itoh, M. Taki, H. Nakao, P. L. Holland, W. B. Tolman, J. L. Que, S. Fukuzumi, *Angew. Chem. Int. Ed.* **2000**, *39*, 398; f) P. L. Holland, K. R. Rodgers, W. B. Tolman, *Angew. Chem. Int. Ed.* **1999**, *38*, 1139; g) A. P. Cole, D. E. Root, P. Mukherjee, E. I. Solomon, T. D. Stack, *Science* **1996**, *273*, 1848.
[10] P. Specht, A. Petrillo, J. Becker, S. Schindler, *Eur. J. Inorg. Chem.* **2021**, 1961.
[11] a) B. Schönecker, T. Zheldakova, Y. Liu, M. Kötteritzsch, W. Günther, H. Görls, *Angew. Chem. Int. Ed.* **2003**, *42*, 3240; b) B. Schönecker, T. Zheldakova, C. Lange, W. Günther, H. Görls, M. Bohl, *Chem. Eur. J.* **2004**, *10*, 6029; c) Y. Y. See, A. T. Herrmann, Y. Aihara, P. S. Baran, *J. Am. Chem. Soc.* **2015**, *137*, 13776.
[12] R. Trammell, Y. Y. See, A. T. Herrmann, N. Xie, D. E. Díaz, M. A. Siegler, P. S. Baran, I. Garcia-Bosch, *J. Org. Chem.* **2017**, *82*, 7887.
[13] G. Blay, E. Climent, I. Fernández, V. Hernández-Olmos, J. R. Pedro, *Tetrahedron: Asymmetry* **2006**, *17*, 2046.
[14] a) G. Blay, E. Climent, I. Fernández, V. Hernández-Olmos, J. R. Pedro, *Tetrahedron: Asymmetry* **2007**, *18*, 1603; b) G. Blay, L. R. Domingo, V. Hernández-Olmos, J. R. Pedro, *Chem. Eur. J.* **2008**, *14*, 4725.
[15] J. Becker, P. Gupta, F. Angersbach, F. Tuczek, C. Näther, M. C. Holthausen, S. Schindler, *Chem. Eur. J.* **2015**, *21*, 11735.
[16] J. Becker, Y. Y. Zhyhadlo, E. D. Butova, A. A. Fokin, P. R. Schreiner, M. Förster, M. C. Holthausen, P. Specht, S. Schindler, *Chem. Eur. J.* **2018**, *24*, 15543.
[17] a) M. Schatz, M. Becker, O. Walter, G. Liehr, S. Schindler, *Inorg. Chim. Acta* **2001**, *324*, 173; b) T.-D. J. Stumpf, M. Steinbach, C. Würtele, J. Becker, S. Becker, R. Fröhlich, R. Göttlich, S. Schindler, *Eur. J. Inorg. Chem.* **2017**, *2017*, 4246.
[18] S. Zhang, R. Trammell, A. Cordova, M. A. Siegler, I. Garcia-Bosch, *J. Inorg. Biochem.* **2021**, *223*, 111557.
[19] K. Warm, G. Tripodi, E. Andris, S. Mebs, U. Kuhlmann, H. Dau, P. Hildebrandt, J. Roithová, K. Ray, *Angew. Chem. Int. Ed.* **2021**, *60*, 23018.

EurJIC
European Journal of Inorganic Chemistry

Research Article
doi.org/10.1002/ejic.202100970

Chemistry Europe
European Chemical Societies Publishing

[20] a) K. D. Karlin, D.-H. Lee, S. Kaderli, A. D. Zuberbühler, *Chem. Commun.* **1997**, 475; b) Y. Rondelez, M.-N. Rager, A. Duprat, O. Reinaud, *J. Am. Chem. Soc.* **2002**, *124*, 1334.
[21] M. Lerch, M. Weitzer, T.-D. J. Stumpf, L. Laurini, A. Hoffmann, J. Becker, A. Miska, R. Göttlich, S. Herres-Pawlis, S. Schindler, *Eur. J. Inorg. Chem.* **2020**, *2020*, 3143.
[22] a) C. Citek, B.-L. Lin, T. E. Phelps, E. C. Wasinger, T. D. P. Stack, *J. Am. Chem. Soc.* **2014**, *136*, 14405; b) C. Citek, J. B. Gary, E. C. Wasinger, T. D. P. Stack, *J. Am. Chem. Soc.* **2015**, *137*, 6991; c) F. Strassl, B. Grimm-Lebsanft, D. Rukser, F. Biebl, M. Biednov, C. Brett, R. Timmermann, F. Metz, A. Hoffmann, M. Rübhausen, S. Herres-Pawlis, *Eur. J. Inorg. Chem.* **2017**, *2017*, 3350; d) H. R. Lucas, L. Li, A. A. N. Sarjeant, M. A. Vance, E. I. Solomon, K. D. Karlin, *J. Am. Chem. Soc.* **2009**, *131*, 3230.
[23] a) S. Herres, A. J. Heuwing, U. Flörke, J. Schneider, G. Henkel, *Inorg. Chim. Acta* **2005**, *358*, 1089; b) L. Q. Hatcher, M. A. Vance, A. A. Narducci Sarjeant, E. I. Solomon, K. D. Karlin, *Inorg. Chem.* **2006**, *45*, 3004; c) R. Haase, T. Beschnitt, U. Flörke, S. Herres-Pawlis, *Inorg. Chim. Acta* **2011**, *374*, 546.
[24] a) T. Abe, Y. Morimoto, T. Tano, K. Mieda, H. Sugimoto, N. Fujieda, T. Ogura, S. Itoh, *Inorg. Chem.* **2014**, *53*, 8786; b) T. Abe, Y. Shiota, S. Itoh, K. Yoshizawa, *Dalton Trans.* **2020**, *49*, 6710; c) S. Itoh, *Acc. Chem. Res.* **2015**, *48*, 2066.
[25] P. L. Holland, K. R. Rodgers, W. B. Tolman, *Angew. Chem. Int. Ed.* **1999**, *38*, 1139.
[26] T. Schaefer, J. Schindelka, D. Hoffmann, H. Herrmann, *J. Phys. Chem. A* **2012**, *116*, 6317.
[27] a) S. Da Choi, H. Lee, F. Tieves, Y. W. Lee, E. J. Son, W. Zhang, B. Shin, F. Hollmann, C. B. Park, *ACS Catal.* **2019**, *9*, 10562; b) G.-D. Roiban, R. Agudo, A. Ilie, R. Lonsdale, M. T. Reetz, *Chem. Commun.* **2014**, *50*, 14310; c) R. Agudo, G.-D. Roiban, R. Lonsdale, A. Ilie, M. T. Reetz, *J. Org. Chem.* **2015**, *80*, 950; d) A. Ilie, K. Harms, M. T. Reetz, *J. Org. Chem.* **2018**, *83*, 7504.
[28] a) H. Sundén, M. Engqvist, J. Casas, I. Ibrahem, A. Córdova, *Angew. Chem. Int. Ed.* **2004**, *43*, 6532; b) Y. Yang, F. Moinodeen, W. Chin, T. Ma, Z. Jiang, C.-H. Tan, *Org. Lett.* **2012**, *14*, 4762.
[29] J. Legros, J. Dehli, C. Bolm, *Adv. Synth. Catal.* **2005**, *347*, 19.
[30] a) I. Gamba, S. Palavicini, E. Monzani, L. Casella, *Chem. Eur. J.* **2009**, *15*, 12932; b) G. E. O'Mahony, A. Ford, A. R. Maguire, *J. Org. Chem.* **2012**, *77*, 3288.
[31] a) L. Olbe, E. Carlsson, P. Lindberg, *Nat. Rev. Drug Discovery* **2003**, *2*, 132; b) R. Bentley, *Chem. Soc. Rev.* **2005**, *34*, 609.
[32] F. Stöhr, N. Kulhanek, J. Becker, R. Göttlich, S. Schindler, *Eur. J. Inorg. Chem.* **2021**.
[33] D. F. Shriver, *Inorg. Synth.* **1979**.
[34] G. M. Sheldrick, *Acta crystallographica. Section A, Foundations and advances* **2015**, *71*, 3.
[35] G. M. Sheldrick, *Acta crystallographica. Section C, Structural chemistry* **2015**, *71*, 3.
[36] M. Weitzer, M. Schatz, F. Hampel, F. W. Heinemann, S. Schindler, *Dalton Trans.* **2002**, 686.
[37] Gaussian 16, Revision B.01, M. J. Frisch, G. W. Trucks, H. B. Schlegel, G. E. Scuseria, M. A. Robb, J. R. Cheeseman, G. Scalmani, V. Barone, G. A. Petersson, H. Nakatsuji, X. Li, M. Caricato, A. V. Marenich, J. Bloino, B. G. Janesko, R. Gomperts, B. Mennucci, H. P. Hratchian, J. V. Ortiz, A. F. Izmaylov, J. L. Sonnenberg, D. Williams-Young, F. Ding, F. Lipparini, F. Egidi, J. Goings, B. Peng, A. Petrone, T. Henderson, D. Ranasinghe, V. G. Zakrzewski, J. Gao, N. Rega, G. Zheng, W. Liang, M. Hada, M. Ehara, K. Toyota, R. Fukuda, J. Hasegawa, M. Ishida, T. Nakajima, Y. Honda, O. Kitao, H. Nakai, T. Vreven, K. Throssell, J. A. Montgomery, Jr., J. E. Peralta, F. Ogliaro, M. J. Bearpark, J. J. Heyd, E. N. Brothers, K. N. Kudin, V. N. Staroverov, T. A. Keith, R. Kobayashi, J. Normand, K. Raghavachari, A. P. Rendell, J. C. Burant, S. S. Iyengar, J. Tomasi, M. Cossi, J. M. Millam, M. Klene, C. Adamo, R. Cammi, J. W. Ochterski, R. L. Martin, K. Morokuma, O. Farkas, J. B. Foresman, and D. J. Fox, Gaussian, Inc., Wallingford CT, **2016**.
[38] a) M. Tao, J. P. Perdew, V. N. Staroverov, G. E. Scuseria, *Phys. Rev. Lett.* **2003**, *91*, 146401; b) V. N. Staroverov, G. E. Scuseria, J. Tao, J. P. Perdew, *J. Chem. Phys.* **2003**, *119*, 12129 and Erratum **2004**, 121, 11507(E).
[39] a) F. Weigend, R. Ahlrichs, *Phys. Chem. Chem. Phys.* **2005**, *7*, 3297–305; b) A. Schäfer, C. Huber, R. Ahlrichs, *J. Chem. Phys.* **1994**, *100*, 5829; c) K. Eichkorn, F. Weigend, O. Treutler, R. Ahlrichs, *Theor. Chem. Acc.* **1997**, *97*, 119; d) F. Weigend, M. Häser, H. Patzelt, R. Ahlrichs, *Chem. Phys. Lett.* **1998**, *294*, 143.
[40] a) S. Grimme, S. Ehrlich, L. Goerigk, *J. Comput. Chem.* **2011**, *32*, 1456; b) L. Goerigk, S. Grimme, *Phys. Chem. Chem. Phys.* **2011**, *13*, 6670; c) For TPSSh, the values of the original paper have been substituted by the corrected values kindly provided by S. Grimme as private communication and published in; d) A. Hoffmann, R. Grunzke, S. Herres-Pawlis, *J. Comput. Chem.* **2014**, *35*, 1943.

Manuscript received: November 10, 2021
Revised manuscript received: December 14, 2021
Accepted manuscript online: December 14, 2021

3.2 Expanding the Clip-and-Cleave Concept: Approaching Enantioselective C−H Hydroxylations by Copper Imine Complexes Using O_2 and H_2O_2 as Oxidants

This article has been published in

Journal of the American Chemical Society

Alexander Petrillo, Kevin F. Kirchgeßner-Prado, David Hiller, Kim A. Eisenlohr, Giacomo Rubin, Christian Würtele, Remy Goldberg, Dominic Schatz, Max C. Holthausen, Isaac Garcia-Bosch, and Siegfried Schindler

J. Am. Chem. Soc. **2024**, *146*, 25689.

Reprinted with permission from https://doi.org/10.1021/jacs.4c07777.

JACS
JOURNAL OF THE AMERICAN CHEMICAL SOCIETY
pubs.acs.org/JACS
Article

Expanding the Clip-and-Cleave Concept: Approaching Enantioselective C−H Hydroxylations by Copper Imine Complexes Using O_2 and H_2O_2 as Oxidants

Alexander Petrillo, Kevin F. Kirchgeßner-Prado, David Hiller, Kim A. Eisenlohr, Giacomo Rubin, Christian Würtele, Remy Goldberg, Dominic Schatz, Max C. Holthausen,* Isaac Garcia-Bosch,* and Siegfried Schindler*

Cite This: J. Am. Chem. Soc. 2024, 146, 25689−25700

ABSTRACT: Copper-mediated aromatic and aliphatic C−H hydroxylations using benign oxidants (O_2 and H_2O_2) have been studied intensively in recent years to meet the growing demand for efficient and green C−H functionalizations. Herein, we report an enantioselective variant of the so-called clip-and-cleave concept for intramolecular ligand hydroxylations by the application of chiral diamines as directing groups. We tested the hydroxylation of cyclohexanone and 1-acetyladamantane under different oxidative conditions (Cu^I/O_2; Cu^I/H_2O_2; Cu^{II}/H_2O_2) in various solvents. As an outstanding example, we obtained (*R*)-1-acetyl-2-adamantol with a yield of 37% and >99:1 enantiomeric excess from hydroxylation in acetone using Cu^I and O_2. Low-temperature stopped-flow UV−vis measurements in combination with density functional theory (DFT) computations revealed that the hydroxylation proceeds via a bis(μ-oxido) dicopper intermediate. The reaction product represents a rare example of an enantiopure 1,2-difunctionalized adamantane derivative, which paves the way for potential pharmacological studies. Furthermore, we found that 1-acetyladamantane can be hydroxylated in a one-pot reaction under air with isolated yields up to 36% and enantiomeric ratios of 96:4 using Cu^{II}/H_2O_2 in MeOH.

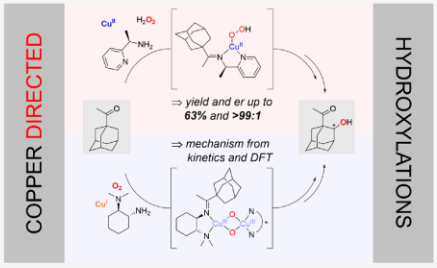

INTRODUCTION

Copper-containing enzymes catalyze various selective oxidations and hydroxylations utilizing dioxygen (O_2) as an oxidant.[1,2] Important examples are methane monooxygenase, which catalyzes the aerobic oxygenation of methane to methanol,[3−5] and dopamine-β-monooxygenase (DβM), which performs the enantioselective hydroxylation of the benzylic CH_2 group in dopamine during biosynthesis of noradrenaline.[1,2] Related to DβM is the enzyme peptidylglycine-α-hydroxylating monooxygenase (PHM) that catalyzes the enantioselective oxygenation of C-terminal glycine residues, a post-translational modification of peptides during hormone biosynthesis.[6] DβM and PHM are classified as Cu-monooxygenases and are thought to follow similar mechanisms.[1] Crystal structure determination of a precatalytic PHM complex in 2004 demonstrated the presence of two non-coupled Cu centers 11 Å apart (Scheme 1),[6] with the Cu_H site coordinated by three histidine residues and the Cu_M site by one methionine and two histidine residues. O_2 was found bound to the Cu_M site in an end-on η^1 fashion to form a superoxido intermediate, and it was proposed that the Cu_H site is responsible for electron transfer to the Cu_M site to close the catalytic cycle.[7] Various mechanisms have been proposed in the following years that posit mononuclear Cu^{II} superoxido or hydroperoxido species as primary oxidants (e.g., Scheme 1iii).[1,8−11] However, in a detailed crystallographic study on a DβM dimer from 2016, Vendelboe et al. demonstrated the existence of an open form (Cu_H−Cu_M = 14 Å) together with a closed form (Cu_H−Cu_M = 4−5 Å) of the active site and opened a debate around the involvement of dinuclear intermediates in the catalytic cycle of PHM and DβM.[12,13] A recent quantum mechanics/molecular mechanics (QM/MM) study[14] indicated that the open active site allows entry of the cosubstrate ascorbate into the Cu_M binding site, which readily undergoes hydrogen atom abstraction (HAA) by the Cu^{II}−O_2 intermediate formed upon subsequent O_2 binding. Facile interconversion to the closed active site then initiates O−OH

Received: June 10, 2024
Revised: August 12, 2024
Accepted: August 13, 2024
Published: September 6, 2024

https://doi.org/10.1021/jacs.4c07777
J. Am. Chem. Soc. 2024, 146, 25689−25700

Scheme 1. (i) Enantioselective Oxygenation of C-Terminal Peptidylglycine by PHM;[1] (ii) Enantioselective Oxygenations of Dopamine by DβM;[1] (iii) Active Site of PHM Based on the Crystal Structure Reported by Prigge et al. in 2004 and One Example of an in the Following Years Prosed Reaction Path via a Mononuclear Intermediate;[6,8,9] (iv) Active Sites of the DβM Dimer Based on the Crystal Structure Reported by Vendelboe et al. in 2016 and Proposed Reaction Path by Wu et al. Involving a Coupled Dicopper Intermediate[12,14]

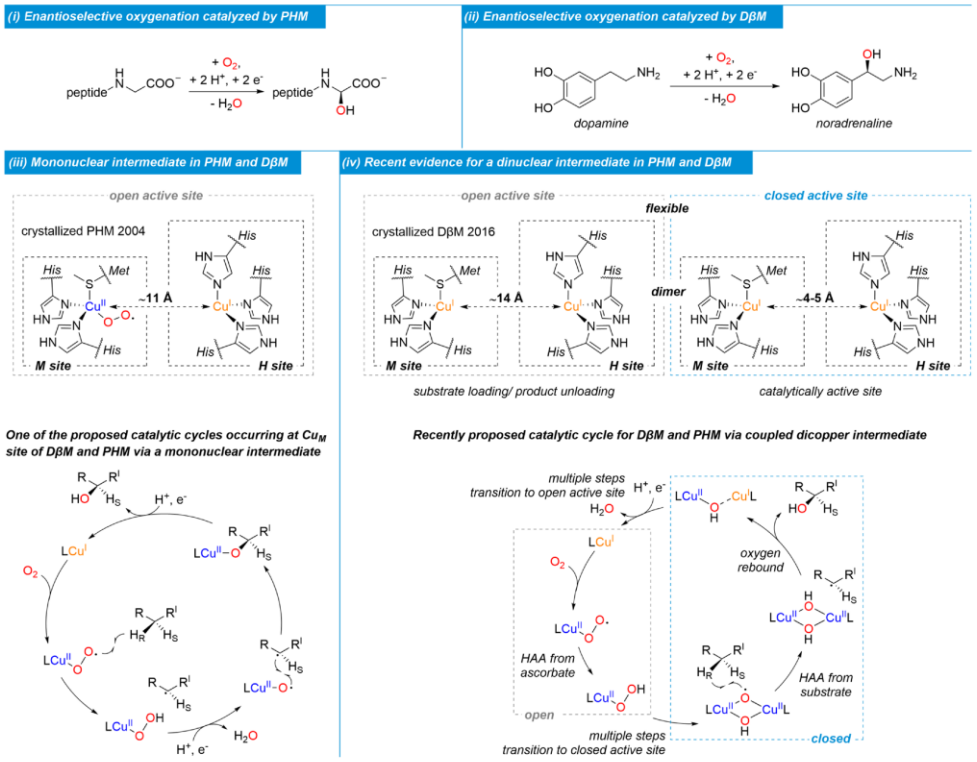

cleavage of the resulting hydroperoxido intermediate to form a dinuclear (μ-O$^{\bullet}$)(μ-OH)Cu^{II}Cu^{II} species, which is suggested as the key reactive intermediate for substrate CH-hydroxylation (Scheme 1iv).

Detailed insight into the mechanism of such metalloenzymes is paramount since these aerobic hydroxylations often represent role models for industrially relevant transformations.[3,5,15] Research activities along these lines have led to various biomimetic approaches to utilize Cu complexes with dioxygen as the greenest conceivable oxidant.[15,16] A concise example is the so-called clip-and-cleave concept,[17−20] which was developed for preparatively simple aerobic regioselective oxygenations of substrate ketones and aldehydes (Scheme 2), based on preceding works of Schönecker et al.[21,22] as well as Feringa and co-workers.[23] Spectroscopic studies provided evidence that the intramolecular hydroxylation reactions proceed via dinuclear Cu^{III}Cu^{III} bis(μ-oxido) intermediates.[17−19] Practical synthetic use of the Schönecker oxidation has further been established by Baran and co-workers, who significantly improved reaction yields and reaction times using sodium ascorbate (Na asc.) as a reducing agent.[24] Furthermore, the groups of Garcia-Bosch and Baran demonstrated improved yields upon addition of H_2O_2 in combination with Cu^{II} or Cu^{I} precursor complexes, a finding that was interpreted in terms of a strictly mononuclear reaction mechanism (Scheme 2ii).[25−28]

Direct asymmetric oxygenations with the benign oxidants O_2 or H_2O_2 are very rare but also of high relevance, due to the growing demand for efficient and green C−H functionalizations.[29] The Schönecker oxidation is a diastereoselective reaction when applied to 17-ketosteroids.[21,22,24] Product stereochemistry, however, is predetermined by the chiral steroid substrate. While chiral directing groups (DGs) have successfully been used to alter the site selectivity (D vs E ring in pentacyclic triterpenoids) of clip-and-cleave-type hydroxylations,[30] an enantioselective variant of the concept to hydroxylate achiral substrates is still elusive.

In this study, we thus explored chiral modifications of established DGs (Scheme 2) to investigate enantioselective clip-and-cleave reactions. We found earlier that bidentate

https://doi.org/10.1021/jacs.4c07777
J. Am. Chem. Soc. 2024, 146, 25689−25700

Scheme 2. (i) General Scheme of the Clip-and-Cleave Concept; (ii) Exemplary Products Obtained by the Garcia-Bosch and Baran Groups under Different Conditions by Oxygenation via a Copper Hydroperoxido Intermediate;[24−26] (iii) Exemplary Products Obtained by the Schindler Group via a Bis(μ-oxido) Intermediate;[17−19] NMR or Gas Chromatography (GC) Conversions

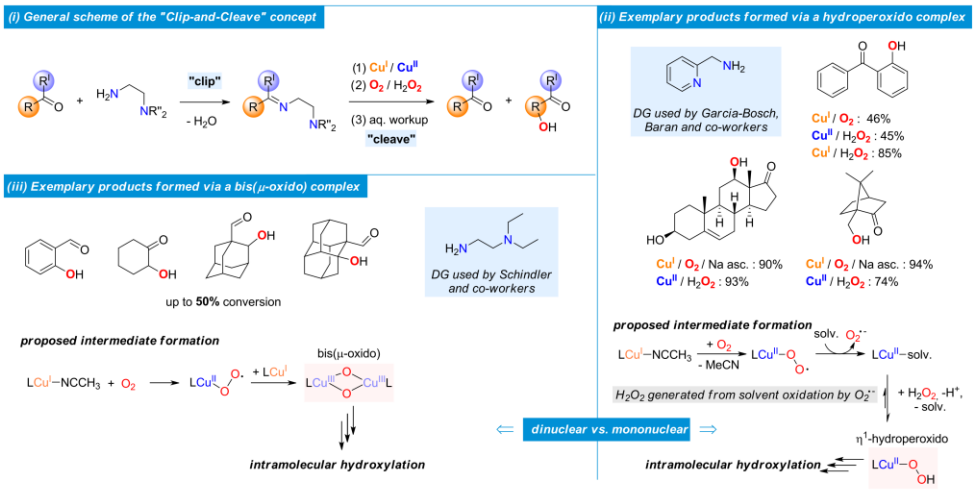

ligands are generally superior to tri- or tetradentate ligands in terms of yield and selectivity.[19,27] Further, ligands that form five-membered chelate rings yield better results than those that form six-membered chelate rings.[19,27] The latter often deactivate Cu^{I} complexes and may alter the mechanism (mononuclear vs dinuclear intermediate, intramolecular vs intermolecular oxygenation).[31,32]

Based on these observations, we chose three different chiral DGs for the present study (Scheme 3). DGs (***R,R***)**-a** and (***R,R***)**-b** represent chiral variants of the ethylene diamine-based DGs employed earlier.[17−19,27] We used (***R,R***)**-a** with two reactive amino groups to test whether binding of two substrates to one ligand could result in improved yields. DG

Scheme 3. Directing Groups Used for Intramolecular Ligand Hydroxylations

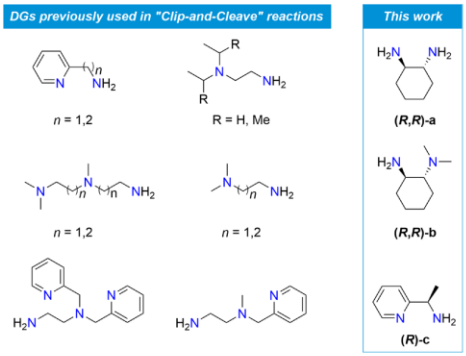

(***R***)**-c** is the simplest chiral derivative of 2-picolylamine, a well-established DG in clip-and-cleave chemistry.[21,24,25] We employed Cu^{I}/O_2, Cu^{I}/H_2O_2, as well as Cu^{II}/H_2O_2 for oxygenation in combination with six different solvents.

RESULTS AND DISCUSSION

We chose cyclohexanone (**1**) as the initial substrate for a proof of concept as it is the simplest substrate with enantiotopic CH_2 groups and has previously been hydroxylated in such reactions.[19] To highlight the synthetic potential of the concept, we opted for 1-acetyladamantane (**2**) as a more convenient substrate compared to adamantane-1-carbaldehyde used previously (Scheme 2iii).[18] Adamantanes are widely used in the pharmaceutical industry based on 1,3-derivatives.[33,34] The realization of enantioselective 1,2-substitutions is, however, challenging,[33,35,36] and the availability of an enantioselective clip-and-cleave variant represents a highly rewarding goal (Scheme 4). To evaluate the enantiomeric ratios (er), the (*R*)- and (*S*)-enantiomers of all ligands have been synthesized. In view of the significance of small changes in ligand structure discussed previously,[32] **2-MPy** was prepared for comparison with (***R***)**-2c** in terms of yields and reaction mechanism. Synthesis of a ligand using substrate **2** and (***R,R***)**-a** as DG was not successful under various conditions, most likely due to the steric bulk of the adamantane residue.

Ligand hydroxylation was studied in six different solvents (MeOH, dichloromethane (DCM), tetrahydrofuran (THF), acetone, MeCN, and hexafluoroisopropanol (HFIP)), and the reaction conditions were chosen in line with previous investigations (Scheme 4).

Cyclohexanone-Based Ligands. Screening results for the cyclohexanone-based ligands are summarized in Table 1. The conversion equals the amount of hydroxylation product obtained after the reaction of a ligand under the reaction

https://doi.org/10.1021/jacs.4c07777
J. Am. Chem. Soc. 2024, 146, 25689−25700

Scheme 4. (i) Chiral Ligands Investigated in This Work; (ii) Oxidative Conditions Applied to All Ligands in Various Solvents[a]

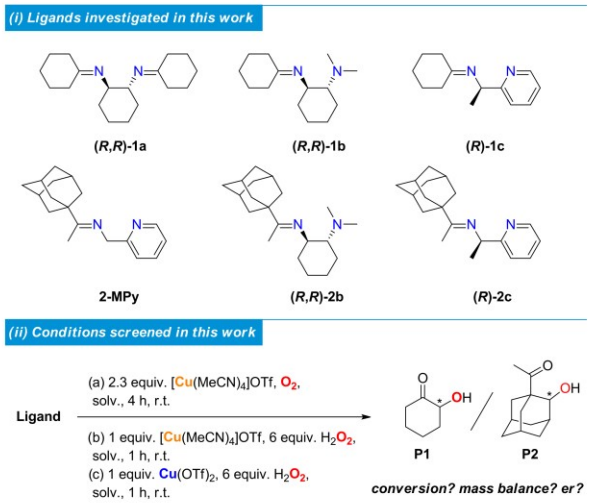

[a]Reactions under all three conditions were followed by acidic workup.

Table 1. Screening Results of Cyclohexanone-Based Ligands

	solvent	Cu^{I}/O_2	Cu^{I}/H_2O_2	Cu^{II}/H_2O_2	Cu^{I}/O_2	Cu^{I}/H_2O_2	Cu^{II}/H_2O_2	Cu^{I}/O_2	Cu^{I}/H_2O_2	Cu^{II}/H_2O_2
conv.<20%	MeOH	**7** (97) 39:61	**0** (37) /	**1** (36) /	**4** (31) /	**3** (21) /	**9** (23) 88:12	**0** (26) /	**2** (8) /	**32** (35) 64:36
	DCM	**14** (88) 51:49	**0** (47) /	**0** (25) /	**2** (26) /	**1** (22) /	**0** (10) /	**0** (13) /	**0** (1) /	**20** (48) 53:47
conv. ≥20%	THF	**47** (74) 50:50	**1** (32) /	**0** (28) /	**3** (34) /	**4** (23) /	**7** (26) 82:18	**0** (69) /	**2** (4) /	**40** (42) 63:37
	acetone	**35** (60) 50:50	**0** (66) /	**0** (37) /	**8** (30) /	**2** (13) /	**0** (5) /	**0** (40) /	**0** (3) /	**0** (87) /
conv. ≥50% or er >80:20	MeCN	**7** (28) 39:61	**0** (71) /	**0** (31) /	**13** (37) 60:40	**0** (2) /	**0** (3) /	**1** (48) /	**9** (40) /	**0** (39) /
	HFIP	**7** (72) 40:60	**3** (82) /	**1** (67) /	**0** (58) /	**0** (24) /	**0** (44) /	**2** (59) /	**0** (4) /	**4** (35) /

[a]The conversion (conv.) of ligand to the hydroxylated product **P1** was determined by GC-MS using 1,3,5-trimethoxybenzene as internal standard. The mass balance (mb) equals the sum of conversions to **P1**, **1**, and 1,2-cyclohexanedione. The enantiomeric ratio (er) was determined using chiral GC (β-TBDAc).

conditions chosen. The mass balance (mb) equals the sum of the quantified unreacted substrate, hydroxylation product, and known side products and serves as a measure for unidentified side products. We generally observed low conversion and mass balance for the majority of conditions tested. Ligand **(*R*,*R*)-1a** gave modest conversions of up to 47% in acetone and THF using Cu^{I}/O_2, in keeping with the 50% conversion threshold expected under these conditions.[17−19] Enantiomeric excess, however, was not observed. The use of H_2O_2 was unproductive with this ligand.

In contrast, **(*R*,*R*)-1b** gave the best results using Cu^{II}/H_2O_2 in MeOH and THF. A low conversion of at most 9% was observed, but the associated enantiomeric ratio of 88:12 (*S*/*R*) demonstrated the potential of the reaction to generate enantiomerically enriched products. Also **(*R*)-1c** yielded the best results in MeOH and THF using Cu^{II}/H_2O_2, increasing the conversion up to 40% but at the same time reducing the er to 63:37 (*S*/*R*). The use of an aromatic DG affords the highest conversion with Cu^{II}/H_2O_2. Attempts to increase conversion and er by running the reaction at −80, −30, and 0 °C or by

https://doi.org/10.1021/jacs.4c07777
J. Am. Chem. Soc. 2024, 146, 25689−25700

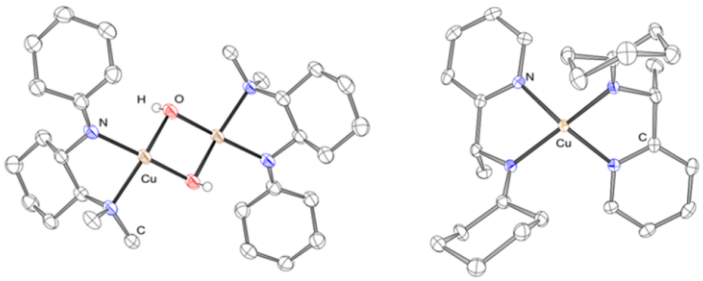

$[Cu^{II}_2(\mathbf{1b})_2(\mu\text{-}OH)_2](OTf)_2$ $[Cu^{II}((\mathbf{R})\text{-}\mathbf{1c})_2](OTf)_2$

Figure 1. Oak Ridge thermal ellipsoid plots (ORTEP) of the molecular structures of $[Cu_2((\mathbf{R},\mathbf{R})\text{-}\mathbf{1b})_2(\mu\text{-}OH)_2](OTf)_2$ and $[Cu((\mathbf{R})\text{-}\mathbf{1c})_2](OTf)_2$. Anions and carbon-bound hydrogen atoms have been omitted for the sake of clarity. Ellipsoids are drawn at a 50% probability.

Table 2. Screening Results of 1-Acetyladamantane-Based Ligands

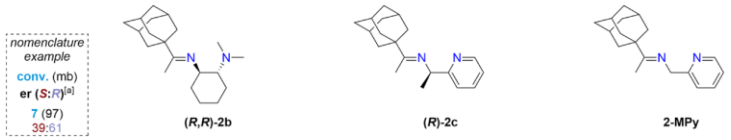

	solvent	Cu^I/O_2	Cu^I/H_2O_2	Cu^{II}/H_2O_2	Cu^I/O_2	Cu^I/H_2O_2	Cu^{II}/H_2O_2	Cu^I/O_2	Cu^I/H_2O_2	Cu^{II}/H_2O_2
conv. <20%	MeOH	**17** (51) >99:1	**3** (72) /	**0** (87) /	**38** (75) 71:29	**30** (34) 71:29	**64** (79) 72:28	**39** (70)	**34** (43)	**69** (78)
	DCM	**32** (59) >99:1	**0** (69) /	**6** (60) /	**28** (58) 67:23	**15** (29) 63:27	**34** (73) 72:28	**31** (83)	**20** (50)	**40** (76)
conv. ≥20%	THF	**32** (44) >99:1	**0** (70) /	**8** (82) /	**23** (55) 67:23	**18** (40) 60:40	**40** (77) 67:23	**33** (73)	**29** (68)	**32** (87)
	acetone	**36** (62) >99:1	**3** (63) /	**5** (82) /	**34** (44) 65:35	**22** (34) 65:35	**34** (90) 74:26	**35** (55)	**25** (50)	**32** (81)
conv. ≥50% or er >80:20	MeCN	**6** (74) /	**0** (67) /	**0** (68) /	**6** (82) /	**5** (22) /	**2** (95) /	**0** (80)	**6** (22)	**0** (71)
	HFIP	**3** (70) /	**0** (64) /	**3** (62) /	**30** (73) 75:25	**21** (45) [b]	**0** (33) /	**39** (94)	**20** (30)	**23** (62)

[a]The conversion (conv.) of ligand to **P2** was determined by ^{1}H NMR using 1,3,5-trimethoxybenzene as internal standard. The mass balance (mb) equals the sum of conversions to **P2** and **2**. The enantiomeric ratio (er) was determined using chiral HPLC (Chiralpak IC). [b]er was not determined due to the high formation of side products with overlapping signals in the chromatogram.

using Na ascorbate or CumOOH remained unsuccessful. Since the cyclohexanone-based ligands are prone to hydrolysis already under air, we initially suspected that ligand hydrolysis by water from the aqueous H_2O_2 reagent occurred prior to hydroxylation. We thus repeated the experiment using anhydrous urea hydrogen peroxide instead, but better conversion was not observed. Hence, hydrolysis of the ligand is not the reason for the low conversion. The generally low mass balance is indicative of more efficient side reactions—in fact, $C_{carbonyl}-C_\alpha$ cleavages are common side reactions in cyclic ketone hydroxylations.[37] Furthermore, it was observed earlier that cyclohexanone (formed *in situ* from cyclohexane) can undergo copper-catalyzed formation of adipic acid followed by multiple subsequent oxidative decarboxylations.[38] Additionally, up to 6% 1,2-cyclohexadione was found as a common side product in the hydroxylations of $(\mathbf{R},\mathbf{R})$-**1b** and $(\mathbf{R})$-**1c** with Cu^I/H_2O_2. This side product most likely forms due to subsequent overoxidation after ligand hydroxylation. We crystallized $(\mathbf{R},\mathbf{R})$-**1b** as a $Cu^{II}Cu^{II}$ bis(μ-hydroxido) dicopper complex upon oxygenation in DCM (Figure 1). This kind of complex is often formed from a $Cu^{III}Cu^{III}$ bis(μ-oxido) complex, which we could confirm by low-temperature stopped-flow UV−vis measurements (cf. Supporting Information (SI) Figure S7). Furthermore, $(\mathbf{R})$-**1c** crystallized as a homoleptic 1:2 [Cu:L_2] Cu^{II} complex, which is common for bidentate ligands and often represents a steep thermodynamic sink precluding efficient clip-and-cleave reactivity.[19]

All in all, the results represent an encouraging proof of principle, but the pronounced lability of cyclohexanone derivatives evidently renders this ligand class unsuitable for clip-and-cleave chemistry.

1-Acetyladamantane-Based Ligands. Screening of 1-acetyladamantane-based ligands was carried out employing the same conditions as before (Table 2). As a general observation, we note that ligands with cyclohexyl DGs do not undergo hydroxylation with H_2O_2. Pyridyl-based DGs, on the other hand, yield substantially improved results with Cu^{II}/H_2O_2.

https://doi.org/10.1021/jacs.4c07777
J. Am. Chem. Soc. 2024, 146, 25689−25700

(*R,R*)-**2b** showed moderate conversion to (*S*)-1-acetyl-2-adamantol in up to 36% (>99:1 er) under Cu^{I}/O_2 conditions in acetone, DCM, and THF. Correspondingly, (*R*)-1-acetyl-2-adamantol, (*R*)-**P2**, was readily isolable upon hydroxylation of (*S,S*)-**2b** in acetone using Cu^{I}/O_2 (37% yield and >99:1 er). Vibrational circular dichroism (VCD) spectroscopy was used to determine the absolute product configuration (Figure 2),

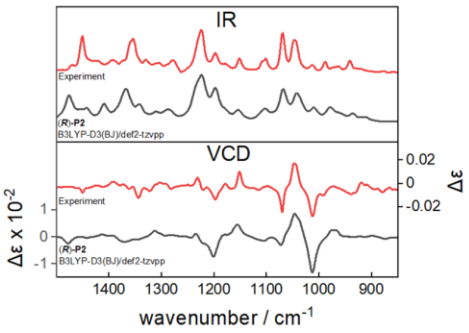

Figure 2. IR and VCD spectra of **P2** isolated from the hydroxylation of (*S,S*)-**2b** using Cu^{I}/O_2 (experimental in red vs computed spectra for (*R*)-**P2** in gray).

and the computational VCD spectra for (*R*)-**P2** matched the experimental spectra. Hence, the (*R*)-ligands investigated preferentially form (*S*)-products, and vice versa. In contrast, Cu^{I}/H_2O_2 and Cu^{II}/H_2O_2 conditions yielded no significant results indicating that the hydroxylation proceeds via a copper dioxygen intermediate that remains inaccessible using H_2O_2. The use of sodium ascorbate as a reducing agent did not improve the conversion of the reaction either.

Low-temperature stopped-flow UV−vis measurements (Figure 3) and TD-DFT computations (Figures S30 and S31) revealed the formation of a $Cu^{III}Cu^{III}$ bis(μ-oxido) dicopper intermediate in acetone at −82 °C (λ = 415 nm; ε_{415nm} = 1.6 mM^{-1} L^{-1}; $\lambda_{TD\text{-}DFT}$ = 407 nm). This intermediate is commonly observed in intramolecular ligand hydroxylations and is debated as possible active hydroxylating species in particulate methane monooxygenase (pMMO).[1,17−19,39−41] Intermediate formation kinetics are first order in both Cu^{I} and dioxygen concentration. In combination with a strongly negative activation entropy calculated from an Eyring plot ($\Delta^{\ddagger}S$ = −28 ± 2 cal K^{-1} mol^{-1}; Figure 3B,ii), an associative formation of a Cu^{II} superoxido complex in the rate-determining step prior to dimerization to the $Cu^{III}Cu^{III}$ bis(μ-oxido) dicopper intermediate is suggested. The intercept in the k_{obs} vs $c(O_2)$ plot (Figure 3B,i) indicates the reversible formation of the dinuclear intermediate, which then irreversibly decays in the course of subsequent hydroxylation. We reported a related kinetic scenario previously.[42]

DFT computations employing the BLYP functional were used for further mechanistic scrutiny (Figure 4). This functional has shown excellent performance for thermodynamic and kinetic properties of bis(μ-oxido) dicopper systems in earlier work.[20,43−46] Starting from monomeric **I1**, O_2 is coordinated via (spin conserving) associative ligand exchange. The resulting triplet Cu^{II} superoxido complex **I3** is unreactive

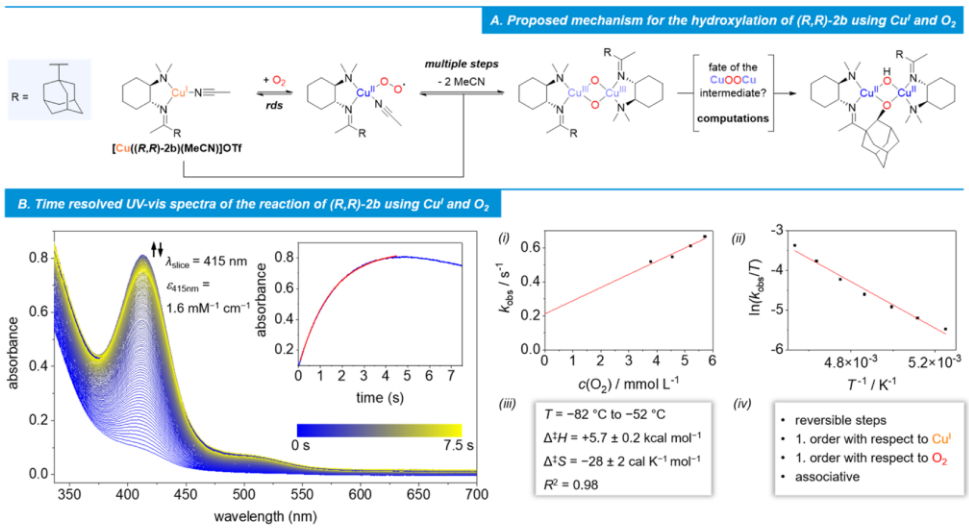

Figure 3. (A) Proposed mechanism for the hydroxylation of (*R,R*)-**2b** using Cu^{I}/O_2 in acetone. (B) Time-resolved UV−vis spectra of the reaction of $[Cu((R,R)\text{-}2b)]^{+}$ (5.10×10^{-4} mol L^{-1}) with dioxygen (5.72×10^{-3} mol L^{-1})[16] in acetone at −82 °C over a period of 7.5 s. The inset displays the time-dependent change in absorbance at 415 nm (blue, experimental fit; red, exponential fit). (B, i) Change of k_{obs} at −82 °C in dependence of the O_2 concentration; (B, ii) Eyring plot obtained from the k_{obs} values determined between −82 and −52 °C; (B, iii) activation parameters obtained from the Eyring plot; (B, iv) interpretation of the kinetic observations.

https://doi.org/10.1021/jacs.4c07777
J. Am. Chem. Soc. 2024, 146, 25689−25700

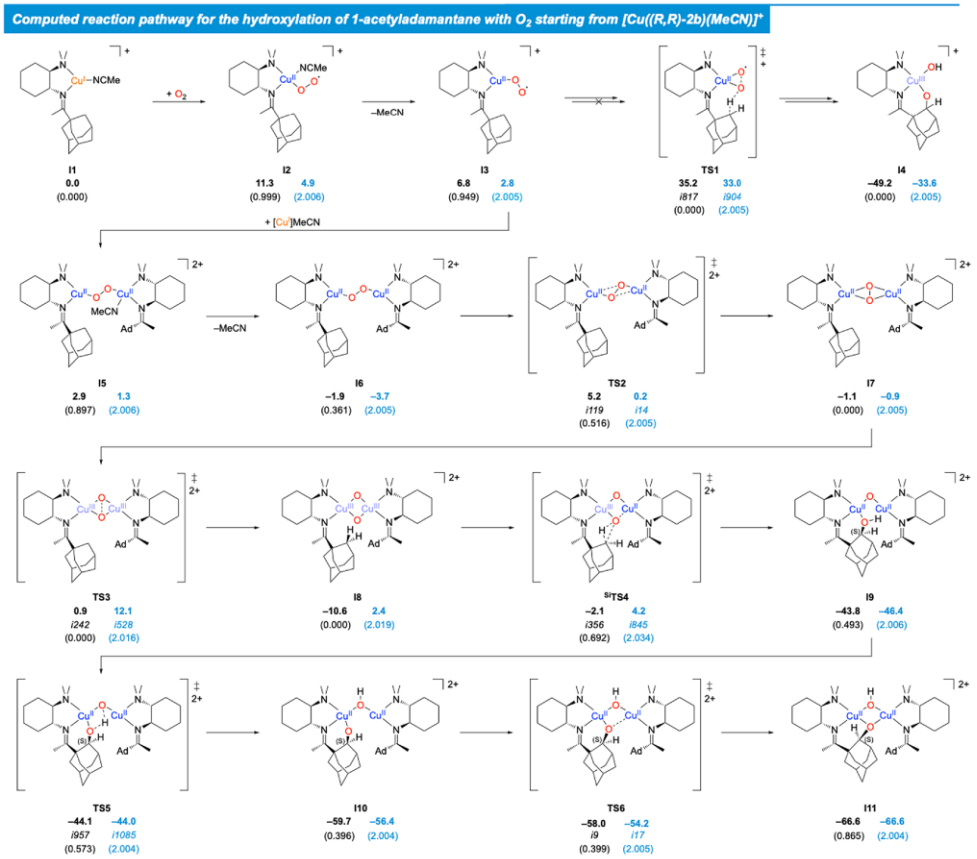

Figure 4. Computed reaction pathways for the C−H activation of 1-acetyladamantane with O_2 starting from [Cu((***R,R***)-**2b**)(MeCN)]$^+$; relative Gibbs free energies (ΔG^{298} in kcal mol^{-1}), imaginary frequencies of transition modes (cm^{-1}) and $\langle S^2 \rangle$ expectation values for singlet (black) and triplet (blue) species at the CPCM-BLYP-D3BJ/def2-TZVP(SDD)//BLYP-D3BJ/def2-TZVP(SDD) level of DFT (solvent: MeOH).

toward hydrogen atom abstraction ($\Delta^{\ddagger}G$ > 35 kcal mol^{-1}).[47] This is consistent with several earlier studies, in which mononuclear Cu^{II} superoxido complexes have been shown to activate only moderately strong C−H bonds with bond dissociation enthalpies (BDE) below 80 kcal mol^{-1}, such as formylglycine, 1-benzyl-1,4-dihydronicotinamide, or 9,10-dihydroanthracene.[11,48−50] With BDE > 95 kcal mol^{-1},[51] C−H bonds in adamantanes resist activation by $[CuO_2]^+$ species. Instead, association of **I1** and **I3**, with concomitant loss of MeCN, leads to the dinuclear Cu^{II}Cu^{II} peroxido complex **I6**. Low barrier isomerization via **TS2** leads to side-on bound **I7**. Hence, up to this point, O_2 binding as well as dimer formation represent a dynamic equilibrium, with close-lying singlet and triplet states for the dinuclear part. O−O cleavage, then, leads to the experimentally observed Cu^{III}Cu^{III} bis(μ-oxido) key intermediate **I8**. This process is favored on the singlet surface ($\Delta^{\ddagger}G_{eff}$ = 5 vs 16 kcal mol^{-1} for the triplet process). Hydrogen atom abstraction of the ^{Si}H atom via ^{Si}**TS4** is kinetically preferred over abstraction of the ^{Re}H atom with an effective reaction barrier of 9 vs 13 kcal mol^{-1} relative to singlet **I8**. Following the intrinsic reaction coordinate (IRC) of ^{Si}**TS4** reveals a barrierless OH rebound on the product side, leading to the strongly exergonic (*S*)-isomer **I9** (Figure 5). An intrinsic bond orbital analysis[52,53] of the **I8** → ^{Si}**TS4** → **I9** reaction step indicates initial hydrogen atom transfer, followed by intramolecular electron transfer from the resulting carbon radical to one of the copper ions with almost synchronous OH$^-$ rebound; this sequence of electronic events collectively represents an oxygen atom insertion into the C−H bond (cf. Section 3.3.5 in the Supporting Information for details). This irreversible step introduces enantioselectivity: The alternative ^{Re}H transfer via ^{Re}**TS4** is kinetically disfavored by 4 kcal mol^{-1}, probably due to steric congestion and less effective overlap of the σ(C−H) orbital with the σ^*(O−O) orbital (a detailed analysis is provided as Supporting Information, cf. Section 3.3.4). Subsequent proton shift toward the bridging, more

https://doi.org/10.1021/jacs.4c07777
J. Am. Chem. Soc. 2024, 146, 25689−25700

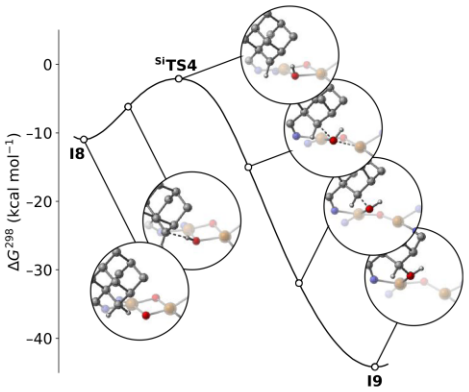

Figure 5. Energy profile obtained from IRC calculations on singlet ^{Si}**TS4** connecting **I8** with **I9**, illustrating the nonsynchronous concerted character of the hydroxylation step.

basic oxygen atom and Cu−O bond formation resulting in **I11** represents a rapid, exergonic sequence of steps. The overall scenario is in accordance with previous studies on aliphatic hydroxylation involving $Cu^{III}Cu^{III}$ bis(μ-oxido) $[Cu_2O_2]^{2+}$ complexes.[20,54,55]

Reactions with Hydrogen Peroxide. Compared to the results obtained with (***R,R***)**-2b**, the hydroxylations of (***R***)**-2c** and **2-MPy** appeared generally more robust under various conditions, but using Cu^I/H_2O_2 results in a significantly lower mass balance than the reactions with Cu^I/O_2 or Cu^{II}/H_2O_2. It is also noteworthy that (***R***)**-2c** and **2-MPy** demonstrate similar reactivity, irrespective of the additional methyl group in (***R***)**-2c**, which we expected to have a drastic influence on the reaction based on previous studies.[31,32,56,57] The best results were achieved in methanol under all three conditions, but Cu^{II}/H_2O_2 conditions stand out, with conversions up to 64% and er up to 72:28. HFIP did not have any advantages in comparison to MeOH. Acetonitrile was the most unproductive solvent, probably precluding the binding of O_2 or H_2O_2. The finding that MeOH outperforms solvents commonly used in clip-and-cleave chemistry i.e., acetone, DCM, and THF,[17−19,25,26] was quite unexpected at first. Protic solvents have long been considered problematic in Cu^I/O_2 chemistry since they often quench the central Cu−O_2 intermediates involved in such reactions. Anyhow, recent studies demonstrated that MeOH can support Cu^I/O_2 chemistry[42] and it was found useful as an additive in clip-and-cleave reactions.[24,25] Also HFIP was productive as a solvent for the hydroxylation of (***R***)**-2c** and **2-MPy** using Cu^I/O_2. Use of H_2O_2, however, did not yield good results in HFIP, potentially because HFIP amplifies the oxidizing power under these conditions causing side reactions.[58] This is supported by the low to modest mass balance of the reactions in HFIP. In view of the particularly high conversion observed, we further screened the hydroxylation of (***R***)**-2c** using Cu^{II}/H_2O_2 in MeOH (Table 3). The key findings were that (i) the reaction time can be reduced to 5 min, (ii) only 1 equiv of H_2O_2 is sufficient to get close to the maximum observed conversion, (iii) neither addition of 2 equiv of Cu^{II} nor addition of HFIP improved conversion, (iv) use of organic peroxides as oxidants resulted in very low conversion, but rather high mass balance, (v) temperature variation does not result in significant changes.

Table 3. Screening of Various Conditions for the Hydroxylation of (*R*)-2c

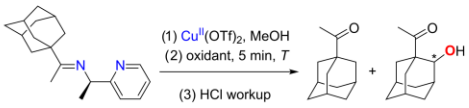

(*R*)-2c 2 P2

entry	equiv Cu(OTf)$_2$	equiv H_2O_2	T/°C	conv. (mb)	er (S/R)
1	1	1	rt	65 (78)	70:30
2	1	2	rt	71 (81)	72:28
3	1	6	rt	72 (83)	71:29
4	1 (1% HFIP)[a]	6	rt	66 (75)	72:28
5	1 (10% HFIP)[a]	6	rt	60 (71)	73:27
6	2	6	rt	65 (81)	72:28
7	1	6	50	70 (82)	71:29
8	1	6	0	60 (76)	72:28
9	1	6	−30	63 (81)	71:29
10	1	6 equiv CumOOH[b]	rt	3 (74)	
11	1	6 equiv *t*BuOOH[b]	rt	3 (74)	
12	1 (1 equiv TEA)	6	rt	27 (29)	79:21
13	1 (1 equiv NMe_4OH)	6	rt	32 (35)	82:18

[a]With respect to solvent volume. [b]Instead of H_2O_2.

We considered deprotonation of H_2O_2 a potentially useful step aiding the formation of reactive hydroxylating Cu^{II} intermediates such as mononuclear hydroperoxido or peroxido complexes, or dinuclear species.[25,26,59] In contrast, we found that the addition of a base significantly decreases conversion and mass balance (Table 3; entries 12 and 13). It thus appears that additional base causes a mechanistic change leading to unproductive side reactions.

The bottleneck for the generation of higher er was found to be the partial racemization of ligand (***R***)**-2c** (er = 26:74) during its synthesis, which naturally limits the er of **P2** (cf. SI Figure S6). We first suspected the purification by kugelrohr distillation at 160 °C to be the problem and attempted a one-pot hydroxylation using the unpurified ligand immediately after synthesis for hydroxylation under Cu^{II}/H_2O_2 conditions in MeOH. We isolated the product in 63% yield with 79:21 er. Increase of the latter by approximately 7% demonstrated that the azeotropic distillation in toluene might have a more significant influence on the er. We consequently changed the solvent to benzene, which has a lower boiling point than toluene. After azeotropic distillation overnight, **P2** was isolated in 29% yield and 93:7 er, in line with our reaction temperature hypothesis. Longer distillation times did not change the yield but lowered the er. In DCM, the reaction gave **P2** in 36% yield and 96:4 er after 4 days (Scheme 5). We thus established a convenient one-pot reaction in which DCM is readily distilled off after ligand formation and methanol is added to redissolve the crude ligand. Subsequently, Cu(OTf)$_2$ and H_2O_2 are added to the mixture to afford the hydroxylation after 5 min of stirring (Scheme 5).

We were unable to obtain crystals of $Cu^{I/II}$ complexes bearing (***R,R***)**-2b** as a ligand. However, starting complexes

https://doi.org/10.1021/jacs.4c07777
J. Am. Chem. Soc. 2024, 146, 25689−25700

Scheme 5. (a) Initial Isolation of P2 from Hydroxylation of (*R*)-2c; (b) Isolation of P2 via One-Pot Hydroxylation of 2[a]

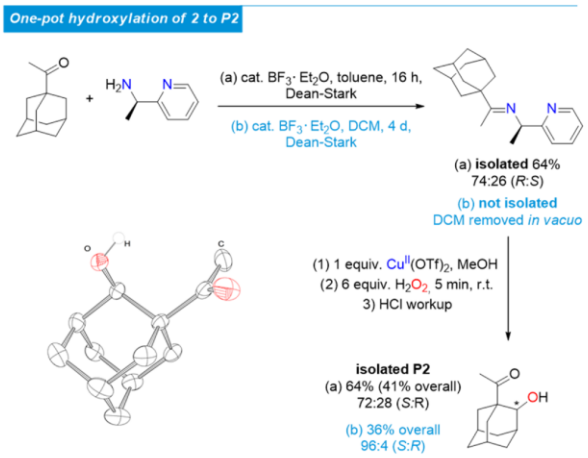

[a]ORTEP plot of the molecular structure of **P2**. Carbon-bound H atoms were omitted for clarity and ellipsoids are drawn at 50% probability.

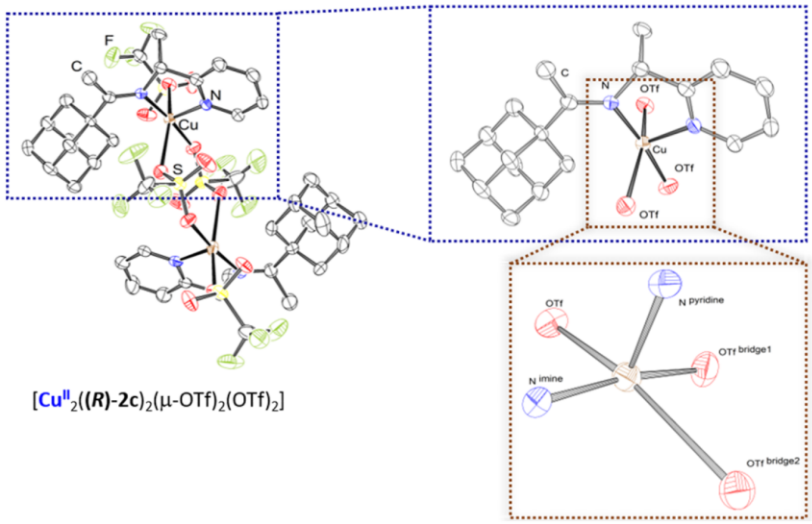

Figure 6. ORTEP plots of the molecular structure of $[Cu_2((R)\text{-}2c)_2(\mu\text{-}OTf)_2(OTf)_2]$. Anions and hydrogen atoms have been omitted for the sake of clarity. Ellipsoids are drawn at 50% probability. The blue and orange boxes indicate a zoomed-in view of the molecular structure.

[Cu(**2-MPy**)(MeCN)]OTf, $[Cu_2(\textbf{2-MPy})_2(\mu\text{-}OTf)_2(OTf)_2]$ (cf. SI), and $[Cu_2((R)\text{-}2c)_2(\mu\text{-}OTf)_2(OTf)_2]$ were analyzed by single crystal X-ray diffraction (SC-XRD) (Figure 6). [Cu(**2-MPy**)(MeCN)]OTf crystallized as trigonal planar monoacetonitrile complex, which is very common for Cu^I complexes with bidentate ligands generated from tetrakis-(acetonitrile)copper(I) salts (cf. SI).[19,25,32] The crystallization of a Cu^I complex bearing ligand (***R***)-**2c** was not successful, but considering the similar reactivity to **2-MPy**, the same coordination sphere can be assumed. Interestingly, Cu^{II} complexes bearing **2-MPy** and (***R***)-**2c** crystallized as triflate-bridged dimers. In both complexes, the Cu^{II} centers possess a square pyramidal coordination sphere with the pyridyl N atom coordinated in the axial position and the imine N in the equatorial position. Furthermore, three triflate anions are coordinated in the equatorial plane, of which two form a bridge to the other Cu^{II} center. This coordination pattern is quite

https://doi.org/10.1021/jacs.4c07777
J. Am. Chem. Soc. 2024, 146, 25689−25700

uncommon for Cu^{II} complexes and might result from the high steric demand of the adamantyl residues.

We investigated the formation of the intermediates responsible for the hydroxylation of **2-MPy** and (***R***)**-2c** by low-temperature stopped-flow UV−vis spectroscopy in MeOH using Cu^{II}/H_2O_2 (cf. SI). At −82 °C, the rapid formation and decomposition of an intermediate gives rise to a signal at 345 nm (ε_{345nm} = 1.7 mM^{-1} cm^{-1}; Figure 7). Signals in this region

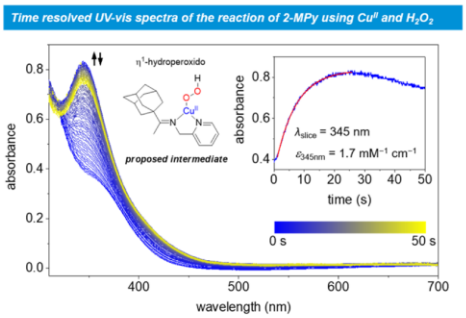

Figure 7. Time-resolved UV−vis spectra of the reaction of $[Cu_2(\mathbf{2\text{-}MPy})_2(\mu\text{-}OTf)_2(OTf)_2]$ (4.96×10^{-4} mol L^{-1}) with H_2O_2 (5.15×10^{-3} mol L^{-1})[16] in MeOH at −82 °C over a period of 50 s. The inset displays the time-dependent change in absorbance at 345 nm (blue experimental; red exponential fit).

are commonly attributed to Cu^{II} hydroperoxido intermediates formed in reactions with H_2O_2.[25−27] The path is dictated by the directing group as previously outlined during the comparison of oxygenations by the Schindler group (dinuclear)[17−19] using aliphatic DGs and the oxygenations by the groups of Garcia-Bosch and Baran (mononuclear) using aromatic DGs.[24,25] However, the signal at 345 nm could also be interpreted as other intermediates such as $Cu^{II}Cu^{II}$ side-on peroxido, or $Cu^{II}Cu^{II}$ bis(μ-hydroxido).[32,60] A more detailed study is required to decipher the correct mechanism.

CONCLUSIONS AND OUTLOOK

In this article, we report an enantioselective variant of the clip-and-cleave concept by the application of chiral diamines as directing groups. The 2-hydroxylation of cyclohexanone with O_2 resulted in rather low conversion. In contrast, the enantioselective 2-hydroxylation of 1-acetyladamantane poses an interesting path to enantiopure 1,2-disubstituted adamantanes and provides unique and easy access to this pharmacologically important class of compounds. Most notably, we were able to obtain (*R*)-1-acetyl-2-adamantol from (***S,S***)**-2b** using Cu^I/O_2 with a yield of 37% and an er of >99:1. Furthermore, in a combined DFT and low-temperature stopped-flow UV−vis kinetic study, we demonstrated that the reaction proceeds via multistep formation of a bis(μ-oxido) intermediate followed by a highly selective concerted C−H bond hydroxylation step.

The hydroxylation can also be run with H_2O_2 as a one-pot reaction via (***R***)**-2c**. In this way, **P2** can be isolated with a 36% yield and er of 96:4. Spectroscopic data was collected for the hydroxylation of **2-MPy** and (***R***)**-2c** using Cu^{II}/H_2O_2 in MeOH using low-temperature stopped-flow UV−vis measurements. The spectroscopic data indicates that the hydroxylation proceeds via a copper hydroperoxido intermediate, as previously described in the literature.[25] However, more detailed studies are required for detailed mechanistic insight.

In future investigations, we plan the application of transient directing groups on enantioselective clip-and-cleave hydroxylations and the development of a catalytic concept.[61] Transient directing groups have already been successfully applied in Cu-catalyzed clip-and-cleave-like sulfonylations.[62] This would significantly improve the practicability of the concept and provide access to more affordable 1,2-difunctionalized adamantanes. The one-pot hydroxylation via (***R***)**-2c** represents an encouraging example in this context.

ASSOCIATED CONTENT

Supporting Information

The Supporting Information is available free of charge at https://pubs.acs.org/doi/10.1021/jacs.4c07777.

Experimental procedures and spectroscopic, kinetic, computational, and crystallographic data (PDF)

Optimized atomic coordinates (TXT)

Accession Codes

CCDC 2333682−2333687 contain the supporting crystallographic data for this paper. These data can be obtained free of charge via www.ccdc.cam.ac.uk/data_request/cif, by emailing data_request@ccdc.cam.ac.uk, or by contacting The Cambridge Crystallographic Data Centre, 12 Union Road, Cambridge CB2 1EZ, UK; fax: +44 1223 336033.

AUTHOR INFORMATION

Corresponding Authors

Max C. Holthausen − *Institute of Inorganic and Analytical Chemistry, Goethe University, 60438 Frankfurt am Main, Germany*; orcid.org/0000-0001-7283-8329; Email: max.holthausen@chemie.uni-frankfurt.de

Isaac Garcia-Bosch − *Department of Chemistry, Carnegie Mellon University, Pittsburgh, Pennsylvania 15213, United States*; orcid.org/0000-0002-6871-3029; Email: igarciab@andrew.cmu.edu

Siegfried Schindler − *Institute of Inorganic and Analytical Chemistry, Justus Liebig University Giessen, 35392 Giessen, Germany*; orcid.org/0000-0002-9991-9513; Email: siegfried.schindler@anorg.chemie.uni-giessen.de

Authors

Alexander Petrillo − *Institute of Inorganic and Analytical Chemistry, Justus Liebig University Giessen, 35392 Giessen, Germany*

Kevin F. Kirchgeßner-Prado − *Institute of Inorganic and Analytical Chemistry, Goethe University, 60438 Frankfurt am Main, Germany*

David Hiller − *Institute of Inorganic and Analytical Chemistry, Goethe University, 60438 Frankfurt am Main, Germany*

Kim A. Eisenlohr − *Institute of Inorganic and Analytical Chemistry, Goethe University, 60438 Frankfurt am Main, Germany*; orcid.org/0009-0002-9463-1331

Giacomo Rubin − *Institute of Inorganic and Analytical Chemistry, Justus Liebig University Giessen, 35392 Giessen, Germany*

Christian Würtele − *Institute of Inorganic and Analytical Chemistry, Justus Liebig University Giessen, 35392 Giessen, Germany*

https://doi.org/10.1021/jacs.4c07777
J. Am. Chem. Soc. 2024, 146, 25689−25700

Remy Goldberg − *Department of Chemistry, Carnegie Mellon University, Pittsburgh, Pennsylvania 15213, United States*
Dominic Schatz − *Institute of Organic Chemistry, Justus Liebig University Giessen, 35392 Giessen, Germany*

Complete contact information is available at: https://pubs.acs.org/10.1021/jacs.4c07777

Notes

The authors declare no competing financial interest.

■ ACKNOWLEDGMENTS

A.P. thanks the German Academic Scholarship Foundation (Studienstiftung des deutschen Volkes) for financial support. The authors thank Prof. Roberto Gil, Karl Schulz, and the NMR Center (Funded in part by NSF grants CHE-9808188 and CHE-1039870) at Carnegie Mellon University. They also thank Dr. Dennis Gerbig and Prof. Peter R. Schreiner for providing access to VCD spectroscopy instruments and Prof. Andrey A. Fokin for useful synthetic advice. Computing resources and excellent service were provided by the NHR Center NHR@SW and the Center for Scientific Computing (CSC) at Goethe University Frankfurt. Research reported in this publication was supported by the National Institute of General Medical Sciences of the National Institutes of Health under Award Number R35GM137914 (to I.G.-B.). The content is solely the responsibility of the authors and does not necessarily represent the official views of the National Institutes of Health.

■ REFERENCES

(1) Liu, J. J.; Diaz, D. E.; Quist, D. A.; Karlin, K. D. Copper(I)-Dioxygen Adducts and Copper Enzyme Mechanisms. *Isr. J. Chem.* **2016**, *56*, 738−755.
(2) Quist, D. A.; Diaz, D. E.; Liu, J. J.; Karlin, K. D. Activation of dioxygen by copper metalloproteins and insights from model complexes. *J. Biol. Inorg. Chem.* **2017**, *22*, 253−288.
(3) Lawton, T. J.; Rosenzweig, A. C. Methane-Oxidizing Enzymes: An Upstream Problem in Biological Gas-to-Liquids Conversion. *J. Am. Chem. Soc.* **2016**, *138* (30), 9327−9340.
(4) Sirajuddin, S.; Rosenzweig, A. C. Enzymatic oxidation of methane. *Biochemistry* **2015**, *54* (14), 2283−2294.
(5) Ross, M. O.; MacMillan, F.; Wang, J.; Nisthal, A.; Lawton, T. J.; Olafson, B. D.; Mayo, S. L.; Rosenzweig, A. C.; Hoffman, B. M. Particulate methane monooxygenase contains only mononuclear copper centers. *Science* **2019**, *364* (6440), 566−570.
(6) Prigge, S. T.; Eipper, B. A.; Mains, R. E.; Amzel, L. M. Dioxygen binds end-on to mononuclear copper in a precatalytic enzyme complex. *Science* **2004**, *304* (5672), 864−867.
(7) Chufán, E. E.; Prigge, S. T.; Siebert, X.; Eipper, B. A.; Mains, R. E.; Amzel, L. M. Differential reactivity between two copper sites in peptidylglycine α-hydroxylating monooxygenase. *J. Am. Chem. Soc.* **2010**, *132* (44), 15565−15572.
(8) Chen, P.; Solomon, E. I. Oxygen activation by the noncoupled binuclear copper site in peptidylglycine alpha-hydroxylating monooxygenase. Reaction mechanism and role of the noncoupled nature of the active site. *J. Am. Chem. Soc.* **2004**, *126* (15), 4991−5000.
(9) Klinman, J. P. The copper-enzyme family of dopamine beta-monooxygenase and peptidylglycine alpha-hydroxylating monooxygenase: resolving the chemical pathway for substrate hydroxylation. *J. Biol. Chem.* **2006**, *281* (6), 3013−3016.
(10) Kim, B.; Brueggemeyer, M. T.; Transue, W. J.; Park, Y.; Cho, J.; Siegler, M. A.; Solomon, E. I.; Karlin, K. D. Fenton-like Chemistry by a Copper(I) Complex and H_2O_2 Relevant to Enzyme Peroxygenase C-H Hydroxylation. *J. Am. Chem. Soc.* **2023**, *145* (21), 11735−11744.
(11) Cowley, R. E.; Tian, L.; Solomon, E. I. Mechanism of O_2 activation and substrate hydroxylation in noncoupled binuclear copper monooxygenases. *Proc. Natl. Acad. Sci. U.S.A.* **2016**, *113* (43), 12035−12040.
(12) Vendelboe, T. V.; Harris, P.; Zhao, Y.; Walter, T. S.; Harlos, K.; El Omari, K.; Christensen, H. E. M. The crystal structure of human dopamine β-hydroxylase at 2.9 Å resolution. *Sci. Adv.* **2016**, *2* (4), No. e1500980.
(13) Rush, K. W.; Eastman, K. A. S.; Welch, E. F.; Bandarian, V.; Blackburn, N. J. Capturing the Binuclear Copper State of Peptidylglycine Monooxygenase Using a Peptidyl-Homocysteine Lure. *J. Am. Chem. Soc.* **2024**, *146* (8), 5074−5080.
(14) Wu, P.; Fan, F.; Song, J.; Peng, W.; Liu, J.; Li, C.; Cao, Z.; Wang, B. Theory Demonstrated a "Coupled" Mechanism for O_2 Activation and Substrate Hydroxylation by Binuclear Copper Monooxygenases. *J. Am. Chem. Soc.* **2019**, *141* (50), 19776−19789.
(15) Allen, S. E.; Walvoord, R. R.; Padilla-Salinas, R.; Kozlowski, M. C. Aerobic copper-catalyzed organic reactions. *Chem. Rev.* **2013**, *113* (8), 6234−6458.
(16) Sterckx, H.; Morel, B.; Maes, B. U. W. Catalytic Aerobic Oxidation of C(sp^3)-H Bonds. *Angew. Chem., Int. Ed.* **2019**, *58* (24), 7946−7970.
(17) Becker, J.; Gupta, P.; Angersbach, F.; Tuczek, F.; Näther, C.; Holthausen, M. C.; Schindler, S. Selective Aromatic Hydroxylation with Dioxygen and Simple Copper Imine Complexes. *Chem. - Eur. J.* **2015**, *21* (33), 11735−11744.
(18) Becker, J.; Zhyhadlo, Y. Y.; Butova, E. D.; Fokin, A. A.; Schreiner, P. R.; Förster, M.; Holthausen, M. C.; Specht, P.; Schindler, S. Aerobic Aliphatic Hydroxylation Reactions by Copper Complexes: A Simple Clip-and-Cleave Concept. *Chem. - Eur. J.* **2018**, *24* (58), 15543−15549.
(19) Specht, P.; Petrillo, A.; Becker, J.; Schindler, S. Aerobic C-H hydroxylation by copper imine complexes: The clip-and-cleave concept − versatility and limits. *Eur. J. Inorg. Chem.* **2021**, *2021*, 1961−1970.
(20) Gupta, P.; Diefenbach, M.; Holthausen, M. C.; Förster, M. Copper-Mediated Selective Hydroxylation of a Non-activated C-H Bond in Steroids: A DFT Study of Schönecker's Reaction. *Chem. - Eur. J.* **2017**, *23* (6), 1427−1435.
(21) Schönecker, B.; Zheldakova, T.; Liu, Y.; Kötteritzsch, M.; Günther, W.; Görls, H. Biomimetic hydroxylation of nonactivated CH_2 groups with copper complexes and molecular oxygen. *Angew. Chem., Int. Ed.* **2003**, *42* (28), 3240−3244.
(22) Schönecker, B.; Zheldakova, T.; Lange, C.; Günther, W.; Görls, H.; Bohl, M. Intramolecular g-hydroxylations of nonactivated C-H bonds with copper complexes and molecular oxygen. *Chem. - Eur. J.* **2004**, *10* (23), 6029−6042.
(23) Zondervan, C.; van den Beuken, E. K.; Kooijman, H.; Spek, A. L.; Feringa, B. L. Efficient Synthesis and Molecular Structure of 2-Hydroxyisophthaldehyde. *Tetrahedron Lett.* **1997**, *38* (17), 3111−3114.
(24) See, Y. Y.; Herrmann, A. T.; Aihara, Y.; Baran, P. S. Scalable C-H Oxidation with Copper: Synthesis of Polyoxypregnanes. *J. Am. Chem. Soc.* **2015**, *137* (43), 13776−13779.
(25) Trammell, R.; See, Y. Y.; Herrmann, A. T.; Xie, N.; Díaz, D. E.; Siegler, M. A.; Baran, P. S.; Garcia-Bosch, I. Decoding the Mechanism of Intramolecular Cu-Directed Hydroxylation of sp^3 C-H Bonds. *J. Org. Chem.* **2017**, *82* (15), 7887−7904.
(26) Trammell, R.; D'Amore, L.; Cordova, A.; Polunin, P.; Xie, N.; Siegler, M. A.; Belanzoni, P.; Swart, M.; Garcia-Bosch, I. Directed Hydroxylation of sp^2 and sp^3 C-H Bonds Using Stoichiometric Amounts of Cu and H_2O_2. *Inorg. Chem.* **2019**, *58* (11), 7584−7592.
(27) Zhang, S.; Trammell, R.; Cordova, A.; Siegler, M. A.; Garcia-Bosch, I. Cu-promoted intramolecular hydroxylation of CH bonds using directing groups with varying denticity. *J. Inorg. Biochem.* **2021**, *223*, No. 111557.
(28) Zhang, S.; Goswami, S.; Schulz, K. H. G.; Gill, K.; Yin, X.; Hwang, J.; Wiese, J.; Jaffer, I.; Gil, R. R.; Garcia-Bosch, I. Regioselective Hydroxylation of Unsymmetrical Ketones Using Cu,

H_2O_2, and Imine Directing Groups via Formation of an Electrophilic Cupric Hydroperoxide Core. *J. Org. Chem.* **2024**, *89* (4), 2622−2636.
(29) Bryliakov, K. P. Catalytic Asymmetric Oxygenations with the Environmentally Benign Oxidants H_2O_2 and O_2. *Chem. Rev.* **2017**, *117* (17), 11406−11459.
(30) Mu, T.; Wei, B.; Zhu, D.; Yu, B. Site-selective C-H hydroxylation of pentacyclic triterpenoids directed by transient chiral pyridine-imino groups. *Nat. Commun.* **2020**, *11* (1), No. 4371.
(31) Schatz, M.; Becker, M.; Thaler, F.; Hampel, F.; Schindler, S.; Jacobson, R. R.; Tyeklár, Z.; Murthy, N. N.; Ghosh, P.; Chen, Q.; Zubieta, J.; Karlin, K. D. Copper(I) complexes, copper(I)/O_2 reactivity, and copper(II) complex adducts, with a series of tetradentate tripyridylalkylamine tripodal ligands. *Inorg. Chem.* **2001**, *40* (10), 2312−2322.
(32) Petrillo, A.; Hoffmann, A.; Becker, J.; Herres-Pawlis, S.; Schindler, S. Copper Mediated Intramolecular vs. Intermolecular Oxygenations: The Spacer makes the Difference! *Eur. J. Inorg. Chem.* **2022**, *2022*, No. e202100970.
(33) Hrdina, R. Directed C−H Functionalization of the Adamantane Framework. *Synthesis* **2019**, *51* (03), 629−642.
(34) Wanka, L.; Iqbal, K.; Schreiner, P. R. The lipophilic bullet hits the targets: medicinal chemistry of adamantane derivatives. *Chem. Rev.* **2013**, *113* (5), 3516−3604.
(35) Todd, M.; Hrdina, R. Synthesis of 1,2-Disubstituted Adamantane Derivatives by Construction of the Adamantane Framework. *Molecules* **2023**, *28* (22), 7636.
(36) Cianfanelli, M.; Olivo, G.; Milan, M.; Klein Gebbink, R. J. M.; Ribas, X.; Bietti, M.; Costas, M. Enantioselective C-H Lactonization of Unactivated Methylenes Directed by Carboxylic Acids. *J. Am. Chem. Soc.* **2020**, *142* (3), 1584−1593.
(37) Tsang, A. S.-K.; Kapat, A.; Schoenebeck, F. Factors That Control C-C Cleavage versus C-H Bond Hydroxylation in Copper-Catalyzed Oxidations of Ketones with O_2. *J. Am. Chem. Soc.* **2016**, *138* (2), 518−526.
(38) Gawlig, C.; Schindler, S.; Becker, S. One-Pot Conversion of Cyclohexane to Adipic Acid Using a μ_4-Oxido-Copper Cluster as Catalyst Together with Hydrogen Peroxide. *Eur. J. Inorg. Chem.* **2020**, *2020* (3), 248−252.
(39) Citek, C.; Herres-Pawlis, S.; Stack, T. D. P. Low temperature syntheses and reactivity of Cu_2O_2 active-site models. *Acc. Chem. Res.* **2015**, *48* (8), 2424−2433.
(40) Citek, C.; Gary, J. B.; Wasinger, E. C.; Stack, T. D. P. Chemical Plausibility of Cu(III) with Biological Ligation in pMMO. *J. Am. Chem. Soc.* **2015**, *137* (22), 6991−6994.
(41) Gary, J. B.; Citek, C.; Brown, T. A.; Zare, R. N.; Wasinger, E. C.; Stack, T. D. P. Direct Copper(III) Formation from O_2 and Copper(I) with Histamine Ligation. *J. Am. Chem. Soc.* **2016**, *138* (31), 9986−9995.
(42) Lerch, M.; Weitzer, M.; Stumpf, T.-D. J.; Laurini, L.; Hoffmann, A.; Becker, J.; Miska, A.; Göttlich, R.; Herres-Pawlis, S.; Schindler, S. Kinetic Investigation of the Reaction of Dioxygen with the Copper(I) Complex $[Cu(Pim^{iPr2})(CH_3CN)]CF_3SO_3$ {Pim^{iPr2} = Tris[2-(1,4-diisopropylimidazolyl)]phosphine}. *Eur. J. Inorg. Chem.* **2020**, *2020* (33), 3143−3150.
(43) Goswami, V. E.; Walli, A.; Förster, M.; Dechert, S.; Demeshko, S.; Holthausen, M. C.; Meyer, F. Acid/base triggered interconversion of μ-η2:η2-peroxido and bis(μ-oxido) dicopper intermediates capped by proton-responsive ligands. *Chem. Sci.* **2017**, *8* (4), 3031−3037.
(44) Herres-Pawlis, S.; Verma, P.; Haase, R.; Kang, P.; Lyons, C. T.; Wasinger, E. C.; Flörke, U.; Henkel, G.; Stack, T. D. P. Phenolate hydroxylation in a bis(μ-oxo)dicopper(III) complex: lessons from the guanidine/amine series. *J. Am. Chem. Soc.* **2009**, *131* (3), 1154−1169.
(45) Gherman, B. F.; Cramer, C. J. Quantum chemical studies of molecules incorporating a $Cu_2O_2^{2+}$ core. *Coord. Chem. Rev.* **2009**, *253* (5−6), 723−753.
(46) Lewin, J. L.; Heppner, D. E.; Cramer, C. J. Validation of density functional modeling protocols on experimental bis(μ-oxo)/m- η^2: η^2-peroxo dicopper equilibria. *J. Biol. Inorg. Chem.* **2007**, *12* (8), 1221−1234.
(47) Wu, P.; Zhang, J.; Chen, Q.; Peng, W.; Wang, B. Theoretical perspective on mononuclear copper-oxygen mediated C−H and O−H activations: A comparison between biological and synthetic systems. *Chin. J. Catal.* **2022**, *43* (4), 913−927.
(48) De Tovar, J.; Leblay, R.; Wang, Y.; Wojcik, L.; Thibon-Pourret, A.; Reglier, M.; Simaan, A. J.; Le Poul, N.; Belle, C. Copper-oxygen adducts: new trends in characterization and properties towards C−H activation. *Chem. Sci.* **2024**, *15*, 10308−10349.
(49) Quek, S. Y.; Debnath, S.; Laxmi, S.; van Gastel, M.; Krämer, T.; England, J. Sterically Stabilized End-On Superoxocopper(II) Complexes and Mechanistic Insights into Their Reactivity with O-H, N-H, and C-H Substrates. *J. Am. Chem. Soc.* **2021**, *143* (47), 19731−19747.
(50) Diaz, D. E.; Quist, D. A.; Herzog, A. E.; Schaefer, A. W.; Kipouros, I.; Bhadra, M.; Solomon, E. I.; Karlin, K. D. Impact of Intramolecular Hydrogen Bonding on the Reactivity of Cupric Superoxide Complexes with O−H and C−H Substrates. *Angew. Chem.* **2019**, *131* (49), 17736−17740.
(51) Luo, Y.-R. *Comprehensive Handbook of Chemical Bond Energies*; CRC Press, 2007.
(52) Knizia, G.; Klein, J. E. M. N. Electron flow in reaction mechanisms—revealed from first principles. *Angew. Chem., Int. Ed.* **2015**, *54* (18), 5518−5522.
(53) Knizia, G. Intrinsic Atomic Orbitals: An Unbiased Bridge between Quantum Theory and Chemical Concepts. *J. Chem. Theory Comput.* **2013**, *9* (11), 4834−4843.
(54) Spuhler, P.; Holthausen, M. C. Mechanism of the aliphatic hydroxylation mediated by a bis(μ-oxo)dicopper(III) complex. *Angew. Chem., Int. Ed.* **2003**, *42* (48), 5961−5965.
(55) Itoh, S.; Taki, M.; Nakao, H.; Holland, P. L.; Tolman, W. B.; Que, J. L.; Fukuzumi, S. Aliphatic Hydroxylation by a Bis(μ-oxo)dicopper(III) Complex. *Angew. Chem., Int. Ed.* **2000**, *39* (2), 398−400.
(56) Itoh, S. Developing mononuclear copper-active-oxygen complexes relevant to reactive intermediates of biological oxidation reactions. *Acc. Chem. Res.* **2015**, *48* (7), 2066−2074.
(57) Abe, T.; Shiota, Y.; Itoh, S.; Yoshizawa, K. Theoretical rationalization for the equilibrium between (μ-η^2:η^2-peroxido)-$Cu^{II}Cu^{II}$ and bis(μ-oxido)$Cu^{III}Cu^{III}$ complexes: perturbational effects from ligand frameworks. *Dalton Trans.* **2020**, *49* (20), 6710−6717.
(58) Motiwala, H. F.; Armaly, A. M.; Cacioppo, J. G.; Coombs, T. C.; Koehn, K. R. K.; Norwood, V. M.; Aubé, J. HFIP in Organic Synthesis. *Chem. Rev.* **2022**, *122* (15), 12544−12747.
(59) Osako, T.; Nagatomo, S.; Tachi, Y.; Kitagawa, T.; Itoh, S. Low-Temperature Stopped-Flow Studies on the Reactions of Copper(II) Complexes and H_2O_2: The First Detection of a Mononuclear Copper(II)−Peroxo Intermediate. *Angew. Chem., Int. Ed.* **2002**, *41* (22), 4325−4328.
(60) Mirica, L. M.; Ottenwaelder, X.; Stack, T. D. P. Structure and spectroscopy of copper-dioxygen complexes. *Chem. Rev.* **2004**, *104* (2), 1013−1045.
(61) Higham, J. I.; Ma, T.-K.; Bull, J. A. When is an Imine Directing Group a Transient Imine Directing Group in C-H Functionalization? *Chem. - Eur. J.* **2024**, *30*, No. e202400345.
(62) Higham, J. I.; Bull, J. A. Amine-Catalyzed Copper-Mediated C-H Sulfonylation of Benzaldehydes via a Transient Imine Directing Group. *Angew. Chem., Int. Ed.* **2022**, *61* (27), No. e202202933.

https://doi.org/10.1021/jacs.4c07777
J. Am. Chem. Soc. 2024, 146, 25689−25700

4 References

[1] Deutsche Gesellschaft für Katalyse, *Katalytische Oxidationsreaktionen als Schlüsseltechnologie*. *Positionspapier*, DECHEMA Gesellschaft für Chemische Technik und Biotechnologie e.V., Frankfurt am Main, **2015**.

[2] H. Sterckx, B. Morel, B. U. W. Maes, *Angew. Chem. Int. Ed.* **2019**, *58*, 7946.

[3] A. Huang, R. S. Delima, Y. Kim, E. W. Lees, F. G. L. Parlane, D. J. Dvorak, M. B. Rooney, R. P. Jansonius, A. G. Fink, Z. Zhang, C. P. Berlinguette, *J. Am. Chem. Soc.* **2022**, *144*, 14548.

[4] J. A. Keith, P. M. Henry, *Angew. Chem. Int. Ed.* **2009**, *48*, 9038.

[5] S. J. Blanksby, G. B. Ellison, *Acc. Chem. Res.* **2003**, *36*, 255.

[6] P. Gandeepan, T. Müller, D. Zell, G. Cera, S. Warratz, L. Ackermann, *Chem. Rev.* **2019**, *119*, 2192.

[7] K. Liao, S. Negretti, D. G. Musaev, J. Bacsa, H. M. L. Davies, *Nature* **2016**, *533*, 230.

[8] Deutsche Gesellschaft für Katalyse, *KATALYSE Eine interdisziplinäre Schlüsseltechnologie zur nachhaltigen Wirtschaftsentwicklung*, DECHEMA Gesellschaft für Chemische Technik und Biotechnologie e.V., Frankfurt am Main, **2023**.

[9] J. Wencel-Delord, F. Glorius, *Nat. Chem.* **2013**, *5*, 369.

[10] B. Hong, T. Luo, X. Lei, *ACS Cent. Sci.* **2020**, *6*, 622.

[11] W. G. Mcbride, *The Lancet* **1961**, *278*, 1358.

[12] S. Wnendt, M. Finkam, W. Winter, J. Ossig, G. Raabe, K. Zwingenberger, *Chirality* **1996**, *8*, 390.

[13] P. Höglund, T. Eriksson, S. Björkman, *J. Pharmacokinet. Pharmacodyn.* **1998**, *26*, 363.

[14] a) R. Noyori, *Nobel Lecture* **2001**; b) N. B. Johnson, I. C. Lennon, P. H. Moran, J. A. Ramsden, *Acc. Chem. Res.* **2007**, *40*, 1291.

[15] K. P. Bryliakov, *Chem. Rev.* **2017**, *117*, 11406.

[16] J. Wencel-Delord, T. Dröge, F. Liu, F. Glorius, *Chem. Soc. Rev.* **2011**, *40*, 4740.

[17] I. Garcia-Bosch, K. D. Karlin in *PATAI'S Chemistry of Functional Groups* (Ed.: Zvi Rappoport), John Wiley & Sons, Ltd., Chichester, UK, **2014**, pp. 1–52.

[18] I. A. Koval, P. Gamez, C. Belle, K. Selmeczi, J. Reedijk, *Chem. Soc. Rev.* **2006**, *35*, 814.

[19] E. I. Solomon, D. E. Heppner, E. M. Johnston, J. W. Ginsbach, J. Cirera, M. Qayyum, M. T. Kieber-Emmons, C. H. Kjaergaard, R. G. Hadt, L. Tian, *Chem. Rev.* **2014**, *114*, 3659.

[20] J. J. Liu, D. E. Diaz, D. A. Quist, K. D. Karlin, *Isr. J. Chem.* **2016**, *56*, 9.

[21] D. A. Quist, D. E. Diaz, J. J. Liu, K. D. Karlin, *J. Biol. Inorg. Chem.* **2017**, *22*, 253.

[22] L. M. Mirica, X. Ottenwaelder, T. D. P. Stack, *Chem. Rev.* **2004**, *104*, 1013.

[23] A. Brinkmeier, R. A. Schulz, M. Buchhorn, C.-J. Spyra, S. Dechert, S. Demeshko, V. Krewald, F. Meyer, *J. Am. Chem. Soc.* **2021**, *143*, 10361.

[24] P. M. Colman, H. C. Freeman, J. M. Guss, M. Murata, V. A. Norris, J. A. M. Ramshaw, M. P. Venkatappa, *Nature* **1978**, *272*, 319.

[25] S. T. Prigge, B. A. Eipper, R. E. Mains, L. M. Amzel, *Science* **2004**, *304*, 864.

[26] Y. Matoba, T. Kumagai, A. Yamamoto, H. Yoshitsu, M. Sugiyama, *J. Biol. Chem.* **2006**, *281*, 8981.

[27] R. J. Quinlan, M. D. Sweeney, L. Lo Leggio, H. Otten, J.-C. N. Poulsen, K. S. Johansen, K. B. R. M. Krogh, C. I. Jørgensen, M. Tovborg, A. Anthonsen, T. Tryfona,

C. P. Walter, P. Dupree, F. Xu, G. J. Davies, P. H. Walton, *Proc. Natl. Acad. Sci.* **2011**, *108*, 15079.

[28] J. A. Guckert, M. D. Lowery, E. I. Solomon, *J. Am. Chem. Soc.* **1995**, *117*, 2817.

[29] H. B. Gray, B. G. Malmström, R. J. Williams, *J. Biol. Inorg. Chem.* **2000**, *5*, 551.

[30] J. A. Tainer, E. D. Getzoff, J. S. Richardson, D. C. Richardson, *Nature* **1983**, *306*, 284.

[31] T. V. Vendelboe, P. Harris, Y. Zhao, T. S. Walter, K. Harlos, K. El Omari, H. E. M. Christensen, *Sci. Adv.* **2016**, *2*, e1500980.

[32] E. E. Chufán, S. T. Prigge, X. Siebert, B. A. Eipper, R. E. Mains, L. M. Amzel, *J. Am. Chem. Soc.* **2010**, *132*, 15565.

[33] a) G. Tian, J. A. Berry, J. P. Klinman, *Biochemistry* **1994**, *33*, 226; b) W. A. Francisco, D. J. Merkler, N. J. Blackburn, J. P. Klinman, *Biochemistry* **1998**, *37*, 8244.

[34] a) A. Crespo, M. A. Martí, A. E. Roitberg, L. M. Amzel, D. A. Estrin, *J. Am. Chem. Soc.* **2006**, *128*, 12817; b) K. Yoshizawa, N. Kihara, T. Kamachi, Y. Shiota, *Inorg. Chem.* **2006**, *45*, 3034; c) A. de La Lande, O. Parisel, H. Gérard, V. Moliner, O. Reinaud, *Chem. Eur. J.* **2008**, *14*, 6465.

[35] a) J. P. Klinman, *J. Biol. Chem.* **2006**, *281*, 3013; b) P. Chen, E. I. Solomon, *J. Am. Chem. Soc.* **2004**, *126*, 4991.

[36] P. Wu, F. Fan, J. Song, W. Peng, J. Liu, C. Li, Z. Cao, B. Wang, *J. Am. Chem. Soc.* **2019**, *141*, 19776.

[37] A. Volbeda, W. G. Hol, *J. Mol. Biol.* **1989**, *209*, 249.

[38] T. Klabunde, C. Eicken, J. C. Sacchettini, B. Krebs, *Nat. Struct. Mol. Biol.* **1998**, *5*, 1084.

[39] J. N. Hamann, B. Herzigkeit, R. Jurgeleit, F. Tuczek, *Coord. Chem. Rev.* **2017**, *334*, 54.

[40] E. Solem, F. Tuczek, H. Decker, *Angew. Chem. Int. Ed.* **2016**, *55*, 2884.

[41] G. Prota, *Med. Res. Rev.* **1988**, *8*, 525.

[42] M. R. Loizzo, R. Tundis, F. Menichini, *Compr. Rev. Food Sci. Food Saf.* **2012**, *11*, 378.

[43] N. Fujieda, M. Murata, S. Yabuta, T. Ikeda, C. Shimokawa, Y. Nakamura, Y. Hata, S. Itoh, *J. Biol. Inorg. Chem.* **2013**, *18*, 19.

[44] M. Rolff, J. Schottenheim, H. Decker, F. Tuczek, *Chem. Soc. Rev.* **2011**, *40*, 4077.

[45] G. Vaaje-Kolstad, B. Westereng, S. J. Horn, Z. Liu, H. Zhai, M. Sørlie, V. G. H. Eijsink, *Science* **2010**, *330*, 219.

[46] L. Ciano, G. J. Davies, W. B. Tolman, P. H. Walton, *Nat. Catal.* **2018**, *1*, 571.

[47] B. Wang, E. M. Johnston, P. Li, S. Shaik, G. J. Davies, P. H. Walton, C. Rovira, *ACS Catal.* **2018**, *8*, 1346.

[48] B. Bissaro, Å. K. Røhr, G. Müller, P. Chylenski, M. Skaugen, Z. Forsberg, S. J. Horn, G. Vaaje-Kolstad, V. G. H. Eijsink, *Nat. Chem. Biol.* **2017**, *13*, 1123.

[49] B. Bissaro, B. Streit, I. Isaksen, V. G. H. Eijsink, G. T. Beckham, J. L. DuBois, Å. K. Røhr, *Proc. Natl. Acad. Sci.* **2020**, *117*, 1504.

[50] B. Wang, P. H. Walton, C. Rovira, *ACS Catal.* **2019**, *9*, 4958.

[51] L. Rieder, A. A. Stepnov, M. Sørlie, V. G. H. Eijsink, *Biochemistry* **2021**, *60*, 3633.

[52] X. Li, W. T. Beeson, C. M. Phillips, M. A. Marletta, J. H. D. Cate, *Structure* **2012**, *20*, 1051.

[53] E. A. Lewis, W. B. Tolman, *Chem. Rev.* **2004**, *104*, 1047.

[54] C. E. Elwell, N. L. Gagnon, B. D. Neisen, D. Dhar, A. D. Spaeth, G. M. Yee, W. B. Tolman, *Chem. Rev.* **2017**, *117*, 2059.

[55] R. Trammell, K. Rajabimoghadam, I. Garcia-Bosch, *Chem. Rev.* **2019**, *119*, 2954.

[56] a) N. Kitajima, T. Koda, S. Hashimoto, T. Kitagawa, Y. Morooka, *J. Am. Chem. Soc.* **1991**, *113*, 5664; b) A. Wada, M. Harata, K. Hasegawa, K. Jitsukawa, H. Masuda, M. Mukai, T. Kitagawa, H. Einaga, *Angew. Chem. Int. Ed.* **1998**, *37*, 798; c) M. Schatz, V. Raab, S. P. Foxon, G. Brehm, S. Schneider, M. Reiher, M. C. Holthausen, J. Sundermeyer, S. Schindler, *Angew. Chem. Int. Ed.* **2004**, *43*, 4360; d) T. Fujii, S. Yamaguchi, Y. Funahashi, T. Ozawa, T. Tosha, T. Kitagawa, H. Masuda, *Chem. Commun.* **2006**, 4428; e) D. Maiti, J. S. Woertink, A. A. Narducci Sarjeant, E. I. Solomon, K. D. Karlin, *Inorg. Chem.* **2008**, *47*, 3787.

[57] K. Fujisawa, M. Tanaka, Y. Moro-oka, N. Kitajima, *J. Am. Chem. Soc.* **1994**, *116*, 12079.

[58] J. A. Halfen, S. Mahapatra, E. C. Wilkinson, S. Kaderli, V. G. Young, L. Que, A. D. Zuberbühler, W. B. Tolman, *Science* **1996**, *271*, 1397.

[59] C. Würtele, E. Gaoutchenova, K. Harms, M. C. Holthausen, J. Sundermeyer, S. Schindler, *Angew. Chem. Int. Ed.* **2006**, *45*, 3867.

[60] S. Schindler, *Eur. J. Inorg. Chem.* **2000**, *2000*, 2311.

[61] M. Bhadra, W. J. Transue, H. Lim, R. E. Cowley, J. Y. C. Lee, M. A. Siegler, P. Josephs, G. Henkel, M. Lerch, S. Schindler, A. Neuba, K. O. Hodgson, B. Hedman, E. I. Solomon, K. D. Karlin, *J. Am. Chem. Soc.* **2021**, *143*, 3707.

[62] a) L. S. Kau, D. J. Spira-Solomon, J. E. Penner-Hahn, K. O. Hodgson, E. I. Solomon, *J. Am. Chem. Soc.* **1987**, *109*, 6433; b) J. L. DuBois, P. Mukherjee, T. D. P. Stack, B. Hedman, E. I. Solomon, K. O. Hodgson, *J. Am. Chem. Soc.* **2000**, *122*, 5775.

[63] R. R. Jacobson, Z. Tyeklar, A. Farooq, K. D. Karlin, S. Liu, J. Zubieta, *J. Am. Chem. Soc.* **1988**, *110*, 3690.

[64] H. R. Lucas, L. Li, A. A. N. Sarjeant, M. A. Vance, E. I. Solomon, K. D. Karlin, *J. Am. Chem. Soc.* **2009**, *131*, 3230.

[65] C. Würtele, O. Sander, V. Lutz, T. Waitz, F. Tuczek, S. Schindler, *J. Am. Chem. Soc.* **2009**, *131*, 7544.

[66] M. Schatz, M. Becker, F. Thaler, F. Hampel, S. Schindler, R. R. Jacobson, Z. Tyeklár, N. N. Murthy, P. Ghosh, Q. Chen, J. Zubieta, K. D. Karlin, *Inorg. Chem.* **2001**, *40*, 2312.

[67] M. Weitzer, M. Schatz, F. Hampel, F. W. Heinemann, S. Schindler, *Dalton Trans.* **2002**, 686.

[68] S. Itoh, H. Nakao, L. M. Berreau, T. Kondo, M. Komatsu, S. Fukuzumi, *J. Am. Chem. Soc.* **1998**, *120*, 2890.

[69] S. Itoh, M. Taki, H. Nakao, P. L. Holland, W. B. Tolman, J. L. Que, S. Fukuzumi, *Angew. Chem. Int. Ed.* **2000**, *39*, 398.

[70] M. Weitzer, S. Schindler, G. Brehm, S. Schneider, E. Hörmann, B. Jung, S. Kaderli, A. D. Zuberbühler, *Inorg. Chem.* **2003**, *42*, 1800.

[71] Y. Rondelez, M.-N. Rager, A. Duprat, O. Reinaud, *J. Am. Chem. Soc.* **2002**, *124*, 1334.

[72] H. Hayashi, S. Fujinami, S. Nagatomo, S. Ogo, M. Suzuki, A. Uehara, Y. Watanabe, T. Kitagawa, *J. Am. Chem. Soc.* **2000**, *122*, 2124.

[73] T. Osako, Y. Ueno, Y. Tachi, S. Itoh, *Inorg. Chem.* **2003**, *42*, 8087.

[74] T. Osako, S. Terada, T. Tosha, S. Nagatomo, H. Furutachi, S. Fujinami, T. Kitagawa, M. Suzuki, S. Itoh, *Dalton Trans.* **2005**, 3514.

[75] L. Q. Hatcher, M. A. Vance, A. A. Narducci Sarjeant, E. I. Solomon, K. D. Karlin, *Inorg. Chem.* **2006**, *45*, 3004.

[76] S. Gamboa-Ramirez, B. Faure, M. Réglier, A. J. Simaan, M. Orio, *Chem. Eur. J.* **2022**, *28*, e202202206.

[77] D. Maiti, D.-H. Lee, K. Gaoutchenova, C. Würtele, M. C. Holthausen, A. A. Narducci Sarjeant, J. Sundermeyer, S. Schindler, K. D. Karlin, *Angew. Chem. Int. Ed.* **2008**, *120*, 88.

[78] B. Kim, M. T. Brueggemeyer, W. J. Transue, Y. Park, J. Cho, M. A. Siegler, E. I. Solomon, K. D. Karlin, *J. Am. Chem. Soc.* **2023**, *145*, 11735.

[79] K. D. Karlin, P. L. Dahlstrom, S. N. Cozzette, P. M. Scensny, J. Zubieta, *J. Chem. Soc., Chem. Commun.* **1981**, 881.

[80] K. D. Karlin, J. C. Hayes, Y. Gultneh, R. W. Cruse, J. W. McKown, J. P. Hutchinson, J. Zubieta, *J. Am. Chem. Soc.* **1984**, *106*, 2121.

[81] K. D. Karlin, M. S. Nasir, B. I. Cohen, R. W. Cruse, S. Kaderli, A. D. Zuberbuehler, *J. Am. Chem. Soc.* **1994**, *116*, 1324.

[82] S. Ryan, H. Adams, D. E. Fenton, M. Becker, S. Schindler, *Inorg. Chem.* **1998**, *37*, 2134.

[83] P. L. Holland, K. R. Rodgers, W. B. Tolman, *Angew. Chem. Int. Ed.* **1999**, *38*, 1139.

[84] J. Becker, P. Gupta, F. Angersbach, F. Tuczek, C. Näther, M. C. Holthausen, S. Schindler, *Chem. Eur. J.* **2015**, *21*, 11735.

[85] B. Schönecker, T. Zheldakova, Y. Liu, M. Kötteritzsch, W. Günther, H. Görls, *Angew. Chem. Int. Ed.* **2003**, *42*, 3240.

[86] B. Schönecker, T. Zheldakova, C. Lange, W. Günther, H. Görls, M. Bohl, *Chem. Eur. J.* **2004**, *10*, 6029.

[87] Y. Y. See, A. T. Herrmann, Y. Aihara, P. S. Baran, *J. Am. Chem. Soc.* **2015**, *137*, 13776.

[88] P. Gupta, M. Diefenbach, M. C. Holthausen, M. Förster, *Chem. Eur. J.* **2017**, *23*, 1427.

[89] R. Trammell, Y. Y. See, A. T. Herrmann, N. Xie, D. E. Díaz, M. A. Siegler, P. S. Baran, I. Garcia-Bosch, *J. Org. Chem.* **2017**, *82*, 7887.

[90] S. Zhang, R. Trammell, A. Cordova, M. A. Siegler, I. Garcia-Bosch, *J. Inorg. Biochem.* **2021**, *223*, 111557.

[91] J. Becker, Y. Y. Zhyhadlo, E. D. Butova, A. A. Fokin, P. R. Schreiner, M. Förster, M. C. Holthausen, P. Specht, S. Schindler, *Chem. Eur. J.* **2018**, *24*, 15543.

[92] R. Trammell, L. D'Amore, A. Cordova, P. Polunin, N. Xie, M. A. Siegler, P. Belanzoni, M. Swart, I. Garcia-Bosch, *Inorg. Chem.* **2019**, *58*, 7584.

[93] P. Specht, A. Petrillo, J. Becker, S. Schindler, *Eur. J. Inorg. Chem.* **2021**, 1961.

[94] I. Garcia-Bosch, M. A. Siegler, *Angew. Chem. Int. Ed.* **2016**, *55*, 12873.

[95] M. Schatz, M. Becker, O. Walter, G. Liehr, S. Schindler, *Inorg. Chim. Acta* **2001**, *324*, 173.